

UNIVERSITY OF CALIFORNIA

Los Angeles

Activated Sludge Process Improvements:
Benefits of Bioaugmentation and Improved Monitoring

A dissertation submitted in partial satisfaction of the
requirements for the degree Doctor of Philosophy
in Civil Engineering

by

Shao-Yuan Leu

2009

UMI Number: 3374955

INFORMATION TO USERS

The quality of this reproduction is dependent upon the quality of the copy submitted. Broken or indistinct print, colored or poor quality illustrations and photographs, print bleed-through, substandard margins, and improper alignment can adversely affect reproduction.

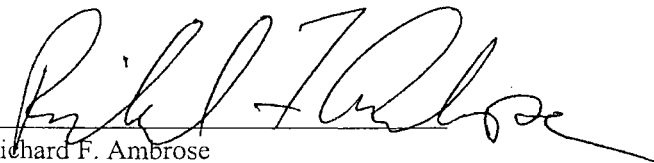
In the unlikely event that the author did not send a complete manuscript and there are missing pages, these will be noted. Also, if unauthorized copyright material had to be removed, a note will indicate the deletion.



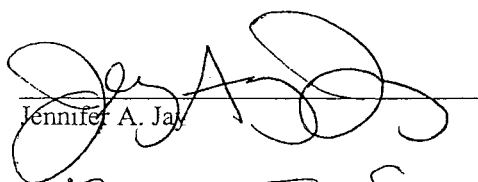
UMI Microform 3374955
Copyright 2009 by ProQuest LLC
All rights reserved. This microform edition is protected against
unauthorized copying under Title 17, United States Code.

ProQuest LLC
789 East Eisenhower Parkway
P.O. Box 1346
Ann Arbor, MI 48106-1346

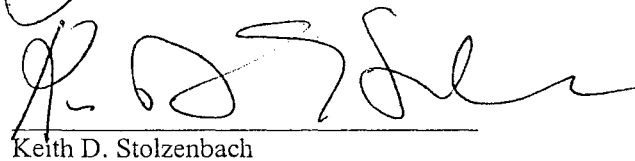
The dissertation of Shao-Yuan Leu is approved.



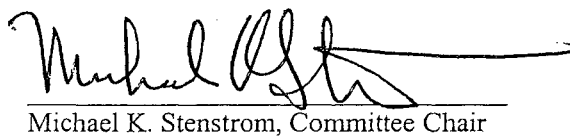
Richard F. Ambrose



Jennifer A. Jay



Keith D. Stolzenbach



Michael K. Stenstrom, Committee Chair

University of California, Los Angeles

2009

TABLE OF CONTENTS

LIST OF FIGURES AND TABLES	iii
ACKNOWLEDGEMENTS	ix
VITA	x
ABSTRACT OF THE DISSERTATION	xi
1. INTRODUCTION	1
2. LITERATURE REVIEW	6
2.1 Wastewater Composition	6
2.2 Simulation Models	8
2.2.1 ASP Models	8
2.2.1.1 Development of Unstructured and Structured Models	10
2.2.1.2 Comparison of the Modern ASP Models	13
2.2.1.2 Parameters and Model Calibration of ASM Models	18
2.2.2 Gas Transfer Model	20
2.2.2.1 General Theory	20
2.2.2.2 Conversion Gas Transfer Coefficient among Gases	22
2.2.2.3 CO ₂ Transfer and pH Simulation	23
2.3 Introduction to Off-Gas Test	26
2.4 Application of Off-Gas Test and Gas Phase Simulation in ASP Models	29
3. BIOAUGMENTATION TO IMPROVE HAZARDOUS POLLUTANTS	30
3.1 Summary	30
3.2 Experimental Methods	36
3.3 Model Development	41
3.4 Results and Discussion	45
3.4.1 Steady State Results	45

3.4.2 Shock Loading and Reacclimation Experiments	48
3.4.3 Dynamic Simulations	51
3.4.4 Model Calibration	55
3.4.5 Simulation of the <i>In-Situ</i> Process	57
3.4 Conclusion	60
4. BIOAUGMENTATION TO IMPROVE NITRIFICATION	63
4.1 Summary	63
4.2 Theoretical Background	64
4.2.1 Bioaugmentation Schemes	64
4.2.2 Simulation of bioaugmentation processes	69
4.3 Results and Discussion	75
4.3.1 Steady-State Analysis	75
4.3.2 Results of Dynamic Simulations	79
4.3.3 Effects of Temperature and Aeration Volumes	85
4.3.4 Comparison between <i>In-situ</i> and ER Approaches	87
4.4 Conclusion	89
5. MONITORING AERATION EFFICIENCY	90
5.1 Introduction	90
5.2 Material and Methods	94
5.2.1 Field Experiments	94
5.2.2 Design of a Real-Time Off-gas Analyzer	97
5.2.3 Oxygen Uptake Rate Model	100
5.3 Results and Discussion	105
5.3.1 The 24-Hour Experiments	105
5.3.2 Oxygen Demand Simulation	108

5.3.3 Remarks on Air Supply System	112
5.3.4 Application I. – Optimal Cleaning of Fine-Pore Diffusers	112
5.3.5 Application II. – Optimization of the Peak Power Loadings	115
5.4 Conclusion	121
6. QUANTIFYING NITROGEN REMOVAL BY MONITORING OFF-GAS O ₂ /CO ₂	
6.1 Introduction	123
6.2 Materials and methods	126
6.2.1 Background of tested Treatment Plant	126
6.2.2 Off-Gas Tests	127
6.2.3 Activated Sludge Model	129
6.2.4 Simulation of Gas Transfer	132
6.3 Results and Discussion	135
6.3.1 Primary Analysis of Off-Gas Data	135
6.3.2 Model Calibration and Sensitivity Analysis	140
6.3.3 Dynamic Simulation	143
6.4 Conclusions	145
7. CONCLUSIONS	149
REFERENCES	151

LIST OF FIGURES

Figure 1.1 Concept schematic of three bioaugmentation processes	4
Figure 1.2 Setup and equipments of an off-gas test	5
Figure 2.1 Figure 2.1 Reaction schematic of a nitrifying activated sludge process	6
Figure 2.2 Schematic diagram of a CMAS process	9
Figure 2.3 Flow diagrams of the Clift and Andrews Activated Sludge Model	15
Figure 2.4 Flow diagram of the IAWQ Activated Sludge Model No.1	16
Figure 2.5 Flow diagram of the IAWQ Activated Sludge Model No.3	17
Figure 2.7 Equilibrium of carbonate system versus pH	24
Figure 3.1 (a) Concept schematic of the enricher-reactor bioaugmentation process	33
Figure 3.1 (b) Concept schematic of the on-line <i>in-situ</i> bioaugmentation process	34
Figure 3.2 Laboratory setup of bioaugmentation experiments for 1-NA	39
Figure 3.3 Biomass concentration versus bioaugmentation levels	48
Figure 3.4 Effluent 1-NA breakthrough in bioaugmentation experiments	50
Figure 3.5 Simulation results of 1-NA breakthrough in shock loading experiments	52
Figure 3.6 Simulation results of 1-NA breakthrough in reacclimation experiments	54
Figure 3.7 Simulation results of performance of different bioaugmentation methods	59
Figure 4.1 (a) Concept schematic of parallel plant approach	65
Figure 4.1 (b) Concept schematic of enricher-reactor approach	67
Figure 4.1 (c) Concept schematic of <i>in-situ</i> approach	68
Figure 4.2 Simulation results of three bioaugmentation approaches	74
Figure 4.3 Simulation results of the studied wastewater treatment plant	82
Figure 4.4 Simulation results of nitrogen removal under stressed conditions	84
Figure 4.5 Simulations of bioaugmentation scenarios under changing temperature	85
Figure 4.6 Simulations of bioaugmentation scenarios under changing volumes	87

Figure 5.1 Schematic Diagram of the tested treatment plant	95
Figure 5.2 Schematic of a real-time off-gas monitoring system	99
Figure 5.3 Results of off-gas monitoring during a 24-hr cycle	106
Figure 5.4 Correlation between α SOTE, α , and diffuser air flux	107
Figure 5.5 Simulated oxygen uptake rate versus the rate of oxygen transferred	110
Figure 5.6 Energy expenditure of aeration cost	114
Figure 5.7 Energy consumption of blowers versus the hourly power rate	116
Figure 5.8 Energy saving practices by flow control	118
Figure 6.1 Tank geometry and schematic diagram of tested treatment plant	128
Figure 6.2 Experiment results of real-time off-gas tests and nitrification status	137
Figure 6.3 Correlations of off-gas measured CTR and OTR	138
Figure 6.4 Calibrated parameter values at different testing temperatures	141
Figure 6.5 Effects of unexpected pH change to CPR simulations	143
Figure 6.6 Simulation results of the three parameters	144
Figure 6.7 Block diagram of simulation procedure	146

LIST OF TABLES

Table 2.1 Typical raw wastewater characteristics	7
Table 2.2 Timeline of literatures developing the modern activated sludge models	14
Table 2.3 Reference values of Monod parameters	19
Table 3.1 Operational characteristics of laboratory reactors	40
Table 3.2 Measured effluent biomass and soluble COD	46
Table 3.3 Monod kinetics used in the simulations	48
Table 4.1 Selected parameters in literature of on-site bioaugmentation studies	77
Table 4.2 Wastewater properties of tested treatment plant	80
Table 4.3 Selected Monod kinetics for autotrophic species in simulations	80
Table 4.4 Mass yield matrix used in simulations	81
Table 4.5 Designed bioaugmentation scenarios under overloaded conditions	83
Table 5.1 Operation background of tested treatment plant	96
Table 5.2 Matrix of mass yield from stoichiometry	108
Table 5.3 Monod kinetics of activated sludge model at 20°C	109
Table 5.4 Results of off-gas tests	113
Table 5.5 Aeration costs of different plant operation strategy	120
Table 6.1 Wastewater composition of the tested treatment plant	127
Table 6.2 Model matrix of yield coefficient and model kinetics	131
Table 6.3 Average plant monitoring results and off-gas tests	135
Table 6.4 Mass balance of special elements	139
Table 6.5 Selected Monod kinetics used in simulations	140

ACKNOWLEDGMENTS

This research was partially supported by the California Energy Commission and Southern California Edison Inc., a power company in California, U.S.A. The technology published is in public domain. The author thanks Professor Stenstrom for academic advices and his patience, creativity, and encouragement are what have made this dissertation a success. The author also thanks Diego Rosso, Min-Mo Chung, Pan Jiang, and Li-Cheng Chan for their assistance with the 24-hour experiments, Judy Libra and her research group for data collection, and Sim-Lin Lau for the water quality analysis.

VITA

November 18, 1975	Born, Taipei, Taiwan
1997	B. A., Forestry National Taiwan University Taipei, Taiwan
1997- 1999	M. S., Forestry National Taiwan University Taipei, Taiwan
1999- 2001	Solider Clerk Air Force Base, Hsin-Chu, Taiwan
2001- 2003	Research Assistant National Taiwan University Taipei, Taiwan
2003- 2005	M. S., Civil and Environmental Engineering University of California, Los Angeles

PUBLICATIONS

- Kaliman, A, Rosso, D., Leu, S.-Y., and Stenstrom, M.K. (2008) Fine-pore aeration diffusers: Accelerated membrane ageing studies, *Wat. Research*, **42**: 467-475.
- Leu, S.-Y., Babcock, R., Tzeng, C.-J., and Stenstrom, M.K. (2009) Modeling the Performance of Hazardous Wastes Removal in Bioaugmented Activated Sludge Processes, *Wat. Environ. Research*, (accepted)
- Leu, S.-Y., Rosso, D., Larson, L., and Stenstrom, M.K. (2009) Real-Time Monitoring Aeration Efficiency in the Activated Sludge Process and Methods to Reduce Energy Consumption, *Wat. Environ. Research*, (accepted)
- Leu, S.-Y., and Stenstrom, M.K. (2009) Quantification and Evaluation of Nitrogen Removal in Bioaugmentation Processes, *Wat. Research*, (in review)
- Leu, S.-Y., Libra, J., and Stenstrom, M.K. (2009) Monitoring the real-time nitrogen removal performance in activated sludge processes by off-gas test, *Wat. Research*, (in preparation)

ABSTRACT OF THE DISSERTATION

Activated Sludge Process Improvements:
Benefits of Bioaugmentation and Improved Monitoring

by

Shao-Yuan Leu

Doctor of Philosophy in Civil Engineering

University of California, Los Angeles, 2009

Professor Michael K. Stenstrom, Chair

This dissertation investigated two techniques to improve the activated sludge process for wastewater treatment. Bioaugmentation is a technique that uses specially acclimated biomass cultures to increase the degradation of the “target component(s)” in otherwise conventional activated sludge processes. Off-gas is a real-time monitoring technique that can be used to estimate aeration costs and nitrification efficiency. Mathematical modeling coupled with field studies and laboratory observations was used to develop the theoretical basis to evaluate four process improvements: bioaugmentation for improved removals of hazardous wastes; bioaugmentation to improve nitrification; real-time monitoring to save energy and reduce peak energy consumption, and the use of off-gas carbon dioxide concentration to quantify nitrification efficiency.

Bioaugmentation was applied to degrade a selected hazardous waste (1-naphthylamine, 1-NA). This aromatic compound is normally not degradable in ASP and is an inhibitor to nitrifiers. A model was developed to simulate the consumption of 1-NA and validated using results from lab-scale experiments studying the relationship between waste removal performance and bioaugmentation rates at different influent loadings.

A similar modeling approach was performed for ammonia removal to compare three commonly used bioaugmentation schemes, i.e. ER-process, *in-situ* process, and parallel plant process. The simulation results concluded that the ER-process and *in-situ* process modifications can significantly improve treatment and both are better than using a parallel plant to produced acclimated biomass.

The monitoring strategies proposed in this dissertation are based on off-gas analysis, which is the best technique for measuring real-time oxygen transfer efficiency in process water. Field studies coupled with mathematical modeling demonstrated the value of real-time off-gas analyses to quantify diffuser cleaning schedules and flow equalization.

Finally the carbon dioxide transfer rate, measured by off-gas analysis with the oxygen transfer rate, can serve as a new index to estimate nitrification rate. This is possible because nitrification is autotrophic and the reaction by-products can be independently calculated. A structured model was developed and calibrated to study the observation. The validated model successfully simulated the nitrification performance and predicted the discharge of ammonia.

1. INTRODUCTION

The activated sludge process (ASP) is the most popular technique for municipal wastewater treatment. When properly operated, this process provides almost complete COD removal and up to 80% removal of the nitrogenous pollutants if nitrification/denitrification (NDN) is also used. The main challenges of using ASPs for modern and future wastewater management are to reduce the operation costs and guarantee the nutrient removal performance without significant and costly modifications of ASPs constructed during the previous 30 years. Many if not most of the ASPs constructed in the 1970s and 1980s are still in operation and were not designed to remove nutrients. The essential problem of reusing this existing wastewater treatment infrastructure is upgrading these plants at minimal cost (i.e. upgrading a “carbon-only” plant to NDN processes). This dissertation investigates two major techniques to improve ASPs: 1) using bioaugmentation to enhance the removal of “target pollutants” of special interest, such as a hazardous waste, pharmaceutical or ammonia (i.e., improving nitrification); and 2) improving/developing real-time monitoring strategies to reduce operation costs and improving the nitrification reliability.

Bioaugmentation is a proposed approach that can effectively improve removal of the target compound(s) in ASPs without significantly increasing the tank volume (Parker and Wanner, 2007). By dosing specific acclimated cultures into the main reactors, activated sludge processes can increase their removal of the target compound(s), or operate under

conditions that would otherwise be unfavorable (e.g., too low an MCRT or temperature). Based upon this concept, many bioaugmentation approaches with various plant configurations have been developed, but few studies have compared the benefits of different approaches. This dissertation compares several bioaugmentation approaches to enhance the removal of a selected aromatic hazardous waste and nitrogenous pollutants.

In aeration basins, oxygen transfer efficiency (OTE, %) is one of the most important growing factors to carefully maintain to provide a suitable habitat for microorganisms, especially for nitrifiers. Nitrification failure can easily occur if sufficient oxygen can not be supplied. Also aeration is the most energy intensive unit operation in ASPs.

Monitoring OTE in real-time can be useful to minimize power consumption or to reduce aeration costs by estimating diffuser fouling or flow equalization. Off-gas analysis is the process water OTE measurement with the highest accuracy and precision (ASCE, 1997), and it is the only technique that can determine OTE in real-time. A lightweight and inexpensive off-gas analyzer that can be routinely used in treatment plants will be beneficial to energy savings.

In addition, monitoring O_2 and CO_2 transfer in an off-gas analysis (proposed in this dissertation) may become a new method to estimate nitrification performance. The proposed method is based upon the differences in CO_2 production since the by-products of the treatment of carbonaceous and nitrogenous compounds are different. Although both reactions consume O_2 , consumption of carbonaceous substrate produce CO_2 but

nitrification does not. The molar fraction of CO₂ in the off-gas should be greater if nitrification is limited, or the ratio of nitrogenous compounds in total BOD is smaller. Goals of this dissertation are to investigate how activated sludge processes can be improved by bioaugmentation and off-gas monitoring. Mathematical models with Monod-type growth kinetics were used throughout the study to develop a theoretical understanding between bacteria activities and parameters of interests, such as gas transfer, aeration costs, and removal rates of pollutants. The dissertation contains four major thrusts, each presented in different chapters as independent papers and a general literature review in Chapter 2 which is applicable to all four major thrusts. The chapters are as briefly summarized in the following paragraphs.

Chapters 3 and 4 develop and apply models to evaluate the benefits of bioaugmentation. Three general bioaugmentation methods, shown schematically in Figure 1.1, are (a) parallel plant process, (b) enricher reactor (ER) process, and (c) *in-situ* process. Chapter 3 develops a model of the performance of hazardous wastes removal in bioaugmented ASPs. A simple model was developed based on the experimental data using ER process to treat a selected aromatic hazardous waste (1-naphthylamine, 1-NA), and after calibration the model was used to compare two different bioaugmentation approaches. Chapter 4 compares three bioaugmentation approaches to improve nitrification in wastewater treatment, based upon a similar model structure as presented in Chapter 3.

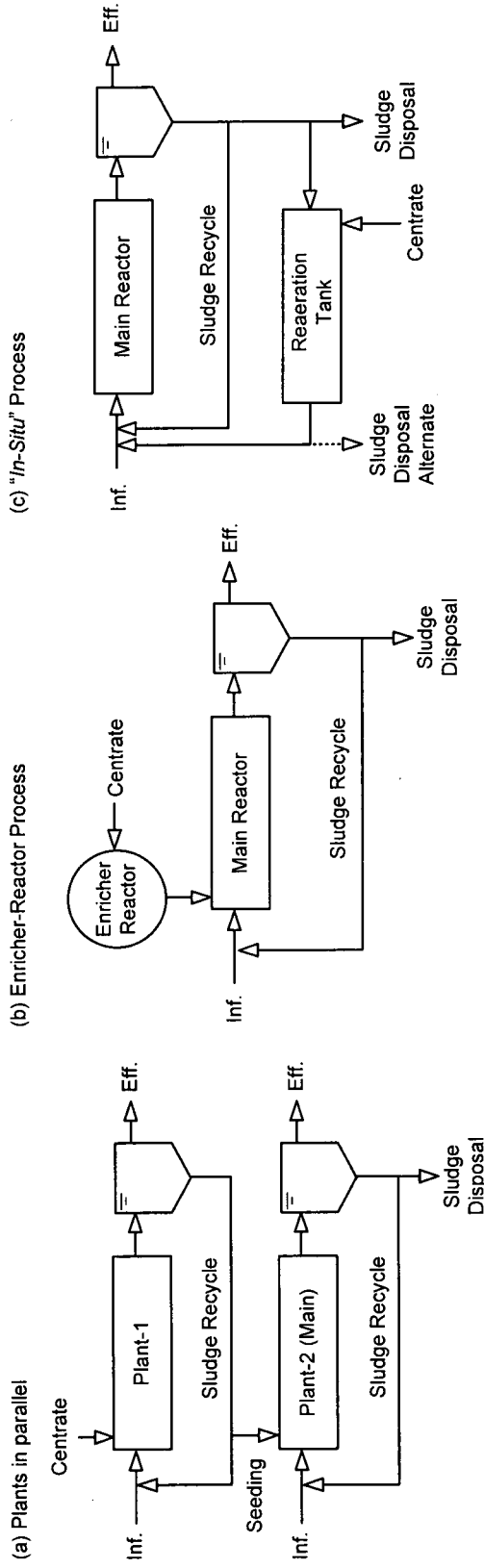


Figure 1.1 Concept schematic of three bioaugmentation processes: (a) parallel plants process, (b) off-line on-site process using enricher-reactor; and (c) on-line *in-situ* process with reaeration.

Chapter 5 demonstrates the benefits of real-time aeration efficiency monitoring and methodologies to reduce energy consumption and power costs. Figure 1.2 shows the application of off-gas analysis at typical treatment plant. A schematic diagram of an automated analyzer and two examples to optimize the operation of the tested treatment plant were also shown. Chapter 6 presents the potential of monitoring off-gas O_2/CO_2 to predict nitrification performance in ASPs. A structured model validated with long-term full-scale observations was used in the study. In the end, conclusions made to summarize the findings from all the studies were presented in Chapter 7.

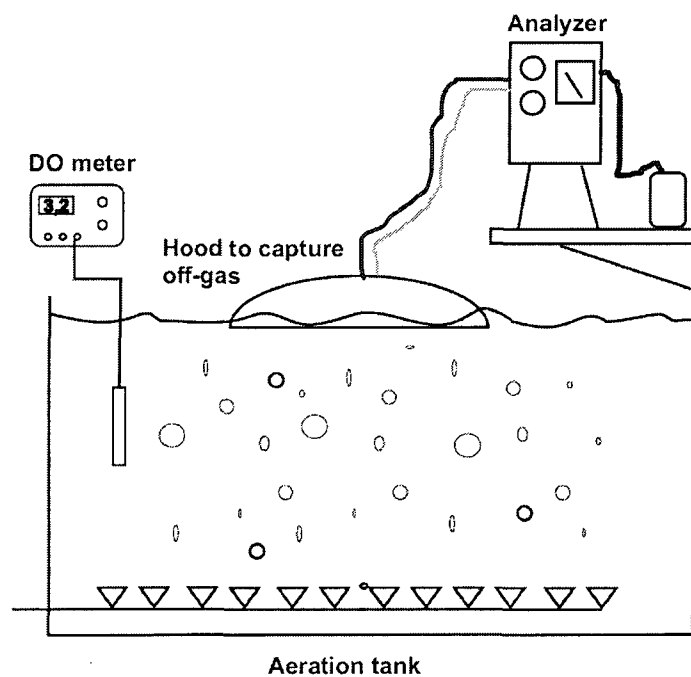


Figure 1.2 Setup and equipments of an off-gas test

2. LITERATURE REVIEW

2.1 Wastewater composition

The aeration tank of activated sludge process is a semi-controlled system. Three phases of the process water system should be considered: the liquid phase, biological phase, and the gas phase. To calculate treatment plant performance, the amount and composition of pollutants and products in different phases must be quantified. A schematic diagram of the components and the corresponding reactions are shown in Figure 2.1. Dissolved compounds include carbonaceous substrate, ammonia, oxygen, and reaction products. The organisms are described as sludge or biomass, and consists of both heterotrophic and nitrifying species. Among those components, substrate and bacteria cells are the most complex materials to be investigated.

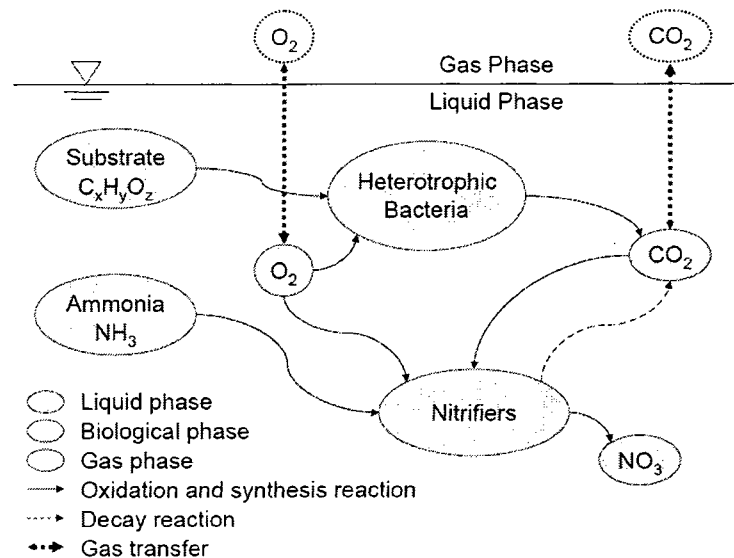


Figure 2.1 Reaction schematic of a nitrifying activated sludge process

The substrate consists of different types of carbonaceous organics. Depending on the properties of the organics, substrate can be defined by solubility (dissolved or suspended), oxygen demand (BOD, BOD₅, or COD), or biological reactivity (inert or biodegradable). The general composition of municipal wastewater with different strengths is shown in Table 2.1.

Table 2.1 Typical raw wastewater characteristics (adapted from WEF, 2005)

Contaminants	Concentration (mg/L)		Fraction (%)
	Low-strength	High-strength	
Total Solids	390	1230	100
Dissolved solids	270	860	69.2-69.9
Fixed	160	520	41.0-42.3
Volatile	110	340	27.6-28.2
Suspended solids	120	400	30.8-32.5
Fixed	25	85	6.4-6.9
Volatile	95	315	24.3-25.6
Settleable solids	5	20	1.3-1.6
Biological oxygen demand 5-d, 20°C (BOD ₅ , 20°C)	110	350	
Total organic carbon	80	260	
Chemical oxygen demand	250	800	
Total nitrogen as N	20	70	100
Organic nitrogen	8	25	35.7-40
Free ammonia	12	45	60-64.3
Nitrite	0	0	0
Nitrate	0	0	0
Total phosphorous as P	4	12	17.1-20

These materials have complex composition, and to facilitate the use of dynamic models, general, empirical formulas are frequently used to represent substrate and bacteria. For example, $C_5H_7NO_2$ is the general empirical formula for bacteria (Porges, 1955). Alternatives have been proposed by Gujer et al. (1999) who used $(C_4H_6O_2)_n$ and Pratt et al. (2003) who used acetic acids (CH_2O) as the formula of the rapidly biodegradable substrate. The stored organics are usually represented as poly- β -hydroxybutyrate (PHB), which is expressed as $(CH_{1.5}O_{0.5})$ (Majone et al., 1999).

2.2 Simulation models

2.2.1 ASP models

The general structure of modern ASP models are based upon mass conservation equations (Accumulation = Inflow – Outflow \pm Reaction) associated with Monod (1942) type reaction kinetics. Reactors are assumed to be complete-mix activated-sludge (CMAS), which is a single or a series of continuous stirred tank reactors (CSTR) and followed by a clarifier (Figure 2.2). In the reactors, bacteria consume soluble components such as dissolved oxygen, organic substrate, and ammonia on respiration and synthesis. The clarifier functions as a liquid-solid separator to remove the cells and to allow them to be recycled. To simplify the calculations, it is assumed the reactions occur only in the reactors.

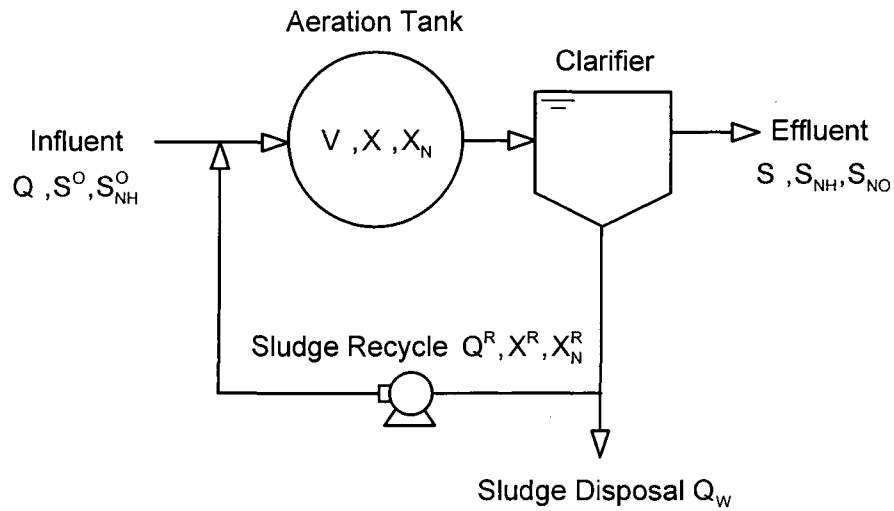


Figure 2.2 Schematic diagram of a CMAS process

The pollutants in wastewater can be soluble or particulate and are defined as substrates (S) while the microorganisms are particulate compounds (X). The Monod function describes the correlation between microbial production rate and substrate concentration; the biomass growth rate initially increases proportionally with increasing substrate concentration and then saturate at a maximum value. The net microbial production rate (r_g) including the Monod function and a first-order decay rate can be written as:

$$r_g = \frac{\mu_{max} \cdot X \cdot S}{(K_s + S)} - K_d \cdot X \quad 2.1$$

where μ_{max} = maximum biomass growth rate (1/day)

K_s = half-velocity coefficient (mg/L);

K_d = the biomass decay coefficient (1/day)

Depending on the reactor geometry and reaction processes, sets of ordinary differential equations (ODE) were developed to simulate the effluent conditions of pollutants, biomass, and/or other compounds in bioreactors.

2.2.1.1 Development of unstructured and structure models

The timeline of the development of ASP models is shown in Table 2.2. Based upon Monod kinetics, Pearson (1967) developed one of the earliest models of biological treatment process. The steady state consumption of single substrate with the production of one biomass was studied. Later, Lawrence and McCarty (1970) proposed their well-known application of this model; this strategy was soon widely used for designing and operating ASPs. Using this simple model, effluent concentrations of substrate and biomass can be both estimated by functions of mean cell retention time (MCRT).

However, since Monod kinetics are measured from steady-state experiments, they are limited when used to perform dynamic simulations with time-dependent variable inputs. For example, single Monod function can not explain the lag phase caused by mass transfer across cell membrane (Powell, 1967). In addition, an extremely rapid initial uptake rate of soluble substrate in bioreactors has long been observed, and applied in real-cases, i.e. the contact-stabilization process. Heukelekian et al. (1947) provided experimental evidence and indicated that the rapid uptake is not due to bacteria metabolism. He demonstrated using sterilized cells that rapid substrate uptake can still occur, showing that the uptake process must be related to adsorption.

To accurately simulate the time-dependent behavior of substrate uptake and bacteria activity, structured models were developed, which divides the treatment process into stages. Tench (1960) divided the activated sludge into three fractions: active and inert biomasses, and a stored fraction. Eckenfelder (1963) used first-order reaction kinetics to estimate the rapid substrate uptake rate. He suggested that the consumption of substrate can be caused by three microbial reactions: storage, growth, and endogenous respiration. Jaquart et al. (1973) used a similar structured model but applied different Monod functions to describe the rate of substrate storage and synthesis reaction. His concept has provided the essential foundation of modern, structured ASP models.

Although the basic ASP structured models have been known since the 1970s, numerical solutions of dynamic models could not be obtained until the widespread use of computers. Westberg (1967) proposed one of the earliest dynamic simulations for living and dead biomass. Andrews (1972) developed a dynamic model simulating the status of soluble substrate and particulate cells in single continuous flow stirred tank reactor (CFSTR). A computer program called CSMP/360 (Speckhart, and Green, 1976) was utilized to numerically solve the mass balance differential equations. In 1975, Bussy and Andrews further adapted the concept of the inert organics and storage mass in this dynamic model. They also improved the model to simulate the system with a series of CFSTRs followed by a clarifier. This change has significantly increased model application to simulate various process designs. Stenstrom and Andrews (1979) further applied the similar structure to develop computer base control strategies. Cliff and Andrews (1981)

continued the development of dynamic models. They separated the simulation of soluble and particulate substrate in the structure and used saturation factors to estimate the storage and entrap rates of soluble and particulate substrate.

In 1983, the International Association on Water Quality (IAWQ) established an international research group to develop general ASP models. In this group, Daigger and Grady (1982) reviewed and reevaluated the Monod kinetics in dynamic simulations. They investigated the storage and growth response of cells based upon former experimental results regarding to RNA fraction and enzyme activities, and they proposed a detailed conceptual model with sets of Monod functions. Dold and Marais (1986) defined the types of substrates in more detail and proposed a new concept of biomass decay. Instead of using the conventional method of endogenous respiration, they developed a death-generation structure to simulate the decay of active biomass. Henze et al. (1987) concluded all the studies and proposed their first general dynamic model for ASP, called Activated Sludge Model No.1, or ASM1.

Since developed, the ASM1 model has been widely applied in simulations of different types of field-scale wastewater treatment plants, i.e. high purity oxygen treatment plant, or HPO plant, (Yuan et al., 1993), nitrification/denitrification process (Gokcay et al., 2004), and sequential batch reactors, SBR, (Rönner-Holm et al., 2006). Calibrations and modifications have been made to improve simulation accuracy. After ASM1, two versions of new ASM models have been published. ASM2 and ASM2d (Henze et al.,

1995a and 1995b) adapted functions of phosphorus removal into ASM1. ASM3 (Gujer et al., 1999) improved the prediction of oxygen uptake and the lysis process of ASM1. A detailed comparison of Cliff-Andrew's model and ASM1 to ASM3 are presented in the following section.

2.2.1.2 Comparison of the modern ASP models

The structure of Cliff and Andrew's Model was shown in Figure 2.3, where the influent carbonaceous compounds, or substrates, were defined as soluble (S_s) that can pass through $4.5 \mu m$ membrane, or particulate (X_s) with larger size. Several processes were considered in this model that both soluble and particulate substrates can be uptake by bacteria. Soluble substrate is uptake and two reactions are processing simultaneously, either the substrate is utilized directly in synthesis reaction or stored in cells. The rate of storage is generally faster than direct synthesis. Particulate substrate can be also uptake (entrapped), stored, transfer, and utilized in synthesis reaction. The product of synthesis reaction is the active cells, or heterotrophic bacteria (X_{bh}), and the decay of the active cells produce carbon dioxide and inert organics (X_i). The stored mass (X_{sto}) is a carbon source for cell growth in the stages with no substrate introduced, for both aerobic and anoxic environment.

Table 2.2 Timeline of literatures developing the modern activated sludge models

Unstructured model		
Year	Author(s)	Contents
1942	Monod	First developed a mathematical function of the microbiological growth rate
1964	Downing et al.	Used Monod function to describe a steady-state nitrification process
1968	Pearson	Developed the basic steady-state single
1970	Lowerance and McCarty	substrate/biomass model
Structure model		
Year	Author(s)	Contents
1960	Tench	First divided biomass composition into three fractions: active mass, inert mass, and stored mass
1963	Eckenfelder	Described the rapid initial substrate storage, cell growth, and decay using 1 st order kinetics
1967	Powell	First described the lag phase of substrate transfer
1967	Siddiqi et al.	Defined the hydrolysis rate of particulate substrate
1967	Westberg	Dynamic simulation of living and dead bacteria
1973	Jacquart, Lefort, and Rovel	Applied Monod functions in storage and synthesis reactions
1973	Lijklema	Dynamic simulation of 1 st stage of nitrification
1974	Poduska	Investigate the two stage reaction kinetics of nitrification
1975	Bubsy and Andrews	Dynamic simulation of a series of reactors
1979	Stenstrom and Andrews	followed by a clarifier; concept of particulate
1981	Cliff and Andrews	components was adapted
1982	Daigger and Grady	Review the reaction kinetics of each stage of structure model
1986	Dold and Marais	Developed the death-generation
1987	Henze et al.	General Activated Sludge Model No.1 (ASM1)
1992	Tzeng and Stenstrom	Adapted and compare gas phase simulation in both
1993	Yuan and Stenstrom	modified ASM1 and Cliff-Andrew's Model of real case (HPO plant) result
1995	Henze et al.	General Activated Sludge Model No.2 (ASM2)
1999	Gujer et al.	General Activated Sludge Model No.3 (ASM3)
2000	Stensel and Horne	Evaluate denitrification kinetics based upon real case observation
2003	Muller et al.	Evaluate yield of heterotrophic bacteria in anoxic zone
2003	Wichern et al.	Applied ASM3 in six real case simulations
2004	Serralta	Adapted pH simulation in activated sludge model
2006	Iacopozzi et al.	Adapted two step nitrification in ASM3

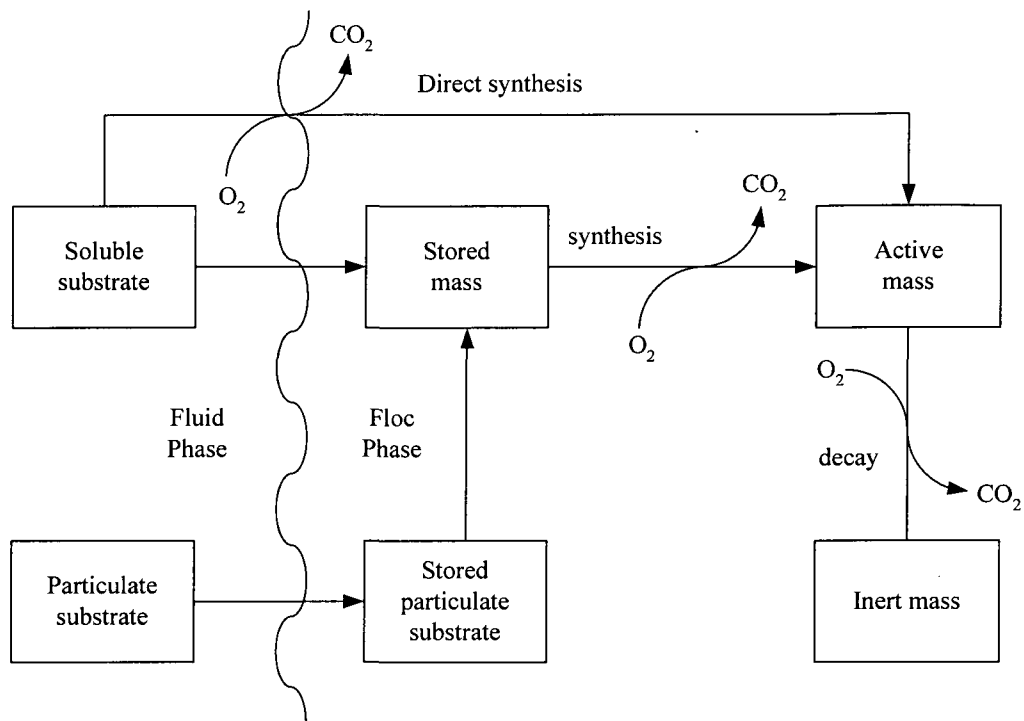


Figure 2.3 Flow diagrams of the Cliff and Andrews Activated Sludge Model

In ASM1, eight processes were considered to simulate the aerobic and anoxic growth and decay of heterotrophic and autotrophic bacteria. The flow diagram of ASM1 is shown in Figure 2.4, where the main difference between Cliff-Andrew's Model and ASM1 is the stored mass and the process of cell decay: in ASM1, all the rapidly biodegradable substrate, which similar to the soluble substrate in Cliff-Andrew's model, is used in synthesis reaction but not stored. A loop was used to describe the decay of heterotrophic bacteria, which a part of the decayed organics is re-uptake/entrapped and then hydrolysis as particulate substrate.

Yuan, et al. (1993) applied a modified ASM1 model and oxygen transfer theory to simulate the oxygen requirement of HPO processes. It was found that the simulation results performed better without the loop of death-generation process. ASM3 (Gujer et al., 1999) is an upgraded/modified version of ASM1 published in 1995. As shown in the flow diagram (Figure 2.5), the loop of decay reaction is taken and the decayed active mass is not recycled to be entrapped substrate. A stage of stored biomass between readily reacted substrate and active mass is also adapted. Two Monod functions and yields are applied to describe the storage and synthesis reactions. The process of uptake/storage reacts faster and with higher yield, preserving the carbon source for aerobic growth and denitrification. The same structure is also used for anoxic zone, with only the differences on electron acceptor and growth kinetics.

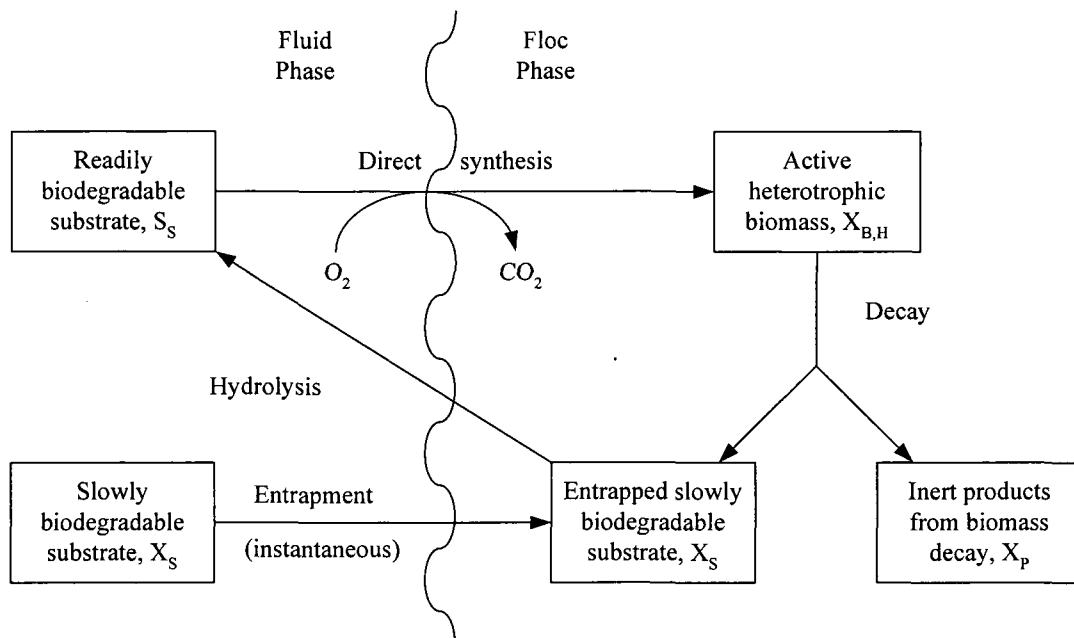


Figure 2.4 Flow diagram of the IAWQ Activated Sludge Model No.1

In ASM3, the reaction process from substrate uptake to cell growth is described by a two-step reaction, which the soluble substrate must be stored first and then utilized in synthesis reaction. However, several studies have shown that the storage of substrate and the growth of cells are processing simultaneously, if influent substrate can be continuously introduced (van Aalst – van Leeuwen et al., 1997; Krishna and van Loosdrecht, 1999; Beun et al., 2000). It was also proposed that structure models with separated pathways, i.e. the direct synthesis and storage reaction, may provide better solution simulating the substrate consumption behavior (van Aalst – van Leeuwen et al., 1997).

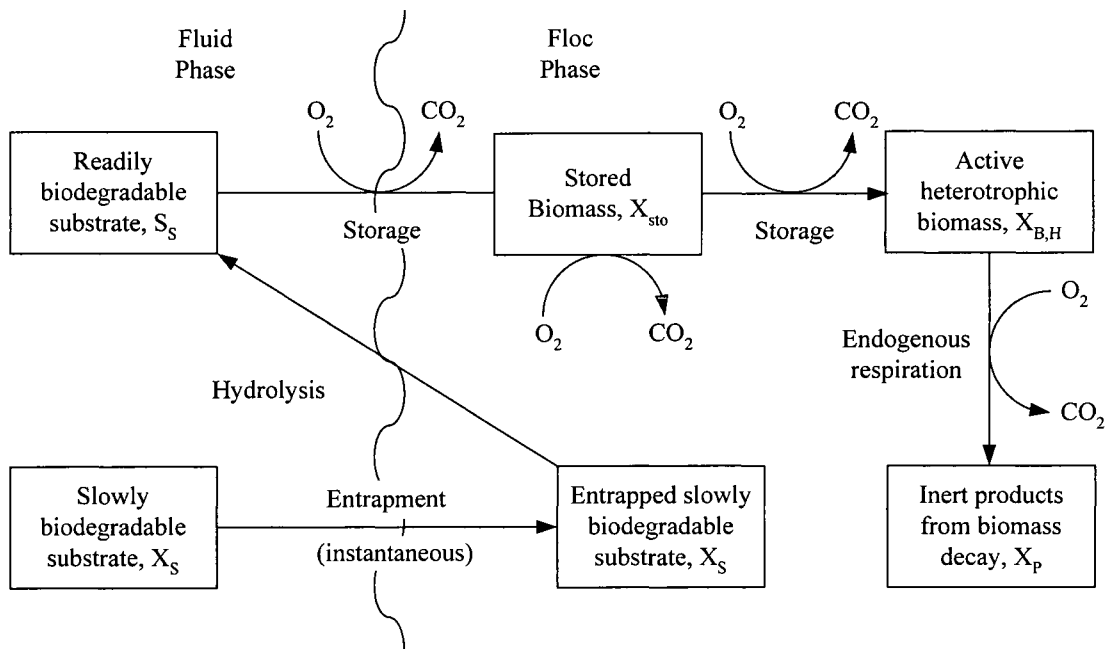


Figure 2.5 Flow diagram of the IAWQ Activated Sludge Model No.3

2.2.1.2 Parameters and model calibration of ASM models

As shown in equation 2.1, the net growth kinetics of bacteria including a Monod function contains three parameters, the maximum cell growth rate ($\hat{\mu}_S$), the half-velocity coefficient (K_s), and the decay rate (K_d). In addition to those factors, a yield coefficient (Y) is used to describe the fraction substrate transforming to biomass. Since introduced, this type of expression has been widely used in simulations of different processes of ASP, such as the growth of heterotrophic bacteria under aerobic and anoxic condition (denitrification), and Nitrifiers. Depending on bacteria species, substrate and nutrient concentration, operation conditions, and other factors, various parameters are required.

The reference values of kinetics, stoichiometry parameters and the corresponding literatures are listed in Table 2.3. Most parameters were obtained from batch experiments with single substrate and culture. Sherrard et al. (1970) started to apply separate carbon sources to test the growth kinetics of heterotrophic bacteria. Poduska et al. (1975) tested the rates of two-step nitrification for autotrophic nitrifiers, i.e. *Nitrosomonas* and *Nitrobacters*. For structure models, coefficients are more specific and may not be simply accessed by direct measurements, e.g. the yield and reaction kinetics of substrate to stored/active mass, and stored mass to active mass. Koch et al. (2000) used acetate as substrate to feed the sludge samples from wastewater treatment plants to calibrate ASM3. A new set of parameters was applied in full-scale simulations, and Wichern (2003) confirmed Koch's adjustments via simulations of six wastewater treatment plants.

Table 2.3 Reference values of Monod parameters

		Carbonaceous				
Wastewater type	Reaction	μ_{max} 1/day	K_s mg/L	K_d 1/day	Y	Reference
Skim milk		2.448	100	0.045	0.48	Gram
Glucose		1.26	355	0.087	0.42	Stack et al.
Domestic	Growth of heterotrophic bacteria	3.752	22	0.07	0.67	Benedex et al.
		3-13.2	5-40	0.06-0.2	0.4	M&E
		6	20	0.12	0.4	
		3.2	60	0.09	0.4	Sherrard
Municipal		0.6-13.2	5-22.5	0.05-1.6	0.57	ASM1
		6	20	0.62	0.67	
	Storage	5	2	0.2	0.85	ASM3
	Growth	2	1	0.2	0.63	
	Storage	12	10	0.3	0.80	Koch et al.
	Growth	3	0.1	0.3	0.80	
		Nitrification				
Wastewater type	Reaction	μ_{max} 1/day	K_n mg/L	K_d 1/day	Y	Reference
Municipal	Nitrification	0.2-0.9	0.5-1	0.05-0.15	0.13	
		0.75	0.74	0.08	0.12	M&E
		1.0	1	0.15	0.24	ASM3
River water	Nitrosomonas	0.9-1.7	0.9-1.9	0.2	0.24	Koch et al.
		0.26-0.61	2.8-3.6	0.050	0.29	Stratton and McCarty
		0.33-0.57	0.3-1.1	0.050	0.08	
ASP	Nitrosomonas	1.08	0.063	0.12	0.05	Poduska
	Nitrobacters	1.44	0.74	0.04	0.12	
Thamesestuary water	Nitrosomonas	0.33	1	-	0.05	Downing et al.
		0.14	2.1	-	0.02	
		0.65-1.5	0.6-1.7	-	0.05	Knowles et al.
	Nitrobacters	0.83-2	1.9-4.7	-	0.05	

2.2.2 Gas transfer model

2.2.2.1 General theory

The modern gas transfer model simulating wastewater aeration is based on the two film theory proposed by Lewis and Whitman in 1924. In this model, the adsorption or stripping of gas molecular is estimated by the diffusion across two stagnant films on the gas/liquid interface, which can be expressed as:

$$\frac{dC}{dt} = K_L a \times (C_{\infty}^* - C) \quad 2.2$$

where $K_L a$ = volumetric mass transfer coefficient

C_{∞}^* = saturated dissolved oxygen concentration

C = effective average DO concentration in the liquid phase

The overall mass transfer coefficient $K_L a$ is a combination of two factors: “ K_L ” represents the resistance of molecular diffusion across the gas/liquid boundary and “ a ” is the effective specific surface area. In real cases, $K_L a$ and C_{∞}^* are functions of different process conditions. For example, K_L could be affected by the change of temperature, bubble size, and the maturity of the stagnant film between liquid and gas phase (Hwang and Stenstrom, 1985, Libra, 1993); different C_{∞}^* may be observed at different depths of the aeration tank. Based upon Henry’s Law, the capacity of saturated dissolved oxygen in water is proportional to its partial pressure in the air bubbles under the same water depth (Stenstrom, 1979). However, for low-solubility gases such as oxygen, the two parameters are generally considered as constants to simplify the calculation. Depending on operation

strategies and aeration devices, significant difference can be observed and estimating K_La and C_{∞}^* from the aeration devices of different plants is necessary.

Based upon oxygen transfer theory, clean water non-steady state testing is one of the most essential methods to estimate these two coefficients. In this test, a part of the aeration system and DO sensor are set up in a small batch reactor. By physical or chemical method, the DO can be stripped; then, K_La can be calculated from measuring DO recovery rate and the coefficient C_{∞}^* , which can be applied from references or the steady state DO concentration measurement (ASCE, 1993).

Furthermore, to correctly estimate transfer in a treatment process, the “clean water” test results must be converted to “wastewater” or process rates by conversion factors.

Converting for the effects of temperature DO concentration, barometric pressure and ionic strength are straight forward. Accounting for the effects of surface active agents in the process is usually difficult. Hwang and Stenstrom (1985) reported that several variables may significantly influence the alpha factor, which accounts for the effect of contaminants on K_L and a . The overall process rate depends on air flow rate, liquid depth, tank geometry, and water quality. Another strategy is to conduct a process water test, which uses process water is a full scale evaluation. However, since it is difficult to measure the oxygen uptake rate from a real treatment process, and because the process must exist in order for it to be tested, process water testing is generally not used for treatment plant design or real-time estimation of treatment performance.

2.2.2.2 Conversion gas transfer coefficient among gases

To estimate the gas transfer coefficient $K_L a$ of other gases, for example carbon dioxide or nitrogen, the surface renewal theory which proposed by Dankwertz (1951) is used. This theory is applicable to a surface that is renewed continuously (no stagnant films).

Therefore, the K_L of a gas can be expressed as:

$$K_L = \sqrt{D \cdot rc} \quad 2.3$$

where D = diffusion coefficient

rc = surface renewal rate

If the value rc in one reactor is a constant, this term can be canceled out by combining two surface renewal equations of oxygen and carbon dioxide. Thus, transfer coefficient can be estimated from:

$$K_L a_{CO_2} = K_L a \sqrt{\frac{D_{CO_2}}{D_{O_2}}} \quad 2.4$$

Therefore, if the oxygen transfer coefficient is known, the transfer rates of other gases, such as CO_2 and N_2 can be estimated. If the system is less turbulent, the correlation between transfer rates varies from the square root of the diffusivity ratios, and ranges from 0.5 to 1.0. Hsieh et al (1993a, b) discusses this relationship in greater detail.

2.2.2.3 CO₂ transfer and pH simulation

Simulation of carbon dioxide transfer is more complex than oxygen. Because carbon dioxide has higher solubility in water, the saturated concentration C_{∞}^* of CO₂ can not be simply assumed as a constant as oxygen; it must be calculated via a function of Henry's constant and partial pressure:

$$DCD_{\infty}^*(t) = H_{CO_2} \cdot pCO_2(t) \quad 2.5$$

where H_{CO_2} = Henry's constant of carbon dioxide

$pCO_2(t)$ = partial pressure of carbon dioxide in head space

In addition, equilibrium of dissolved carbon dioxide serves an important role buffering the change of pH. Since the distribution of dissolved carbon dioxide (H₂CO₃) and bicarbonate (HCO₃⁻) varies with pHs, the solubility of CO₂ therefore changes with pH. Under the normal conditions, the concentration of dissolved CO₂ is generally oversaturated, which means the total dissolved CO₂ is higher than the value calculated from Henry's law. As shown in Figure 2.7, when pH is around 7 and temperature at 20°C, the majority portion of the total dissolved CO₂ is of the format of HCO₃⁻, and the fraction associated with CO₂ stripping i.e. the fraction of H₂CO₃* is only around 18 %; and this value is even lower when temperature rises.

Frahm et al. (2002) estimated processing status for lab-scale bioreactors. He compared the carbon dioxide production rate (CPR) and transfer rate (CTR) of mammalian cell culture via CO₂ measurement and pH test results. Designed ionic strength water was used

with equilibrium equations to calculate the buffering effect of NaHCO_3 . Significant difference between CPR and CTR was found and he suggested that the reduction rate of dissolved CO_2 according to buffer effect can be directly expressed as:

$$\dot{n}_{\text{CO}_2, \text{buffer}} = - \frac{\partial n_{\text{HCO}_3^-}}{\partial t} \quad 2.6$$

where $n_{\text{HCO}_3^-}$ = concentration of HCO_3^-

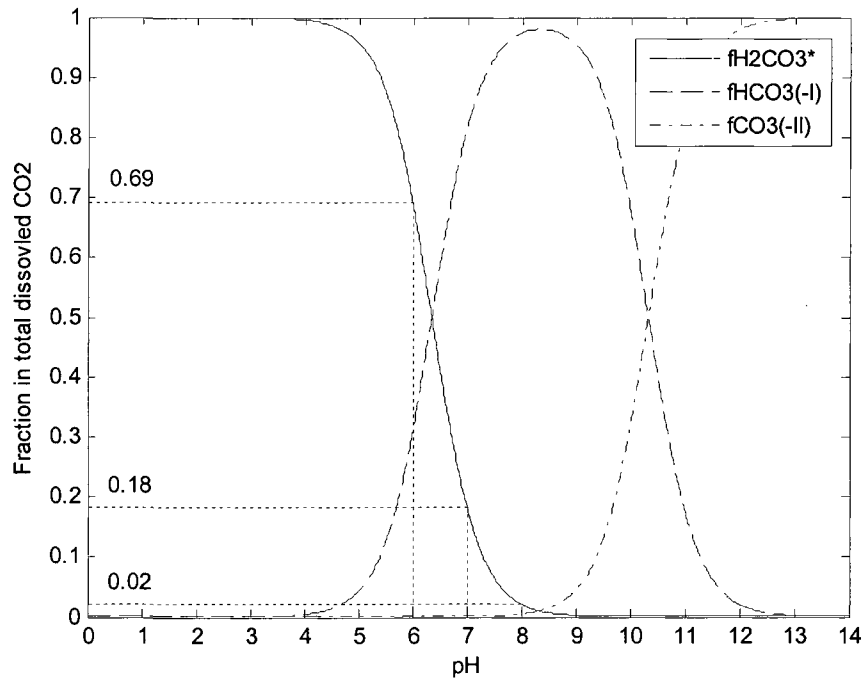


Figure 2.7 Equilibrium of carbonate system versus pH

For operation purpose, the effect of changing pH in ASP also must be carefully monitored. Grunditz and Dalhammar et al. (2001) investigated the pure culture behavior of the two main nitrifying bacteria groups at different pH. They suggested that pH in the tank should be maintained between 7 and 9, which conforms to well-known experimental observations (Painter, 1970). Therefore, simulating pH change in the ASP is desirable.

Carbon dioxide analysis associated with pH simulation has been applied in several studies. Unlike the substrates and microorganisms, pH can not be calculated from mass balance equation. To calculate pH, an alkalinity balance must be used. In ASM1 (Henze, 1987), alkalinity was calculated from the charge balance equation. This estimation is inconvenient since the charge balance can only be applied when all the ion concentrations, including organics and metals, can be measured.

To solve this problem, Serralta (2004) developed a different pH model based on different concept. This model was extended from ASM2d and the alkalinity was basically calculated from proton balance. Consequently, the input data for this simulation were reduced to only the influent pH and carbonate alkalinity, which are much easier to collect from treatment plants. This approach has been applied in simulating the treatment performance of high purity oxygen (HPO) activated sludge process (Stenstrom, 1989, and Tzeng, 2003). In their simulations, the alkalinity (Z) was first calculated by the charge balance of several ions as:

$$Z = -[H^+] + [OH^-] + [HCO_3^-] + 2[CO_3^{2-}] + [NH_3] \quad 2.7$$

Then the pH value was calculated from the quadratic function consists of alkalinity and the molar concentration of ammonia and carbon dioxide as equation 2.7.

$$[H^+]^2 + [H^+] \cdot [Z - [NH_{3(aq)}]] - K_w - \left(K_1 + \frac{2K_1K_2}{[H^+]} \right) \cdot [H_2CO_3^*] = 0 \quad 2.8$$

where K_w = ion product for water

K_1 and K_2 = first and second Keq's for carbon dioxide

$NH_{3(aq)}$ = deprotonated ammonia concentration (mole NH_3 -N/ L^3)

$[H_2CO_3^*]$ = dissolved CO_2 concentration
 $= (CO_{2(aq)})_T - [HCO_3^-] - [CO_3^{2-}]$

Finally, the CO_2 stripping rate was simulated based upon the gas transfer equation and the part of dissolved CO_2

$$\frac{dDCD}{dt} = K_L a \cdot (DCD_{\infty}^* - DCD \cdot f_{CO_2}) \quad 2.9$$

$$\text{where } f_{CO_2} = \frac{[H_2CO_3]}{[H_2CO_2] + [HCO_3^-] + [CO_3^{2-}]}$$

= molar fraction of H_2CO_3 in total dissolved CO_2

2.3 Introduction to off-gas test

In recent years, fine-pore diffusers have been used to reduce energy consumption and provide higher oxygen transfer rates for municipal wastewater treatment. Unfortunately, those diffusers suffer from fouling or scaling problems, and the lifetime of diffusers is hard to estimate. Diffusers made from both ceramic and synthetic membranes are susceptible to fouling. Fouled diffusers suffer a significant drop in OTE. If this situation is not corrected in a short period, greater air flow rate, which represents more energy and operation costs, will be required, eliminating the benefits of fine-pore diffusers. To avoid this problem, better OTE analysis methods have been developed, which can provide real-time data. Several major strategies for estimating OTE have been applied, which are the clean water test, various process water tests, material balance methods, and the

off-gas test. Among these tests, the off-gas test has the benefits of accuracy and requires a short test interval.

The basic concept of off-gas test is to estimate the oxygen consumption from comparing the gas composition in the supplied air and the off-gas. Because the information of off-gas is directly gathered from the processing aeration systems, errors from conversion and estimation can be avoided, and real-time data can be also obtained. The modern off-gas analysis was developed by Redmon et al. (1983) under the sponsorship of EPA and ASCE of U.S. In the analysis process, off-gas collected from a floating hood (see Figure 1.2) on the surface of aeration basin is treated to remove CO₂ and water vapor, and the oxygen partial pressure is measured by an oxygen analyzer. The percentage of oxygen transferred to the process water is:

$$\text{OTE}(\%) = \frac{P_{O_2,IN} - P_{O_2,OUT}}{P_{O_2,IN}} \quad 2.10$$

where p_i = partial pressure of oxygen in the gas stream.

The OTE can be normalized to standard conditions (20°C, 0 mg_{DO}/l, 1 atm, no salinity) to obtain a standard OTE, or SOTE (%) (ASCE, 1984, 1991). In addition, off-gas analyzers also measure the air flow rate passing through the hood. By weighting the area of hood and tank surface, the air flux of the aeration system can be estimated, and oxygen transfer rate (OTR) can be calculated from OTE multiplies by air flow rate.

Hence, based upon OTR measurement and DO, the gas transfer coefficient under process condition ($\alpha K_L a$) can be calculated as:

$$\alpha K_L a = \frac{\text{OTR}}{V \cdot (C_\infty^* - C)} \quad 2.11$$

where V = the volume of aeration tank,

α = ratio of gas transfer coefficient of process water to clean water conditions

Oxygen uptake rate (OUR) is the rate of dissolved oxygen used by microorganisms (M&E, 2002). This factor is generally expressed as mass COD concentration per unit of time (ie. mg/L/hour) and is frequently used in estimating bacteria activity. The OUR from the phase of microbial activity can be expressed as:

$$\text{OUR} = -r_{su} - 1.42 \cdot r_g \quad 2.12$$

where r_{su} is substrate utilization rate; 1.42 is the COD of cell tissue, (mass bsCOD/mass VSS), and r_g is the cell growth rate.

In process water, the oxygen transfer rate across the gas/liquid boundary is not as rapid as the rate dissolved oxygen is utilized. In other word, OUR is limited by the unit volume of OTR. In off-gas test, OUR of the water column covered by hood can be estimated based upon the OTR measured.

The off-gas test is an important analysis method for estimating total oxygen transfer efficiency because of its accuracy and efficiency. Libra (2002) applied this method to compare the performance of several different aeration devices. Krause (2003) used both unsteady-state clean water test and off-gas test to estimate the treatment efficiency of full-scale membrane bioreactors. Furthermore, off-gas analysis has been shown as an appropriate analysis strategy for estimating reactions in small-scale ASP processes.

2.4 Application of off-gas test and gas phase simulation in ASP models

One of the most important aspects to evaluate the structure models is the estimation of the bioreactivity of substrate. Conventional strategy that divide the substrate by $0.45 \mu\text{m}$ membrane has limitation to describe the reactivity of influent substrate. Since both the soluble and particulate substrate are either entrapped or stored in cells, and a certain portion of particulate substrate must be converted to stored mass, to simplify the model structure it could be more convenient to directly estimate the amount of bioreactable substrate instead of defining the substrate by solubility. Koch (2000) proposed that inconsistency to heterotrophic yields could occur if using solubility to define substrate; because batch experiments generally estimate the reaction kinetics of single substrate, and this substrate should not only represent the 'soluble' part of total substrate in wastewater. The most general strategies to evaluate the fraction of rapidly bioreactable substrate in wastewater are by measuring respirometry or the oxygen uptake rate (OUR) (Vanrolleghem et al., 1999), which are easily measured by sensors and/or off-gas test, respectively.

Nevertheless, information with only the respirometry or OUR may be still not adequate to describe the fraction oxygen uptake is used in storage, growth, or endogenous respiration; hence the composition of sludge can not be verified (van Loosdrecht and Heijnen, 2002). Conventional method to quantify the fraction of stored mass in sludge uses lab-scale experiments to directly measure the amount of the stored polymer, or PHB, in microorganisms. This off-line method is labor intensive and usually can not provide the real-time information (Beun et al., 2000). Pratt et al. (2004) combined the carbon dioxide estimation to an ASP model and suggested it can be a new strategy to dynamically estimate the storage process.

In combination with pH analysis, Pratt et al (2003) developed a new method, online titrimetric and off-gas analysis (TOGS), to estimate not only substrate consumption but also nitrification for a batch reactor. This method measures the respirometric-titrimetric signal of ASP systems; the respirometric measurements provide the information of OUR, and the titrimetric results describes the status of buffer effect of process water. In Pratt's study, designed influent wastewater and sample sludge was used in batch reactors; and hydrogen ion production rate (HPR) was measured to estimate the carbon dioxide production rate (CPR). Gernaey et al. (2002a, b) studied the relationship of HPR to each specific process, i.e. the consumption of carbonaceous substrate (if the substrate is an organic acid), the removal of ammonia (from cell uptake and/or nitrification), and CO₂ related production/transfer.

In Gernaey's paper, the calculation of HPR based upon explicit pH data was expressed as:

$$HPR = \frac{m}{x} r_{CH_4O_2} - pr_{NH_3} + n(r_{CO_2} - CTR) \quad 2.13$$

where m, p, n = factor of target components calculated from pH and equilibrium coefficients

$r_{CH_4O_2}, r_{NH_3}$ = reaction rate of product or reactors

CTR = rate of CO_2 transfer across gas/liquid interface

In addition to nitrification and storage process, the strategy of monitoring HPR has also been used to estimate many other processes related to pH change; for example denitrification (Bogaert et al., 1997) and enhanced phosphorous removal (Zeng et al., 2003).

3. BIOAUGMENTATION TO REMOVE HAZARDOUS POLLUTANTS

3.1 Introduction

Bioaugmentation is a method to improve nutrient removal or to enhance the removal of hazardous wastes in activated sludge (AS) processes (Babcock et al., 1993; Parker and Wanner, 2007) and in fixed-film processes (Ro, et al., 1997). Bioaugmentation processes can be classified into three main schemes: 1) adding enriched cultures from “off-site” sources; 2) adding cells produced from an “on-site” reactor, or 3) growing additional biomass *in-situ* with the ordinary biomass, using special reactor geometry. Among these methods, the external or first type bioaugmentation is challenging because the enriched cultures can lose activity when introduced into the process, or may require acclimation to the new process conditions (i.e. different mean cell retention time (MCRT), DO, low substrate supply, or predation). Also the required cell mass for effective bioaugmentation may be too high to affordably acquire from an off-site facility. Babcock et al. (1993) reviewed the difficulties of off-site bioaugmentation for hazardous waste. Rittmann et al. (1996) and Lee (1997) have simulated the high biomass requirements for bioaugmented nitrification, and Head and Oleszkiewicz (2004) have demonstrated the requirements in lab-scale experiments. This chapter considers on-site bioaugmentation and *in-situ* methods since off-site bioaugmentation appears impracticable.

The benefit of the on-site strategy, such as the enricher-reactor (ER), is the ability to grow the enriched cultures at the treatment plant, where they can be quickly produced and

supplied intermittently or continuously, as needed. The ER process has been described previously (Stenstrom et. al., 1989; Cardinal and Stenstrom, 1992; Babcock et. al., 1992; Babcock and Stenstrom, 1993). Figure 3.1 (a) shows the proposed process configuration whereby existing AS systems can be upgraded to treat hazardous wastes that are unavoidably introduced to the wastewater, or to accept additional wastes that would have been unacceptable without bioaugmentation. The ER process allows the existing AS infrastructure to be utilized in the increased capacity of efficient treatment of hazardous wastewaters with reduced possibility of impairing normal operation.

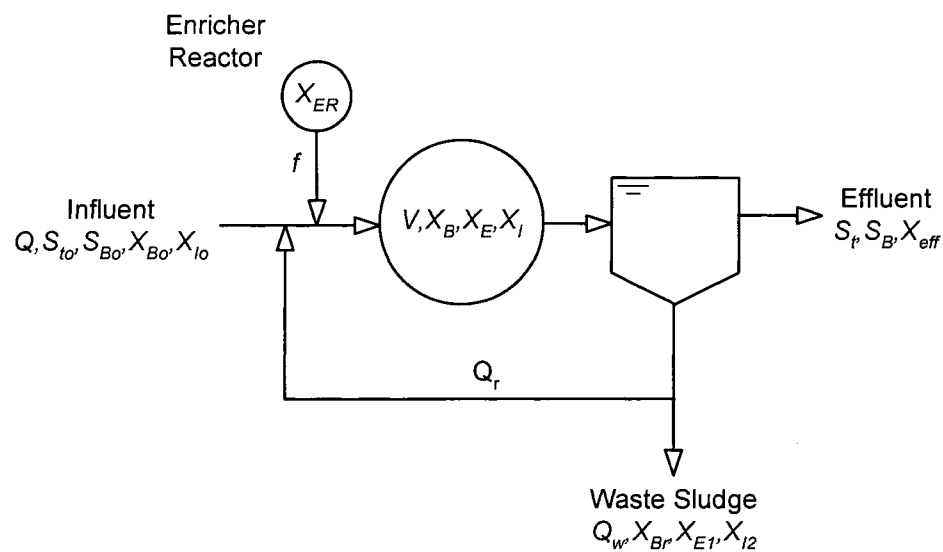


Figure 3.1 (a) Concept schematic of the on-site bioaugmentation process using enricher-reactor

Figure 3.1 (b) shows an example of the on-line, or *in-situ*, bioaugmentation method. This type of processes was originally developed to improve nutrient removal (Bogusch, 1987), and has been successfully applied in full-scale wastewater treatment plants to improve

nitrification (Krhutkova et al., 2005). The key element of this method is that a culture that is capable of degrading the target compounds is grown in a reactor that becomes an integral part of the activated sludge process through the additional of recycled activated sludge. The recycled sludge reactor can be fed with high strength wastewater, e.g. digester supernatant high in ammonia concentration, and re-introduced into the main reactor. The loss in bacteria activity using this method is considered low, due to the similar environment with the main process (Parker and Wanner, 2007).

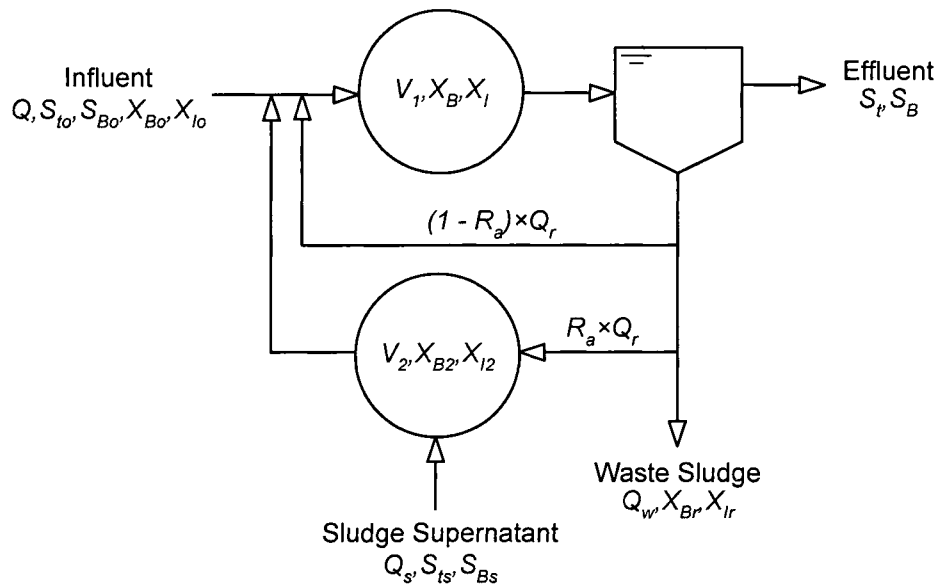


Figure 3.1 (b) Concept schematic of the on-line *in-situ* bioaugmentation process with re-aeration.

The ER process culture can be maintained on either high concentrations of the hazardous target compound (Babcock et. al., 1992), or in the total absence of the target compound using structurally similar or suspected degradation metabolite compounds (Babcock and Stenstrom, 1993). Advantages include the maintenance of acclimation during the

absence of the target compound, greater ability to tolerate shock loads without break-through to the effluent, and the ability to degrade structurally similar compounds without prior acclimation. Improvement in steady state removal efficiency also occurs but this benefit is less dramatic than other benefits.

To better understand the mechanisms involved and the relationships between observation and theory, modeling work was initiated with two goals: The first goal was to examine whether kinetic simulations could accurately predict the experimentally observed dynamic response of complete-mix activated-sludge (CMAS) processes during shock loading and reacclimation periods. CMAS processes are applications of continuous-flow stirred-tank reactors (CFSTR) with biosolids recycle. Degradation kinetics of bioaugmentation cultures following inoculation into CMAS are difficult to directly measure, whereas a simulation model can be useful to explain the underlying kinetic behavior. The second goal was to examine and compare the benefits that might be obtained using the ER and *in-situ* processes. Based upon the validated model, 1-NA degradation was simulated in an *in-situ* reaeration method.

To achieve the goals with a manageable simulation model, we assumed the existence of three populations of organisms: indigenous cells which obtain the ability to degrade the target compound; exogenous cells from the enricher-reactor which have been acclimated to degrade the target compound, and non-1-NA degrading cells which grow only on rapidly degradable COD (bulk substrate) but not the target compound. The dynamic

model incorporated mass balances for each group of microorganisms and each type of substrate. The response of bioaugmented CMAS to transient loadings of the hazardous target-compound (shock loads and changes in influent concentrations) were simulated using the dynamic model and compared to experimental results. The model was calibrated by minimizing the least square error between model data and the observed data from bench-scale experiments. The calibrated model was then used to investigate the dynamics of both the ER and *in-situ* processes.

3.2 Experimental Methods

The model hazardous waste used here consisted of a carcinogenic, amino-substituted polyaromatic hydrocarbon: 1-naphthylamine (1-NA). This compound was noted to be generally resistant to biodegradation (Pitter, 1976) and inhibitory to nitrifying organisms (Hockenbury and Grady, 1977), mutagenic in the Ames assay (McCann et. al., 1975), associated with human bladder cancer (Scott, 1962), and regulated as a carcinogen by OSHA (Federal Register, 1974). 1-Naphthylamine is an intermediate in the manufacture of approximately 150 organic azo-type coloring dyes in current use (Colour Index, 2007), and is probably a trace component of many petrochemical-product manufacturing waste streams (Staff, 1974). It was selected for study because of its industrial importance and the difficulty in eliminating it from use, as might be possible with other hazardous compounds, such as a specific pesticide.

Materials (chemicals and media), setup of AS reactor (SBRs and CMASs), analytical

methods, enrichment techniques, and bioaugmentation procedures have been described in detail previously (Babcock et. al. 1992; Babcock and Stenstrom, 1993, Babcock et al., 1993). Here we briefly describe conditions under which new experiments were conducted and results quantified to acquire the data collected for model calibration and validation.

An AS enrichment culture was developed over a period of 9 months which was then able to rapidly degrade 1-NA as a secondary substrate. Monod-type kinetic parameters of 1-NA degradation were determined, non-biological removal mechanisms were quantified, and mineralization (conversion of 1-NA to CO₂ when present as the sole carbon source) was demonstrated (Babcock et. al., 1993). The enrichment culture was developed and maintained in sequencing-batch reactors (SBRs) where they were exposed to the target compound as well as selective pressures similar to the CMAS (i.e., ability to flocculate and settle well). The enrichment culture was used to bioaugment the main reactors by daily wasting cells from the SBRs to the main reactors.

The ERs were initially seeded with an inoculum from a large municipal wastewater treatment plant which also receives pretreated industrial wastewaters, and an inoculum from a west-coast petroleum refinery activated sludge process. The reactors were operated for five months before they developed significant 1-NA removal, and eventually it was demonstrated that the enrichment culture could use 1-NA as a sole carbon source (Babcock et al., 1993). The laboratory setup of experiments is shown in Figure 3.2. Five

bioaugmented CMAS along with two controls were operated continuously for 12 months (steady-state) prior to their use in these experiments. The unacclimated control was not exposed to 1-NA and did not receive bioaugmentation. The acclimated control was continuously exposed to 1-NA but received no bioaugmentation. The unacclimated CMAS represented the worst-case existing treatment system where the least removal of 1-NA would be expected. The acclimated CMAS represented the best-case conventional system without bioaugmentation. The other CMAS received various daily bioaugmentation doses, and bioaugmentation level was defined as the mass percent of exogenous biomass added per unit mass of non-1-NA degrading biomass (mg exogenous cells per mg MLVSS). Five different bioaugmentation levels: 1%, 2%, 4%, 8%, and 16% were used.

Table 3.1 lists common operating characteristics of the CMAS and SBRs. The nominal 8.9-d CMAS MCRT was controlled by daily removal of 1.37 L of mixed liquor. Immediately following sludge wastage, the required bioaugmentation inoculation was added to the aeration zone. Bioaugmentation inoculum consisted of aerated mixed liquor from the SBRs which was removed just prior to the end of the aeration cycle when the concentration of the target compound (1-NA) had been depleted below the detection limit. Cells used for inoculum were allowed to settle for 0.5 hr in graduated cylinders after which the supernatant was decanted and settled sludge added to the proper CMAS. Additional cells were also removed as necessary to maintain the SBR at 7-d MCRT.

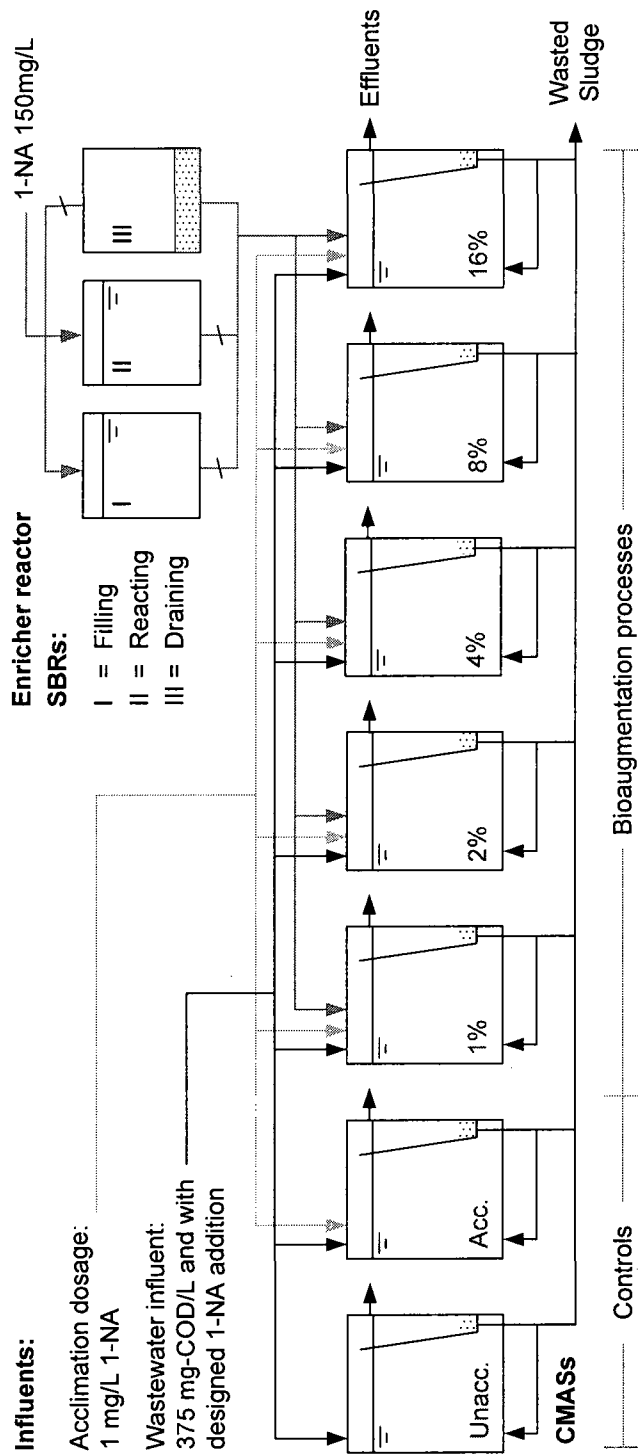


Figure 3.2 Laboratory setup of bioaugmentation experiments. Bioaugmentation level is defined as unit mass enriched culture added per unit mass of bulk biomass in a control reactor.

Table 3.1 Operational characteristics of laboratory reactors

Parameter	Main reactor (CMAS)	Enricher-reactor (SBR)
Volume	12.2 Liter aeration zone 1.5 Liter clarifier	5.0 Liter
HRT	0.458 day (Q = 26.64 L/day)	22 hr aeration 1.0 hr settle 0.5 hr drain 0.5 hr fill
MCRT	8.9 day	7 day
MLVSS	1588-3008 mg/L	2000-4000 mg/L (3415 average)
Loading Rate	810 mg COD/L day	760 mg COD/L day
1-NA Influent	1.0 mg/L	150 mg/L
Aeration Rate	7.1 L/min	2.4 L/min
DO	7.9 mg/L	1-4 mg/L
pH	6.5-7.5	6-7
Temperature	13-23°C	18-30°C

Two experimental regimes were developed to validate dynamic simulations: 1) shock load; and 2) reacclimation to higher influent concentrations. In the shock load experiments, sufficient mass of 1-NA was added to the aeration zone of each CMAS to raise the concentration of 1-NA (to 15 mg/L). The reduction of 1-NA was recorded every two hours to calculate the rate of biodegradation. In the reacclimation experiments, CMAS were acclimated to 3 mg/L 1-NA until achieving steady state, and then the influent 1-NA concentration was decreased to 0 mg/L for 12 days or 1.3 MCRT. The influent 1-NA was then restored to 3 mg/L in order to observe the time to reclamation, and effluent concentration was monitored twice per day for the duration of the experiment.

Samples collected from the aeration off-gas and treated effluent were analyzed by gas chromatography (GC) and high-performance liquid chromatography (HPLC). The detection limit for 1-NA in samples for data reported here was 0.01 mg/L for both GC and HPLC measurements (protocol described by Babcock, et al. 1993). Bulk organic material (soluble substrate) was quantified as filtered chemical oxygen demand (COD) by method 5220B (Standard Methods, 1989) weekly. Biomass concentrations were measured as MLVSS by method 2540E (Standard Methods, 2005) twice per week. Triplicate measurements were always obtained and mean values are presented.

3.3 Model Development

Model formulation generally used the unified approach of Lawrence and McCarty, 1970, since the more complicated structure of advanced models, such as the structured biomass models (Cliff and Andrews, 1981), or the ASMs (Henze et al., 1987, Gujer et al., 1999) were not needed. Two dynamic material balance equations were written for substrates: 1-NA and the non-toxic bulk carbon source (bulk substrate); and three for cells: 1-NA degrading exogenous, 1-NA degrading indigenous, and non-1-NA degrading species. Removal of 1-NA occurs by four mechanisms: 1) volatilization/stripping; 2) adsorption onto activated sludge; 3) biodegradation from the acclimated indigenous culture, and 4) biodegradation from exogenous culture supplied by the enricher-reactors. Adsorption was not considered an important mechanism because adsorbed substrate is quickly metabolized and periodic solvent extraction of waste sludge samples never recovered adsorbed 1-NA. Previous work showed that the biomass rapidly adsorbs 1-NA, but the

sorbed 1-NA is degraded over time, and adsorbed 1-NA disappears before the bulk liquid 1-NA concentration decreases to the 1-NA detection limit. The five mass balances can be written as follows:

$$\frac{dS}{dt} = \frac{1}{\theta_H} \cdot (S_O - S) - r_{su}, \quad 3.1$$

$$\frac{dS_t}{dt} = \frac{1}{\theta_H} \cdot (S_{tO} - S_t) - K_L a \cdot S_t - r_{suE} - r_{suI}, \quad 3.2$$

$$\frac{dX}{dt} = \frac{1}{\theta_H} \cdot \left(X_O - \frac{X}{X + X_E} \cdot X_{eff} \right) - \frac{X}{\theta_X} + r_g, \quad 3.3$$

$$\frac{dX_E}{dt} = \frac{1}{\theta_H} \cdot \left(\frac{fX_{ER}}{Q} - \frac{X}{X + X_E} \cdot X_{eff} \right) - \frac{X_E}{\theta_X} + r_{gE}, \quad 3.4$$

$$\frac{dX_I}{dt} = \frac{1}{\theta_H} \cdot X_{IO} - \frac{X_I}{\theta_X} + r_{gI}, \quad 3.5$$

Figure 3.1 (a) shows all of these variables and their relationship to the physical system. The effluent biomass X_{eff} , which is sometimes neglected in ASP simulations, was needed in the mass balances due to significant loss of effluent suspended solids. In the CMAS the suspended solids and process water were separated by a baffled, quiescent section inside the reactor, function as a clarifier (Figure 3.2). Bacteria flocs were lost in the effluent and the loss was especially high when the reactors were highly augmented. The MLVSS in the reactor mostly consists of two groups of biomass: the exogenous biomass X_E , and the non-1-NA degrading biomass X . The growth of indigenous species X_I due to 1-NA consumption was considered negligible since the influent concentration of 1-NA was

very low (1-3 mg/L) compared to the bulk substrate S (375 mg/L). The effluent VSS was divided into two terms by fraction in Equation 3.3 and 3.4.

Equations 3.4 and 3.5 indicate that both indigenous and exogenous cells consume 1-NA, and that daily additions of exogenous biomass are assumed to be continuous (fX_{ER}).

Monod kinetics were assumed throughout this study for oxidation of both substrate types.

We are aware that Monod kinetics was not developed for degradation of secondary substrates, but in our experiments and in reports from others, the Monod model can fit secondary-substrate degradation data (Babcock et. al., 1993). The correlation between the uptake rates of target substrate for exogenous enriched cultures can be expressed as:

$$r_{suE} = \frac{k_E X_E S_t}{K_t + S_t}, \quad 3.6$$

$$r_{gE} = Y_E \cdot r_{suE} - K_{dE} \cdot X_E, \quad 3.7$$

An important aspect in this model is that the indigenous 1-NA degrading species X_I in Equation 3.5 is an assumed variable that cannot be directly measured from experiments. Former studies (Babcock et al., 1992) showed that after acclimation (several months) and at long $MCRT$, 1-NA can be degraded by normal activated sludge processes without bioaugmentation, although at a slower rate and with consistent uninterrupted feeding of 1-NA. In the mainstream reactor or an *in-situ* reactor, indigenous 1-NA degrading culture must grow with other heterotrophic organisms. It would be difficult to independently

measure indigenous 1-NA degrading organisms, but it is not strictly necessary to measure these organisms independently, but only to simulate their impacts, in a fashion analogous to simulating nitrification in full scale systems. The need for separate balances on the two groups of 1-NA degrading organisms is to quantify the difference in rates of metabolism that occurs because of their previous environmental conditions: within the ER reactor at generally higher 1-NA concentrations, or in main reactor, at lower 1-NA concentration and in competition with other organisms.

Mathematically, we assumed that the non-1-NA degrading biomass (X) degraded only the bulk substrate (S) and were unaffected by the presence of 1-NA or the 1-NA-degrading inoculum; and the growth of exogenous biomass was not affected by the concentration of bulk substrate. The exogenous species is a mixed culture and should be able to adapt to the bulk substrate, but for simplicity we separated this growth from our X_E calculation: to verify the competition between exogenous and indigenous species on bulk substrate, detailed experimental approaches would have been required but were not considered necessary, since the study is not focused on degradation of easily degradable substrate. Since the influent bulk substrate concentration is constant, the total production of the non-1-NA degrading biomass should be steady, independent of the source of the biomass. This assumption simplified the calculation so that Equation 3.3 is independent from Equations 3.4 and 3.5. The model neglects the effect of DO since the reactors always had high DO (> 4 mg/L).

The model was constructed based upon Matlab 7.0 (MathWorks, Natick, Massachusetts) using a fourth-order correct, variable-time-step Runge-Kutta technique (function ode45) to integrate Equations 3.1 through 3.5. Laboratory data from shock load experiments and reacclimation experiments were used for calibration using sensitivity analysis and eventually with a pattern search algorithm (Box, 1965; Tzeng, et al., 2003) to minimize the sum of squares errors between the model output and experimental results.

3.4 Results and Discussion

3.4.1 Steady State Results

Table 3.2 shows the average MLVSS, effluent VSS, and effluent COD versus the bioaugmentation levels after several months of operation at steady state. The bioaugmented CMAS lost significantly more cells and discharged more COD than controls, and the loss increased with bioaugmentation levels. Daily losses of biomass in the reactor effluent were calculated and compared to the mass of cells added for bioaugmentation. The loss and addition rates of VSS are not linearly correlated. At low bioaugmentation level, the daily loss of biomass was more than 100% of the exogenous biomass, but was only 30% of the exogenous mass when the CMAS was highly bioaugmented (8 to 16%). Effluent VSS was composed of both indigenous cells as well as exogenous cells, since the observed improvement in 1-NA removal would not have occurred if the effluent VSS were composed solely of exogenous cells. Degradation of 1-NA at low bioaugmentation level (1 to 4%) improved, even though the MLVSS concentration did not increase.

Table 3.2 Measured effluent biomass and soluble COD

Measurements	Unit	Bioaugmentation levels (%)					
		0	1	2	4	8	16
Average MLVSS	mg/L	1668	1604	2076	1586	2362	3008
Effluent VSS	mg/L	21.7	39.0	62.8	79.2	70.4	99.0
Effluent COD	mg/L	36.7	38.8	29.6	49.4	46.6	60.6
Rate X_E add	mg/day	0	431	861	1703	3400	6826
Rate X_E loss	mg/day	0	461	1095	1532	1297	2059
Loss/added	%	-	107	127	90	38	30

The steady state data were used to calibrate the model shown previously. At steady-state, Equation 3.3 can be rearranged to calculate the concentration of non-1-NA degrading biomass as follows:

$$X = \frac{\theta_X}{\theta_H} \cdot \left[Y(S_O - S) - \frac{X}{X + X_E} \cdot X_{eff} \right] \cdot \frac{1}{1 + K_d \cdot MCRT}, \quad 3.8$$

and for exogenous biomass, Equation 3.4 can be reduced to:

$$X_E = \frac{\theta_X}{\theta_H} \cdot \left[\frac{fX_{ER}}{Q} - \frac{X_E}{X + X_E} \cdot X_{eff} \right] \cdot \frac{1}{1 + K_{dE} \cdot MCRT}, \quad 3.9$$

The production of the suspended solids due to consumption of bulk substrate was first calculated. At zero bioaugmentation (acclimated and unacclimated controls) the MLVSS was assumed to be composed of non-1-NA degrading biomass and a much smaller mass

of 1-NA-degrading cells. The steady state results of the non-1-NA degrading species corresponded to Monod kinetics with the following values: $MLVSS = 1650 \text{ mg/L}$, $X_{eff} = 22 \text{ mg/L}$, influent COD = 375 mg/L, and $MCRT = 8.9 \text{ days}$; then the parameters were provided: $k = 5/\text{day}$; $K_s = 30 \text{ mg/L}$; $K_d = 0.06 \text{ mg/L}$; $Y = 0.4$. These values were assumed for the bulk substrate kinetics for all CMASs regardless of bioaugmentation level. Equation 3.9 was used to calculate the exogenous biomass concentration and K_{dE} is the only parameter that needs to be identified.

Equation 3.8 and 3.9 were solved iteratively with given conditions and the calculated total biomass was plotted in Figure 3.3, with the measured data. The concentration of the non-1-NA degrading biomass (X) and exogenous biomass (X_E) are plotted against the bioaugmentation levels, and the summation of the two is shown as the total biomass. A stable production of non-1-NA degrading biomass is predicted regardless of the level of bioaugmentation: a steady feed of substrate supports a mixed culture with approximately 1000 to 1500 mg/L MLVSS. For the exogenous 1-NA degrading species, observed biomass was lower than predicted with the kinetic parameters described previously. A better fit between model predictions and observations is possible if the value of K_{dE} is increased to 0.12/day. This is reasonable because the exogenous cells have been removed from a 1-NA rich (1-NA = 150 mg/L) environment to an 1-NA poor (1-NA = 3mg/L) environment, and greater decay is to be expected.

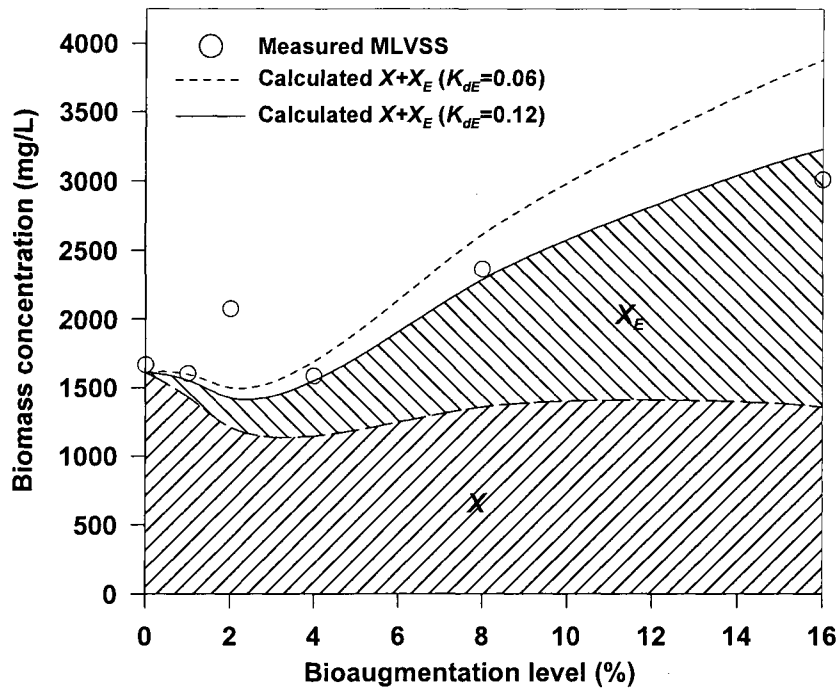


Figure 3.3 Biomass concentration versus bioaugmentation levels.

3.4.2 Shock loading and reacclimation experiments

The effluent 1-NA concentrations from the shock loading experiments are shown in Figure 3.4 (a) and are plotted for various levels of bioaugmentation (0%, 1%, 2%, 4%, 8%, and 16%). In all shock load experiments, effluent 1-NA decreased exponentially to detection limits with increasing levels of bioaugmentation causing greater degradation rates. Degradation of 1-NA initially showed no correlation with bioaugmentation levels (box I); and the difference in biodegradation rates became distinguishable only after the 1-NA concentration decreased to less than 35% of the initial value (box II). The 1-NA decreased to detection limits 4 to 8 hours faster with increasing bioaugmentation levels. The CMAS operating at 4% bioaugmentation was upset during this experiment and the results are not shown.

Figure 3.4 (b) shows the reacclimation in response to a step increase of influent 1-NA to 3 mg/L after operating for 12 days (1.2 MCRT) with no 1-NA. For all CMAS (including the 4% acclimation level, which was now operating properly), effluent 1-NA had decreased to detection limits within 240 hr (10 days). The patterns of breakthrough curves are similar: effluent 1-NA increased with influent concentration to reach a plateau and then decreased after a specific period until being totally degraded. The difference between each test was the peak effluent concentration and the time required for the effluent 1-NA to return to detection limits. As expected higher bioaugmentation reduced the peak 1-NA breakthrough concentration and decreased the time required to reach detection limits. For the case of no bioaugmentation, the effluent 1-NA concentration reached a plateau of approximately 2 mg/L and did not return to detection limits until after 10 days' operation. With low level bioaugmentation (1%, 2%, 4%), the peak effluent concentrations were approximately 0.5 to 1 mg/L and the time to reach detection limits decreased to 8 days. When highly bioaugmented (8% and 16%), there was almost no breakthrough and no recovery period was needed.

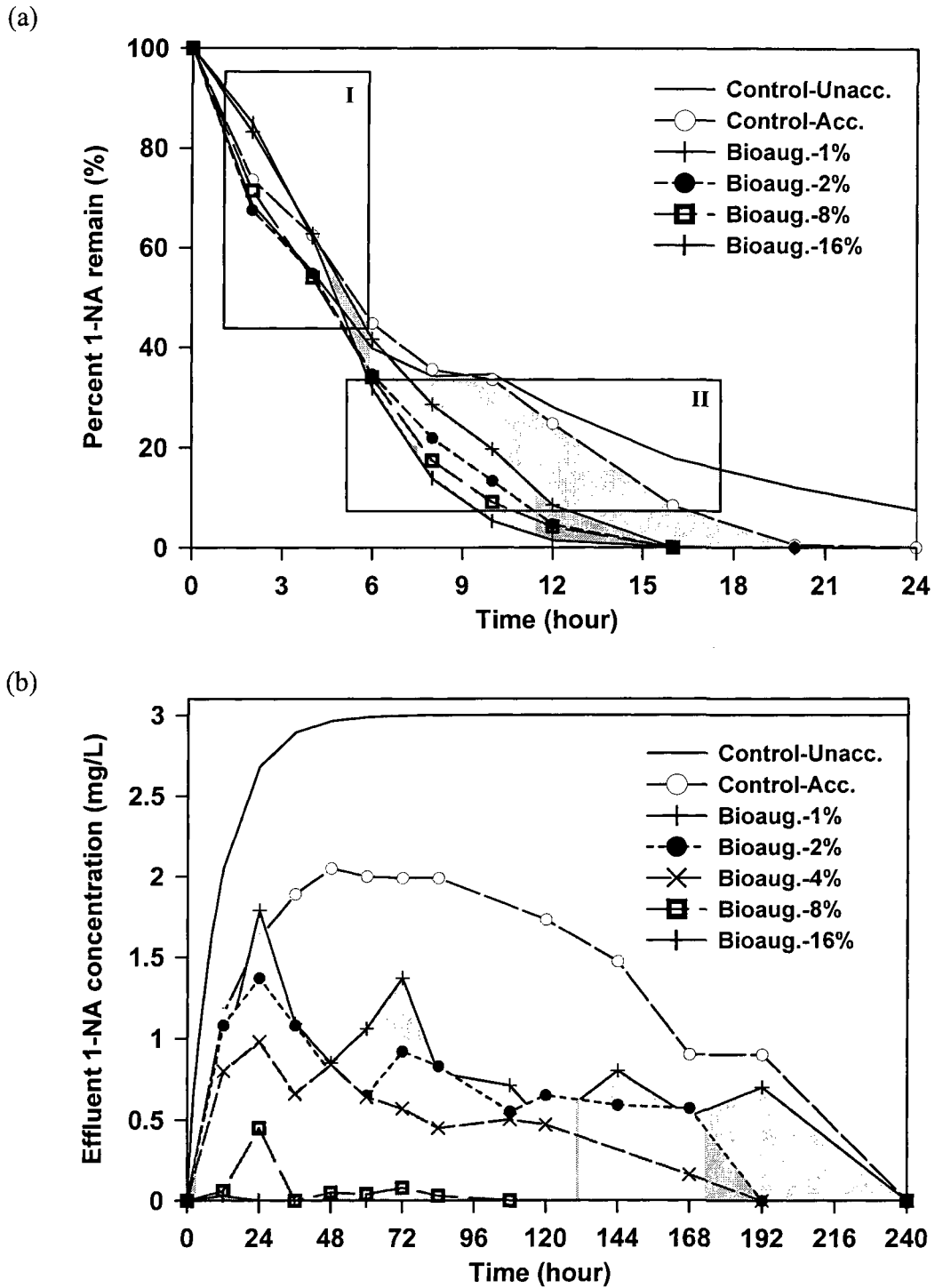


Figure 3.4 Effluent 1-NA breakthrough under different bioaugmentation levels in (a) shock loading experiments. (b) reacclimation experiments.

3.4.3 Dynamic simulations

Simulation results of shock loading experiments are presented in Figure 3.5 (a) through 5 (d) with the parameters shown in Table 3.3.

Table 3.3 Monod kinetics used in the simulations

Parameters	Values	Units
1. Defined parameters		
Yield of bulk biomass on bulk substrate, Y	0.40	-
Yield of acclimated culture on target compound, Y_I, Y_E	0.33	-
Maximum substrate uptake rate of bulk biomass, k	5	1/day
Half velocity coefficient of bulk biomass, K_s	30	mg/L
Half velocity coefficient on target compound, K_t	0.02	mg/L
Decay coefficient of bulk and indigenous biomass, K_d, K_{dI}	0.06	1/day
2. Calibrated parameters		
(1) Stripping and growth		
Gas transfer coefficient of 1-NA, K_La	0.374	1/day
Indigenous maximum uptake rate of target compound, k_I	0.950	1/day
Exogenous maximum uptake rate of target compound, k_E	0.147	1/day
(2) Decay of enriched culture, K_{dE}		
Bioaugmentation level 1%	0.06	1/day
Bioaugmentation level 2%	0.20	1/day
Bioaugmentation level 4%	0.32	1/day
Bioaugmentation level 8%	0.32	1/day
Bioaugmentation level 16%	0.32	1/day

Figure 3.5 (a) shows the 1-NA breakthrough simulated (smooth curves) versus the measured data (open circles) for the unacclimated control experiment. Since no biological degradation was expected from the unacclimated cells, the removal mechanisms are due to washout and stripping.

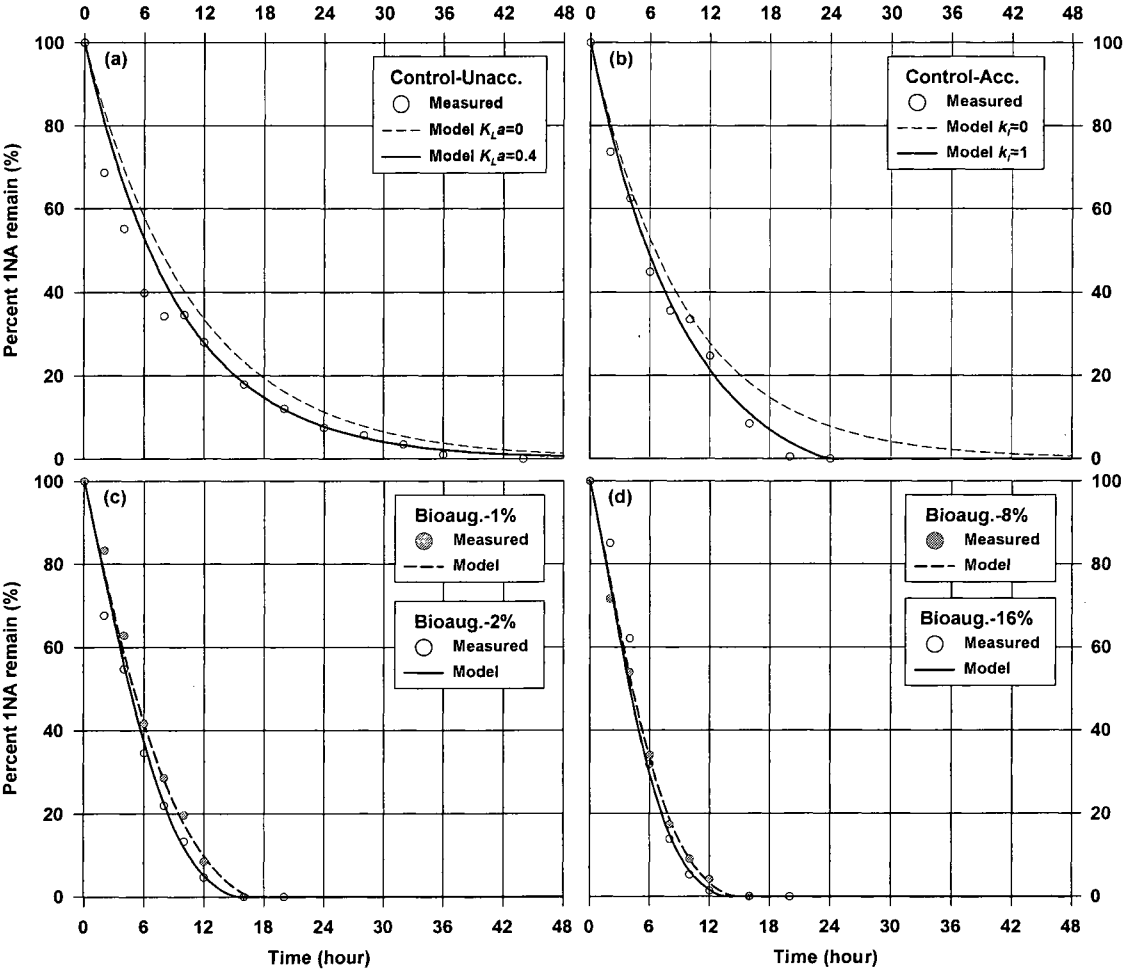


Figure 3.5 Simulation results of 1-NA breakthrough in the shock loading experiments

To illustrate the magnitude of stripping, a second simulated is presented with no stripping ($K_{La} = 0$). The figure shows that stripping of 1-NA is to be expected and the simulation fits better with the gas transfer term (solid line) than without (dash line), using a K_{La} of 0.4/day (Babcock, et al., 1992). Figure 3.5 (b) shows the simulation results of 1-NA loss in the acclimated control. The dashed line shows the results of stripping only, while the solid line simulates stripping and biodegradation provided by X_I . The acclimated control reduced the 1-NA to detection limits in approximately half the time required for the unacclimated control, from 48 hours to 24 hours. Figure 3.5 (c) shows the results of the two low level (1 and 2%) bioaugmentation experiments while Figure 3.5 (d) shows the results from the two high level (8 and 16%) bioaugmentation experiments. The observations and simulation results fit well. The impact of 8% and 16% bioaugmentation are similar, and reduced the time to detection limits to 12 hours.

Figure 3.6 (a) through (d) shows the simulation results of reacclimation experiments. Figure 3.6 (a) shows the 1-NA breakthrough with degradation from indigenous species versus the observations. The simulation output agrees well with the experimental data. The growth kinetics of indigenous biomass collected from this experiment was used throughout all simulations. Figure 3.6 (b) shows the simulation of 1% endogenous bioaugmentation. In order to fit the biomass concentrations, it was necessary to increase K_{dE} , as discussed previously in the steady state results description. The base value of K_{dE} of 0.06/day was used for the acclimated control and 1% bioaugmentation; K_{dE} was increased to 0.20 and 0.32/day for the 2% and 4% to 16%, respectively.

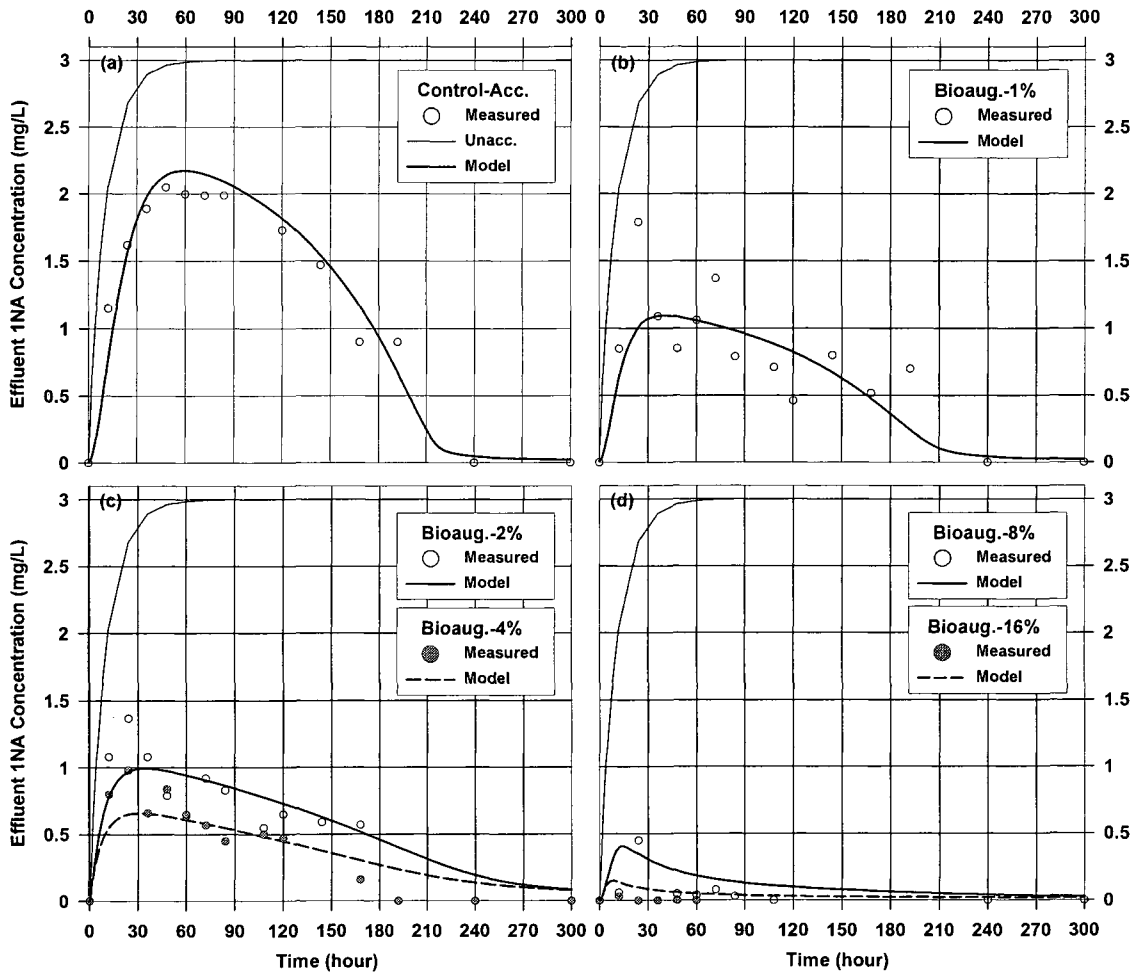


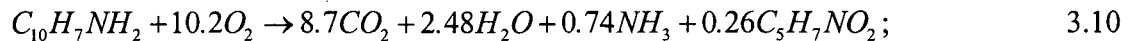
Figure 3.6 Simulation results of 1-NA breakthrough in the reacclimation experiments

The simulations at 8 and 16% bioaugmentation are relatively less accurate, since the effluent 1-NA concentrations are small and approaching detection limits. Higher values of K_{dE} were needed for the higher bioaugmentation levels in order to prevent the model from predicting too great a 1-NA removal efficiency. The fit between observed and predicted solids concentrations are not shown but are roughly the same as in Figure 3.3. More detailed discussion of the parameter estimates are provided in the following section.

3.4.4 Model calibration

The parameters used in the models were validated separately and the average values used in our simulations are shown in Table 3.3. The validated parameters were performed in two groups: 1) defined from references (Y, k, K_s), our previous studies (Y_I, Y_E), or general assumptions (K_t, K_{dt}); and 2) calibrated from the results of experiments designed to identify specific parameters, as follows: gas transfer (K_La) in the un-acclimated control experiments; then the growth kinetics of indigenous species (k_I) in acclimated control experiments; then the average growth kinetics of exogenous species (k_E) from shock loading experiments, and finally the decay coefficient of exogenous species (K_{dE}) from reacclimation experiments.

Yield coefficients of acclimated indigenous species X_I and enriched cultures X_E were calculated based on our previous observations (Cardinal and Stenstrom, 1991; Babcock et al., 1992) which showed that enricher cultures converted approximately 87% of the carbon in 1-NA to CO_2 ; which means the stoichiometry of the microbial growth becomes:



The yield coefficient of the enriched species X_I and X_E is 0.26 molar biomass per molar 1-NA, or 0.33 mass biomass per mass of 1-NA. This value of the yield coefficient, confirms our assumption that the increase in steady-state total biomass is predominantly due to the continuous additions of exogenous biomass and not due to growth on 1-NA.

The influent 1-NA concentration of 1.0 mg/L would only support a steady-state growth of 8.8 mg/day, or at most 6 mg/L MLVSS, whereas our minimum dosage of exogenous biomass (1% bioaugmentation) was about 50 times higher (431 mg/day). For the other parameters, Monod kinetics of the non-1-NA degrading biomass was defined previously; decay coefficient of acclimated 1-NA degrading culture was assumed to be the same as the non-1-NA degrading biomass, since both cultures were reproduced in the main reactor but not from the enricher-reactor.

Monod kinetics of indigenous and exogenous cultures was calibrated by the breakthrough curve of 1-NA. The Monod function represents the growth of microorganisms on the substrate, and each term in the function performs a specific behavior, e.g. in the reacclimation experiments, the maximum substrate uptake rate k_E describes the peak concentration of 1-NA and the time to achieve this value; the half-velocity coefficient K_t represents the residuals of 1-NA; and decay coefficient K_{dE} is correlated to the degradation curves after the peak discharge. The calibration approach used in this chapter is similar to the method used to calibrate structural ASM models. Yuan et al. (1993) applied oxygen uptake rates (OUR) to calibrate the kinetics of substrate consumption in a HPO treatment plant, and Koch et al., (2000) applied the same index to examine the kinetics of the storage function in ASM 3. We defined a low K_t which is close to the detection limit, because 1-NA is degraded to the detection limit at the end of all acclimated experiments. Mathematically, this parameter controls the simulation when the 1-NA concentration is low. The maximum uptake rate k is defined with other parameters

based upon sensitivity analysis: the optimal simulations should lie on a linear function of k , K_t , and K_d . Since the ranges of K_t and K_{dE} were already defined and k_E should not vary significantly throughout the study, the value of 0.147/day was used and fit all experiments equally well.

The decay coefficient of exogenous biomass K_{dE} is one of the more sensitive parameters affecting the simulation. The approach to define K_{dE} separately in each experiment level of bioaugmentation is both a convenient construct which allows us to make the model fit the data and a plausible physical explanation. The endogenous decay parameter is actually a lumped parameter which encompasses both substrate utilization for maintenance of cellular activity (energy) and cell losses due to death (cell lysis) and predation (Metcalf and Eddy, 2003). Increasing K_{dE} should occur with increasing bioaugmentation levels, or the decrease of the F/M ratio. This represents a change of conditions for the cells from “growth-dominate” conditions to “respiration-dominate” conditions. The K_{dE} parameter increased from 0.06 to 0.32/day as the bioaugmentation increased from 0 to 16%.

3.4.5 Simulation of the *in-situ* process

After calibration, the model was used to simulate the *in-situ* bioaugmentation process (Figure 3.1 (b)). Since the growth environment in the reaeration zone is close to the main reactor, we use the same growth kinetics and decay coefficient for indigenous biomass in both reactors, i.e. $k_l = 0.95/\text{day}$, $K_t = 0.02 \text{ mg/L}$, and $K_{dI} = 0.06/\text{day}$. Influent conditions

were similar to the reacclimation experiments that an increase in influent 1-NA from 0 mg/L to a constant 3 mg/L was simulated. Four scenarios were evaluated: 1) acclimated control with no bioaugmentation; 2) with 1% exogenous bioaugmentation; 3) with 4% exogenous bioaugmentation; and 4) with the *in-situ* process. In so far as possible, the ER-process and *in-situ* process were compared using the same conditions. For example, to create sufficient biomass in the ER-process to provide 1% bioaugmentation, approximately 26.5 mg/day of 1-NA is required for cell production. Therefore, in our simulation for the *in-situ* process, the same dosage of 1-NA was used to feed the reaeration tank.

The simulation results of the different scenarios are shown in Figure 3.7 which shows the percent removal of 1-NA as a function of MCRT. The effluent 1-NA mass decreased with increasing MCRT in all scenarios. For the acclimated control simulation (no ER cells and no 1-NA added to the reaeration tank), the reactors performed equivalently, and were able to degrade 1-NA for MCRTs larger than 6 days. Above the wash-out MCRT, the degradation of 1-NA improves with MCRT and removed approximately 60% of the feed 1-NA mass at MCRT = 10 days.

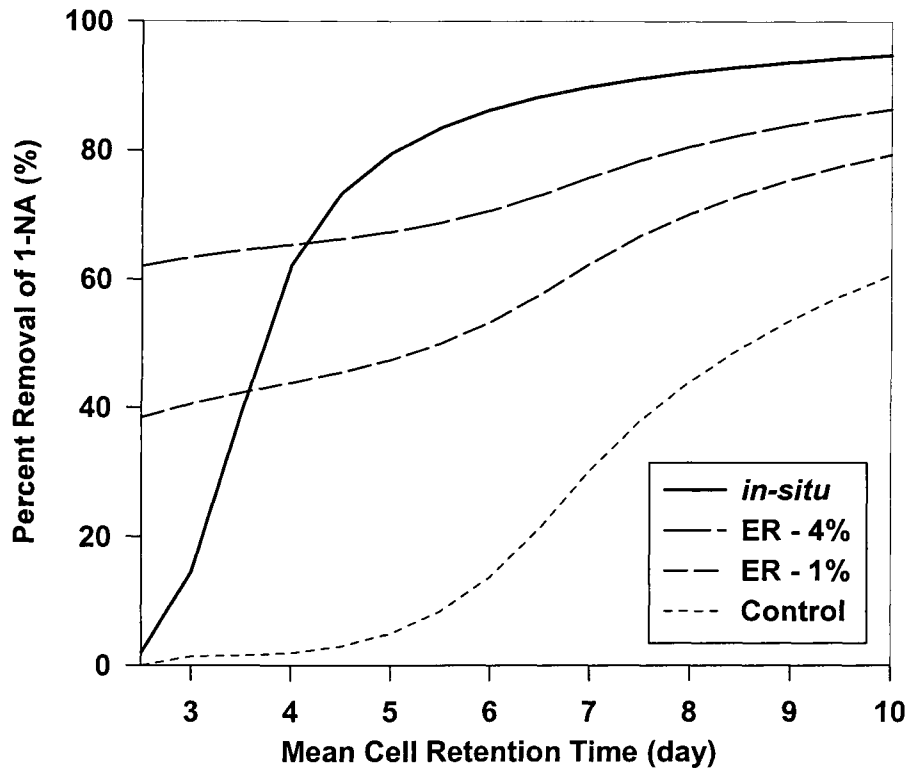


Figure 3.7 Simulation of 1-NA treatment performance of different bioaugmentation methods.

With bioaugmentation, ER-process and the *in-situ* processes both improved 1-NA degradation but performed differently. For the ER-process with 1% bioaugmentation, the removal of 1-NA was approximately 40% at MCRT = 2.5 days, and was 50% at 6 days MCRT. The benefit of this bioaugmentation method over the *in-situ* process is that 1-NA removal occurs at lower MCRTs. However, due to the high decay rate of exogenous biomass, this improvement of 1-NA degradation is not a linear function of the bioaugmentation level; at 4% bioaugmentation removal increases from ~ 40% to ~ 60% at MCRT = 2.5 days, and from ~ 50% to ~ 65% at MCRT = 6 days. This is only a minor improvement for the increased (300%) biomass.

The *in-situ* process performed did not degrade 1-NA well at low MCRT, but excelled at higher MCRTs. The *in-situ* process begins to achieve significant 1-NA removal at MCRT = 4 days and outperforms the ER process at both 1 and 4% bioaugmentation above MCRT = 4 days. The disadvantages of the *in-situ* process over the ER process include the volume required for the reaeration reactor which will be several times larger than the volume of the ER reactor. A second disadvantage is that a significant fraction of biomass in the *in-situ* process is exposed to higher 1-NA concentration as it is recycled through the reaeration reactor. 1-NA is inhibitory or toxic to nitrifiers (Hockenbury and Grady, 1977) and perhaps other organisms which may impact nitrification efficiency or other removal efficiencies. In the ER-process, only the bioaugmentation mass is exposed to the high 1-NA concentrations. Furthermore, multiple ER reactors can be provided; for example, the first ER reactor could provide cells acclimated to 1-NA while the second ER reactor could provide nitrifier biomass or biomass acclimated to a different organic compound.

3.5 Conclusions

1. The benefits of bioaugmentation, using the ER-process, was demonstrated showing that enhanced target compound removal, resistance to shock loads and more rapid reacclimation to a toxic compound are possible. The benefits occur with low amounts of bioaugmentation (1 to 2% by reactor biomass). At higher bioaugmentation levels a large fraction of the added mass decays, reducing the benefits of bioaugmentation.

2. A simulation model is a useful tool to describe microbial behavior which is too difficult or expensive to measure experimentally. In this case, the simulation model was useful to quantify the biomass decay rate, which obviously must occur, but is not easy to measure. The increased decay rate explains the reduced relative benefits of bioaugmentation at higher bioaugmentation levels. The beneficial effects of bioaugmentation using the ER process are limited and the model can become a useful design tool.
3. An alternative strategy to improve the degradation of hazardous waste is to enrich the target culture in the main reactor system, using a reaeration reactor, called “*in-situ*” bioaugmentation. The calibrated model was used to compare the ER-process and the *in-situ* process to show that the *in-situ* process is superior at longer MCRTs. The ER-process has the advantage of not exposing the entire biomass to high concentrations of potentially toxic enrichment substrates, as well as being able to accommodate more than one target compound.
4. Both bioaugmentation methods were able to provide target compound removals at MCRTs below the normal washout MCRT associated with a conventional activated sludge process. This may be an important feature, especially for more commonly encountered treatment goals such as nitrification.

Notation

K_d	decay coefficient, T^{-1}
$K_L a$	gas transfer coefficient, T^{-1}
K_s	half velocity coefficient, ML^{-3}
K_t	half velocity coefficient of target compound, ML^{-3}
Q	volumetric flow rate, $L^3 T^{-1}$
S	substrate, ML^{-3}
V	volume of aeration zone, L^3
X	cell concentrations, ML^{-3}
X_{eff}	effluent suspended solids, ML^{-3}
X_{ER}	biomass concentration from enricher-reactor, ML^{-3}
Y	yield coefficient, mass VSS per mass substrate, MM^{-1}
f	volume of exogenous biomass added per day, $L^3 T^{-1}$
k	maximum substrate uptake rate, T^{-1}
r_{su}	substrate uptake rate, $ML^{-3} T^{-1}$
r_g	growth rate of microbial strains, $ML^{-3} T^{-1}$
θ_H	hydraulic retention time (HRT), T
θ_X	mean cell retention time (MCRT), T

Subscripts

E	exogenous microorganisms
I	indigenous microorganisms
O	influent concentrations
t	target compound (1-NA)

4. BIOAUGMENTATION TO IMPROVE NITRIFICATION

4.1 Summary

Bioaugmentation is a proposed technique to improve nutrient removal in municipal wastewater treatment. Compared with the commonly used nitrification/denitrification (NDN) processes, bioaugmentation processes may be able to reduce tankage or land requirements. Many approaches for bioaugmentation have been developed, but few studies have compared the benefits among different approaches. This chapter quantifies the effectiveness of bioaugmentation processes, based on a validated simulation approach. Three major “on-site” bioaugmentation alternatives were investigated: 1) the parallel plant approach that uses acclimated biomass grown in a nitrifying “long-MCRT” (mean cell retention time) plant to augment a low-MCRT treatment plant; 2) the off-line enricher-reactor (ER) approach which uses an off-line reactor fed with high concentrations of enrichment substrates to produce the augmentation cultures; and 3) the “*in-situ*” reaeration approach which adds enrichment substrates to a reaeration reactor that receives a portion of the recycle activated sludge. Kinetic models were developed to simulate each approach at steady state and dynamic conditions. The benefits of various approaches are presented on the same basis with controllable parameters, such as bioaugmentation rates, aeration tank volume, oxygen demand and sludge production. Examples were given to illustrate the potential benefits of bioaugmentation by upgrading a “carbon-only” wastewater treatment plant to nitrification.

4.2 Theoretical Background

4.2.1 Bioaugmentation Schemes

On-site bioaugmentation processes can be classified into three major strategies: 1) using two or more parallel plants; 2) the enricher-reactor (ER) approach; and 3) the *in-situ* approach. Figures 4.1 (a) through (c) show each of the bioaugmentation approaches and the related literature are reviewed in the following sections. Types 1 and 2 are classified differently because of feed characteristics; a parallel plant treats wastewater while an enricher reactor is fed with a special substrate, usually much more concentrated than a wastewater, such as anaerobic digester centrate. Bioaugmentation has been previously discussed by the authors (Stenstrom et al., 1989; Cardinal and Stenstrom, 1991; Babcock et al., 1992, 1993; and Babcock and Stenstrom, 1993) for removal of recalcitrant organic compounds. For the purpose of this chapter we will be discussing bioaugmentation to improve nitrification.

Parallel plant approach: Figure 4.1 (a) shows the schematic of two parallel plants for bioaugmentation and the parameters used for simulations. This approach uses the excess sludge from the long-MCRT nitrifying plant as seed to enrich the non-nitrifying plant. Simplicity is the benefit of this bioaugmentation approach. Additionally, the construction of a separate nutrient removing parallel plant occurs frequently as treatment plants expand; only the expanded capacity is subject to newer more effluent permit (Carrio et al, 2003; Constantine, 2006). Treatment plants can benefit from bioaugmentation by collecting waste sludge from adjacent plant(s), and few plant

modifications are required, provided sufficient oxygen transfer and biomass thickening capability exists. It is also important to avoid enriching for unwanted biomass, such as *Nocardia* or filamentous organisms. Figure 4.1 (a), plant-1 is the nitrifying system and plant-2 is the bioaugmented process. The sludge centrate is added into plant-1 to increase the production of nitrifier biomass, and the exceeded sludge of plant-1, which is normally wasted, can be used to augment plant-2 for nitrification.

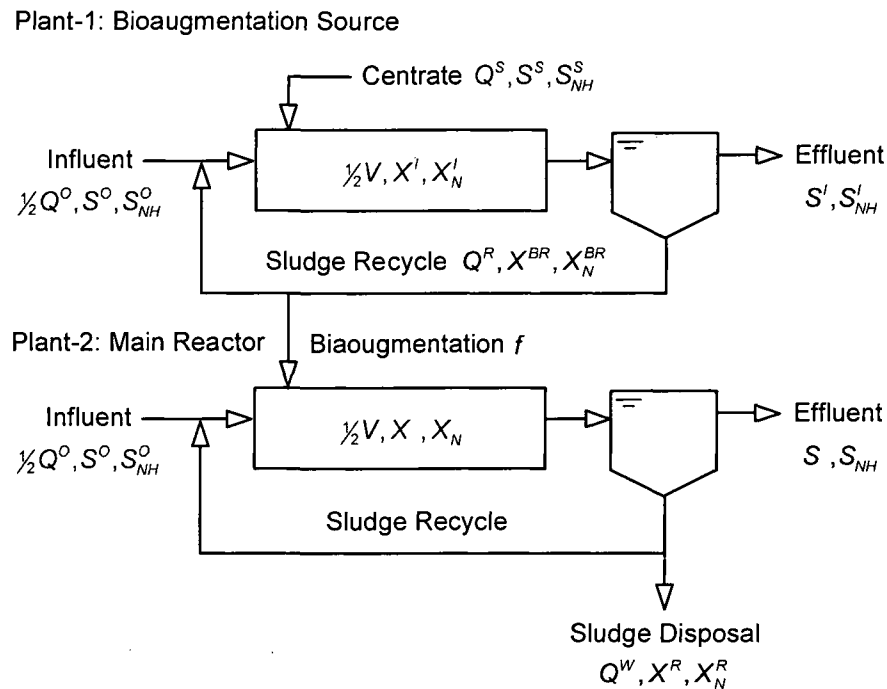


Figure 4.1 (a) Concept schematic of parallel plant approach

The parallel plant approach to improve ammonia removal has been successful in several studies: Daigger et al (1993) improved nitrification under an otherwise nitrifier washed-out condition by adding a trickling filter upstream to the operating ASP.

Neethling et al. (1998) showed that nitrification can be achieved in high purity oxygen (HPO) processes by adding the nitrifier biomass produced in a nitrifying air-type ASP. Plaza et al. (2001) tested and evaluated the bioaugmentation approach of parallel plants and recorded the maximum growth rates of nitrifying biomass in the augmented plant. The full-scale plant that received bioaugmentation was operated under very short MCRT (0.5~1.5 days).

Enricher-Reactor approach: Figure 4.1 (b) shows the ER approach that uses one or more off-line reactor(s) to enrich the nitrifying cultures. The enricher-reactors commonly use sequencing-batch-reactors (SBR). Batch reactors are particularly efficient in treating high strength wastewater, such as anaerobic digester supernatant. Mossakowska et al. (1997) recorded a high removal rate of ammonia by an SBR ($45\text{g NH}_4\text{-N/kg MLVSS}\cdot\text{h}$), for separate treatment of the sludge supernatant from the main reactor. The high production rate of nitrifiers in SBRs provides a source of augmenting cultures. Head and Oleszkiewicz (2004) used the excess biomass from a nitrifying SBR to bioaugment an otherwise non-nitrifying SBR, and achieved full nitrification at low temperature (10°C) and short MCRT. Kos (1998) demonstrated bioaugmentation using a complete mixed activated sludge process (CMAS) as the enricher reactor.

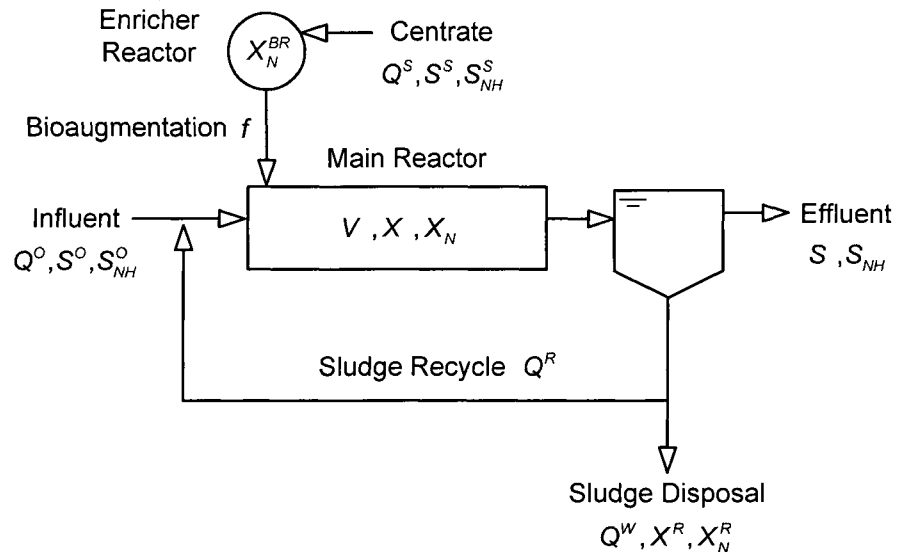


Figure 4.1 (b) Concept schematic of enricher-reactor approach

In-situ approach: this approach grows nitrifier biomass in the recycled sludge by special plant configuration as shown in Figure 4.1 (c). The process withdraws a fraction or all of the recycled sludge to be “reaerated” in a side-stream aerated reactor, where concentrated wastes such as digester filtrate or centrate are fed and to enrich the nitrifying biomass.

A key aspect of all bioaugmentation concepts is to grow organisms that can survive in the main process. Bouchez et al. (2000) reported how enriched cultures produced from off-line ERs are vulnerable to predation of protozoa and/or wash-out in the activated sludge process. Salem et al. (2006) noted an excessive decay rate for the enriched nitrifying cultures. The key concept of the previously cited ER studies is the maintenance of selective pressure to grow flocculating organism since only flocculating and settling organisms will be retained in the SBR or CMAS (Parker and Wanner, 2007).

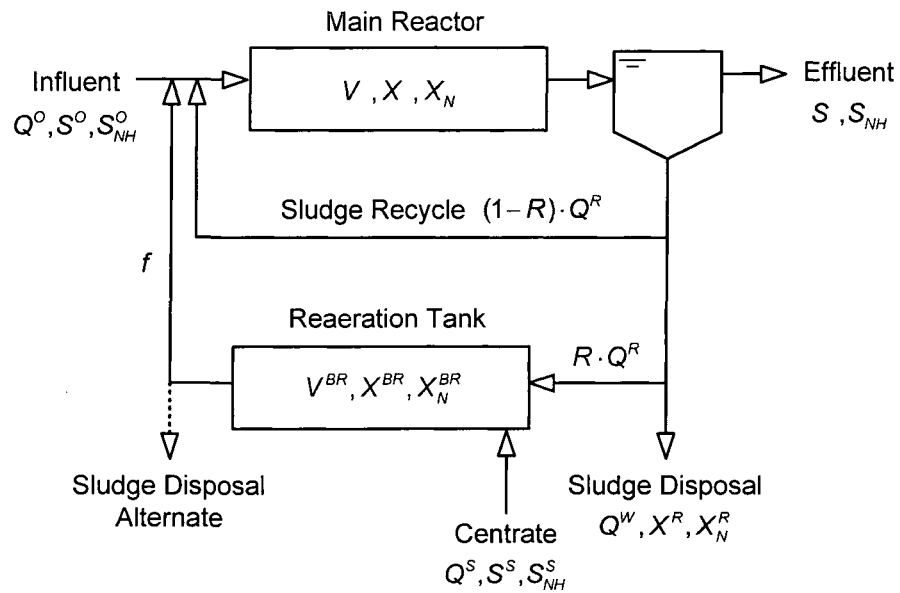


Figure 4.1 (c) Concept schematic of *in-situ* approach

Several bioaugmentation configurations have been developed to treat recycle streams typically found in treatment plants. Grutsch et al. (1978) patented the use of aerobic digesters to nitrify ammonia created from biomass decay and to reintroduce the nitrifying culture back to the activated sludge process. The process was practiced at full scale at the Texas City Amoco refinery and was effective in restoring nitrification and toxic upsets. Bogusch (1987) patented a process to enrich ammonia oxidizing bacteria by introducing high strength ammonia waste stream into the recycle biomass flow with a biomass reaeration zone equal to 5 to 20% of the aeration tank volume. Drury et al (1995) operated a full scale version of the process patented by Bogusch (1987) except that only a portion of the recycle biomass passed through the reaeration zone, and a full-scale

version of the process with partial recycle has been in operation at a Los Angeles County Sanitation Districts wastewater treatment plant since 2001. The MAUREEN process (Mainstream AUtotrophic Recycle Enabling Enhanced N-removal, Katehis et al., 2006) enriched cultures separately using two CMAS in series (the first CMAS is for COD removal and the second for nitrification). Various other process alternatives have been proposed (Regeneration-Denitrification-Nitrification, Wanner et al., 1990 and Krhutková et al., 2006; the BioAugmentation Reaeration or BAR process, Novák and Havrlíková, 2004, and Parker and Wanner, 2007). The BAR process uses the first zone of the aeration basin to treat the high strength ammonia waste stream with the recycled sludge and main process influent is introduced into the downstream zone. The BABE process (Bio-Augmentation Batch Enhanced, (Zilverentant et al., 1999; Salem et al., 2002) divides the reaeration tank into two stages (anoxic/aerobic), followed by a clarifier, to performance denitrification and increase the side-stream MCRT. Biomass can be wasted before sludge reaeration (solid arrow in Figure 4.1 (c), bottom right, Bogusch, 1987, Salem et al., 2002, 2003), or after reaeration (dashed arrow, down left, Grutsch et al., 1978).

4.2.2 Simulation of bioaugmentation processes

Simulations of nitrification in bioaugmented processes are based on the modeling approach of Poduska and Andrews (1975) who showed that the basic structure of the Lawrence and McCarty (1970) model can be used to model nitrification as a two step process of ammonia oxidation to nitrite and nitrite oxidation to nitrate, and using a

modified model structured biomass model (Cliff and Andrews, 1981) similar to ASM3 (Gujer et al., 1999) for COD removal. The concentration of nitrifying biomass controls the oxidation of ammonia, and is a function of bioaugmentation rate, the rates of sludge wastage, and the net specific growth rate. The mass balances of ammonia, concentration of the nitrifying biomass without and with bioaugmentation can be expressed as follows:

Ammonia degradation:

$$\frac{dS_{NH}}{dt} = \frac{1}{\theta_h} \cdot (S_{NH}^O - S_{NH}) - \frac{r_{su}}{Y_N} \quad 4.1$$

Nitrifiers without bioaugmentation:

$$\frac{dX_N}{dt} = -\frac{X_N}{\theta_x} + r_g \quad 4.2$$

Nitrifiers with bioaugmentation:

$$\frac{dX_N}{dt} = \frac{fX_N^{BR}}{V} - \frac{X_N}{\theta_x} + r_g \quad 4.3$$

The relationship between ammonia uptake rate and net growth rate of nitrifying cultures is normally described by Monod kinetics, which can be expressed as:

Ammonia uptake rate:

$$r_{su} = \frac{\mu_{max}^N X_N S_{NH}}{K_n + S_{NH}} \quad 4.4$$

Net growth rate of nitrifiers:

$$r_g = r_{su} - K_{dN} \cdot X_N \quad 4.5$$

Balances for bulk COD, heterotrophic biomass, and oxidation of nitrite can be written in a similar fashion. Since nitrite oxidation in activated sludge processes is normally more rapid than the rate of ammonia oxidation at normal wastewater temperatures (Poduska and Andrews, 1975), nitrification can be simplified by considering it as a single step process.

The sludge age θ_x , or MCRT is the essential operational parameter to control the concentration of suspended solids as well as the nitrification rate. MCRT represents the mean life time of cells staying in the reactor and is controlled by the rate of sludge disposal and recycle. At steady-state and without bioaugmentation (Eq. 2), MCRT can be calculated by the activated mass divided by the waste mass. MCRT is inversely proportional to the net growth rate of nitrifiers and the relationship can be expressed as:

$$\theta_x = \frac{X_N V}{Q^w X_N^R} = \frac{1}{r_g} \quad 4.6$$

In a bioaugmented system, augmenting biomass contributes part of the total biomass in addition to the cell growth. The originally defined operational-based MCRT (left hand side of Eq. 6) if used in a bioaugmented system, will no longer be valid (right hand side

of Eq. 6). Considering this inconsistency, Rittmann (1996) defined a new calculation of MCRT in a bioaugmented system. He suggested that the calculation of MCRT should be based on the growth of biomass excluding the bioaugmentation. The new calculation extends the MCRT definition in a simple fashion: the mass balance of effluent substrates and nitrifying biomass remained the same as before bioaugmentation. This newly-defined relationship is expressed as:

$$\frac{1}{r_g} = \frac{X_N V}{Q^W X_N^R - f X_N^{BR}} = \theta_x \quad 4.7$$

This “cell-based” MCRT is a proper extension for simulation, but this parameter is not directly equal to the “operational” MCRT as normally calculated in plant operation. Lee (1996) and Rittmann (1996) extended the calculation of MCRT to better describe this difference. The relationship between the cell-based MCRT (θ_x) and the operational MCRT (θ_x^{op}) can be calculated as:

$$\frac{\theta_x}{\theta_x^{op}} = \frac{f X_N^{BR}}{XV} \theta_x + 1 \quad 4.8$$

Based upon Monod kinetics and steady state, effluent ammonia and the suspended biomass can be calculated as functions of the bioaugmentation rate; hence Eq. 1 and Eq. 3 can be combined as followed:

$$S_{NH} = \frac{K_n(1 + K_d\theta_x)}{\theta_x(Y\mu_{max} - K_d) - 1} \quad 4.9$$

$$X_N = \frac{\theta_x}{1 + K_d \cdot \theta_x} \cdot \left[\frac{Y(S_0 - S)}{\theta_h} \right] \quad 4.10$$

Mass balances of non-nitrogenous substrate and heterotrophic species are similar to ammonia oxidation except for their different growth rates and parameters.

Figure 4.2 shows examples of steady-state simulation for the three bioaugmentation alternatives using the same total reactor volume. The percent ammonia discharged and concentrations of nitrifying biomass with bioaugmentation are plotted against the operational MCRT, under different bioaugmentation rates. The bioaugmentation rates is defined as the daily mass dosage of enriched biomass per unit of total biomass (mg enriched biomass per mg MLVSS per day). Bioaugmentation rates ranging from 0% to 10% of MLVSS were simulated and all rates reduce the critical MCRT for nitrification. A key factor to affect bioaugmentation performance is the fraction of nitrifying biomass in the bioaugmenting sludge. The ratio of autotrophic to heterotrophic biomass is generally not known, but can be simulated.

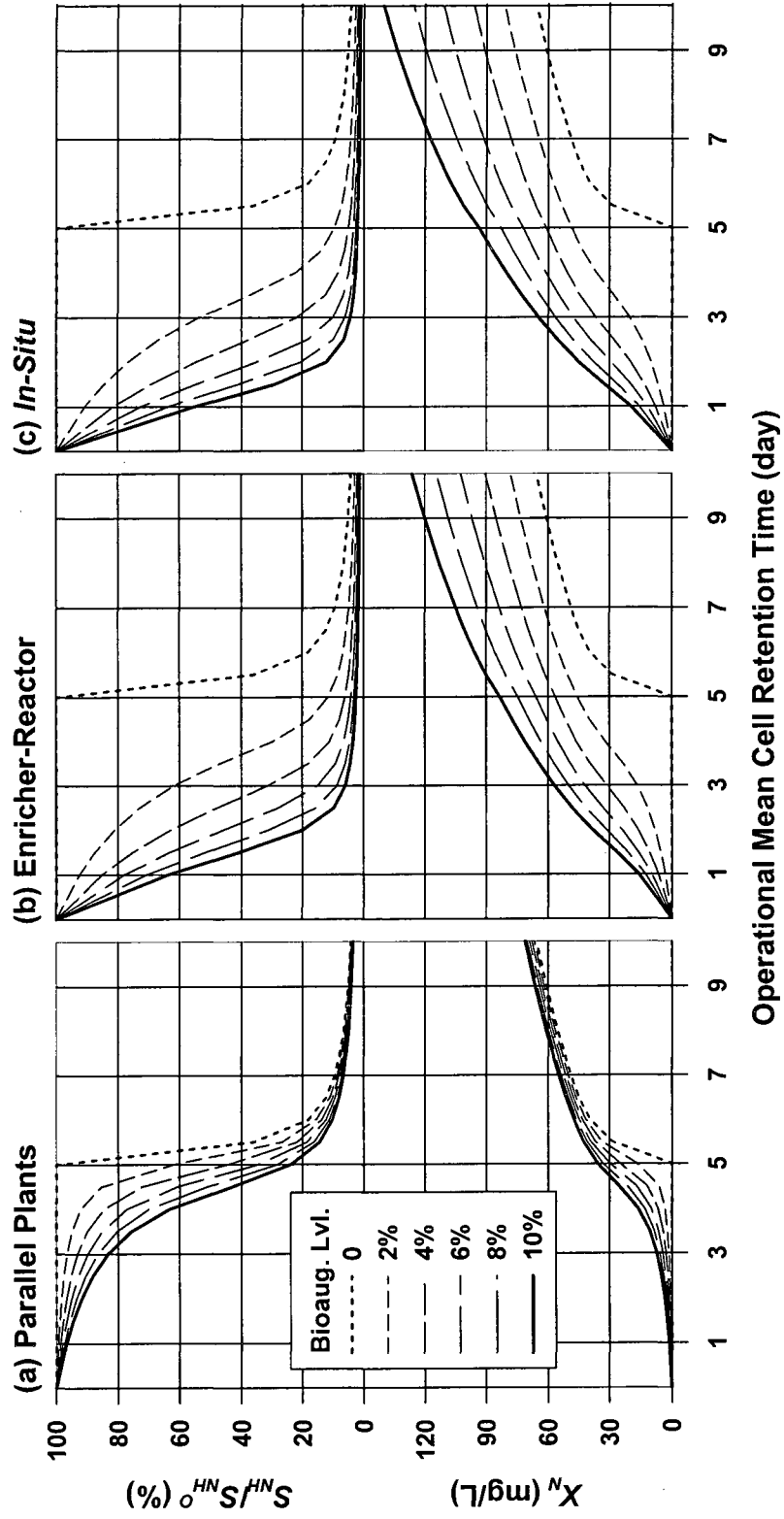


Figure 4.2 Simulation results of three bioaugmentation approaches: (a) parallel plant approach; (b) enricher-reactor approach; (c) *in-situ* approaches. Rows from top to bottom show the simulated percent nitrogen discharged and the concentrations of nitrifying biomass. Bioaugmentation levels of this study = 0~10%.

The sludge production (Eq. 3.8) in different augmenting reactors can be calculated as:

Parallel plants/ER approaches:

$$fX_N^{BR} = \frac{Y_N Q (S_{NH}^O - S_{NH})}{1 + K_{dN} \theta_x^l} \quad 4.11$$

Reaeration approach:

$$fX_N^{BR} = Y_N \cdot [Q^S S_{NH}^S - (RQ^R + Q^S) \cdot S_{NH}^{RA}] \quad 4.12$$

The sludge production of heterotrophic biomass uses a similar approach and the ratio of nitrifiers to total biomass can be calculated. The fraction of nitrifiers in the augmenting biomass is mainly a function of the nitrogen and COD loads in the augmenting reactor with the greatest fraction occurring if the augmenting reactor volume is large enough for complete nitrification.

4.3 Results and Discussion

4.3.1 Steady-State Analysis

Among the three bioaugmentation approaches, augmenting biomass from the parallel plant approach contains the lowest nitrifier biomass. The simulations show that the parallel plant approach is less efficient than the two other alternatives. This occurs because the augmenting biomass includes a large fraction of heterotrophs, which reduces nitrifier biomass. The feed to the parallel plant does not contain a high fraction of ammonia-rich feed, since it usually the ordinary wastewater. Figure 4.2 shows that the

parallel plant bioaugmentation approach can support approximately 15mg/L of nitrifier biomass when receiving 10% bioaugmentation rate at an MCRT (4 days) that would ordinarily be too short to nitrify. The nitrification efficiency of the augmented reactor increases from essential 0 to 40%. Under the same conditions the ER and *in-situ* approaches can sustain five times greater (75mg/L) nitrifier biomass.

To increase the nitrifier fraction in the biomass from a parallel plant, the high strength nitrogen wastewater should be diluted with as little ordinary wastewater as possible (Plaza et al., 2001). The case of two activated sludge plants in series, with the second plant performing nitrification, can be modeled as two plants, but bioaugmentation should be more successful, since the second plant will produce less heterotrophic waste biomass, with a higher proportion of nitrifiers. The wastewater treatment plant of DC-WASA, Washington DC, bioaugments in this way to improve nitrogen removal in the short MCRT first plant.

When the enriched culture is transferred from the augmenting reactor to the main reactor, nitrifying biomass will undergo increased cell loss. The increased loss of nitrifiers can be caused by multiple factors, such as changes of operation temperatures (Head and Oleszkiewicz, 2005), protozoa predation (Bouchez et al, 2000) or high decay rate due to the absence of sufficient substrate for growth (Leu, et al. 2009) . Increased cell loss in bioaugmented processes due to change of environments can be simulated by increasing of decay coefficient, since the decay coefficient K_d is a lumped parameter which accounts all reactions to reduce biomass concentration.

Table 4.1 Selected parameters in literature of on-site bioaugmentation studies

Bioaugmentation approaches	References	Bioaugmentation source reactor							Main reactor			
		θ_x day	T °C	S_N^0 Mg/L	Nitrifying Rate mg N/g VSS-h	Nitrogen Removal %	Type of process	θ_x^{op} day	θ_x day	Nitrifying Rate mg N/g VSS-h	Nitrogen Removal %	
1. Parallel plants	Neethling et al. 1998	12				92	HPO	4.6	>10		91	
	Plaza et al. 2001	5	9-10	290	7		CMAS		Before bioaugmentation (no nitrogen removal)		>90%	
		8	15	290	8	88	CMAS	0.8-2.6				
2. Enricher reactor	Head & Oleszkiewicz 2004	5	20-30	631	<u>1.8</u>	99	Batch	3.3		Failed		
		12	10	631	<u>4.3</u>	99	Batch	3.8	8.2	1.9	31	
		5	20	-	-	-	Batch	4	7.5-23	6.5-8.2	<u>98</u>	
	Zimmerman et al. 2004	5	20	1005	<u>63</u>	27	Batch		Before bioaugmentation (no nitrogen removal)			
		10	20	989	<u>36</u>	81	Batch					
		20	20	996	<u>9-14</u>	99	Batch					
		20	20	1440	<u>23-53</u>	99	Batch					
	Head & Oleszkiewicz 2005	5	20	631	<u>1.8</u>	99	Batch	3.4	11	1.2	39	
		5	2.5	631	<u>1.8</u>	99	Batch	3.4	31	0.5	15	
		5	30	631	<u>1.6</u>	99	Batch	3.4	55	0.3	10	
3. <i>In-situ</i> approach	Salem et al. 2003		No side-stream reaeration					7.5	<u>7.5</u>	3.63	76	
			23	456		74	BABE	8.7	<u>8.7</u>	2.71	69	
	Parker & Wanner 2007						BAR	6.9	<u>9.6</u>	4.33	92	
								5.1	9	<u>0.46</u>	83.8	
									60-100		>95	

*Note: underlined parameters are calculated values based on the relative references

Salem et al (2006) compared the decay of nitrifiers grown in SBRs treating high-N rejected water with their decay after augmenting an activated sludge process, under various oxidation states (i.e. aerobic, anoxic, or anaerobic). They found that the decay rate of the augmented nitrifiers can be ten times higher than in the SBRs (0.02/day versus 0.2/day). They suggested that the main reactor could be a hard environment for the augmented nitrifiers. Head and Oleszkiewicz (2005) augmented SBRs operating at 10°C using nitrifiers grown in SBRs over temperatures ranging from 10 to 30°C and found that nitrogen removal was inversely proportional to the difference in operating temperature (10°C) and growing temperature (10 to 30°C). Loss of nitrifying activity can be reduced when the operating temperature of enricher reactors are as close as possible to the temperature of the main reactor. Leu et al. (2009) simulated the increased decay for enriched exogenous biomass: when removed from a “substrate-rich” enricher reactor to the “substrate-poor” main reactor, the decay coefficients of enriched culture increased from 0.06 to 0.32/day, as the bioaugmentation rate was increased from 0 to 16%.

Table 4.1 shows the parameter values and removal rates of representative literature of the three bioaugmentation approaches. All studies showed significant increase of the MCRT for the augmented cultures and nitrification at MCRTs below normal nitrifier wash-out MCRT. In addition to their value for bioaugmentation, the parallel plants and enricher-reactor approaches nitrify the high strength return wastewater and at least one example in both approaches removed more than 90% nitrogen (Neethling et al., 1998; Plaza et al., 2001; Head and Oleszkiewicz, 2004, 2005; and Zimmerman et al., 2004). For

the *in-situ* approach, investigations mostly focused on whole processes and there is little documentation of the performance of the reaeration tank; only Salem et al (2003) reported the nitrogen removal in the reaeration tank, which accounted for 74% of the nitrogen removal. The loss of the augmenting cultures' viability or their decay rates in the main reactor were not quantified in most of the studies, but generally the nitrifying ability of the augmenting cultures decreased when they were transferred from the augmenting reactors to the main reactors (Head and Oleszkiewicz, 2004, 2005; Zimmerman et al., 2004).

4.3.2 Results of Dynamic Simulations

To illustrate the effects of bioaugmentation on transient removal rates, the Waßmannsdorf, treatment plant in Berlin Germany was simulated. Table 4.2 shows the process conditions and the wastewater compositions of primary effluent and sludge supernatant. The plant is a NDN plant with average capacity of 31,000 m³/day (or 8.2 MGD). The influent total COD is approximately 600 mg/L, and ammonia concentration is approximately 50 mg-N/L. The MCRT of the plant considering the total reactor volume is approximately 8 days in summer to 15 days at winter, and selector volume is approximately 50% of the total aeration tank volume. The plant provides full nitrogen removal during summers (19~22°C) but only reduced removal (0.5~9 mg-N/L) during the winters due to lower temperature (~13°C). Year-round influent and effluent data including flow rates, COD, ammonia, nitrate, DO, MLVSS, and pH were gathered as a part of normal process monitoring and used to calibrate our model.

Table 4.2 Wastewater properties of tested treatment plant

Properties	Primary effluent	Sludge supernatant
Influent flow rate (m ³ /hour)	1350	40
Sludge waste rate (m ³ /hour)	40	-
Temperature (°C)	20	25
Total COD (mg/L)	600	40
Soluble COD (mg/L)	285	40
NH ₃ (mg-N/L)	40	950

Table 4.3 shows the Monod kinetics and Table 4.4 shows the yield coefficient used in the model. The parameters were either selected from references (i.e. Poduska and Andrews, 1975, for the nitrifying species; and Salem et al., 2006, for decay of enriched cultures) or selected within the range of commonly observed parameters in treatment plant investigations or calibrated models (Gujer et al., 1999, and Metcalf and Eddy Inc., 2003, for heterotrophic growth and stored mass).

Table 4.3 Selected Monod kinetics for autotrophic species in simulations

Parameters	Symbol	Value
Biomass yield on NH ₃	Y	0.12
Maximum uptake rate of NH ₃ (1/day)	μ_{max}^N	1.0
Half velocity coefficient on NH ₃ (mg-N/L)	K_n	1.0
Decay coefficient (1/day)	K_{dN}	0.20
Temperature correlation factor	T_N	0.0844

Table 4.3 and 4.4 shows the selected parameter values that best fit the Waßmannsdorf plant data. Figure 4.3 compares the observations and simulation results for oxygen uptake rate (OUR) and effluent ammonia. Oxygen uptake rates (OUR, mg-DO/L/hour), measured by off-gas testing (ASCE, 1997), and effluent ammonia both fit well with measured data. During the monitoring period on two occasions the nitrogen load increased sharply and produced higher effluent ammonia concentrations (>1 mg-N/L), which the model successfully predicted. The model calibration approach using OUR and off-gas technique associated with liquid phase monitoring is similar to Yuan et al. (1993) method.

Table 4.4 Mass yield matrix used in simulations

Reactions	Simulated compounds					
	<i>S</i>	<i>X</i>	<i>DO</i>	<i>NH</i>	<i>NO</i>	<i>X_N</i>
Heterotrophic growth	-1	1.06	-0.22	-0.13		
Autotrophic growth			-4.10	-1	0.97	0.24
Decay		-1	-1.42	0.12		

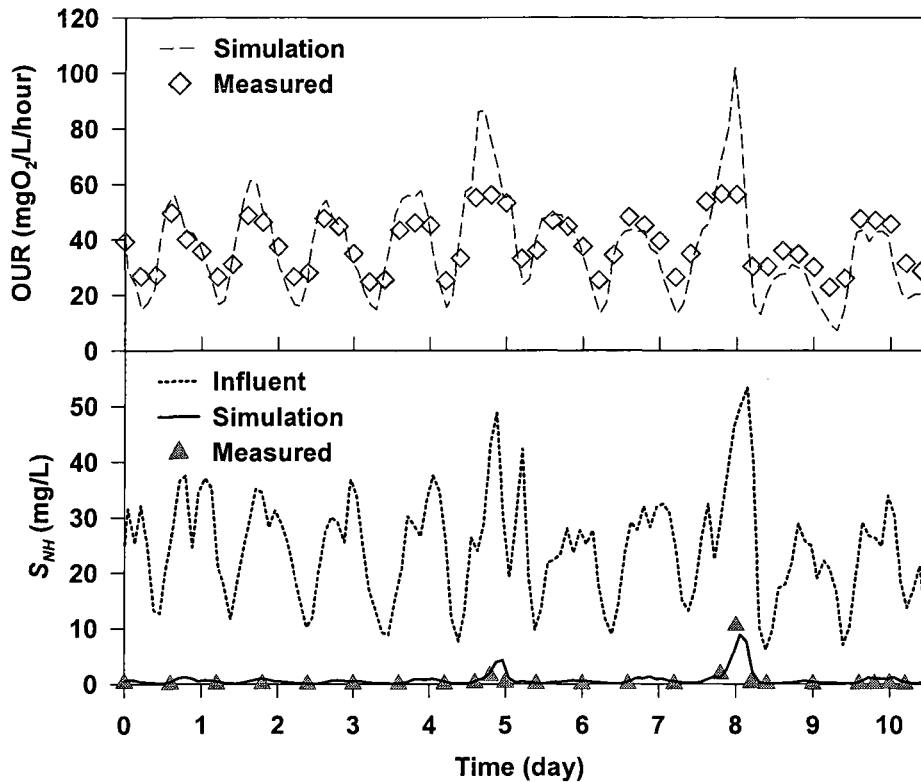


Figure 4.3 Simulation results of the studied wastewater treatment plant. Oxygen uptake rate (OUR, mg-O₂/L/hour), and effluent ammonia, are measured to validate the model.

Table 4.5 shows the hypothetical application of three bioaugmentation scenarios and a control case. The control study is the current operation with no bioaugmentation. Plant flows are doubled in the scenarios to create an over-loaded, poorly nitrifying condition to test the bioaugmentation alternatives. The scenarios and control study are compared at the same basis: additional aeration volume of 3000m³, total flow rates of sludge wastage (Q_w) and sludge recycle (Q_r) are the same, and the same temperatures are assumed for both the side stream and main reactors. The additional aeration volume is used to extend the aeration tanks for the control study and the parallel plant scenario. The aerobic MCRT (calculated neglecting selector volume) of the control process is reduced from 4 days to

2.4 days due to doubled plant flow, but increased to 2.9 days after tank extension. In the parallel plant approach, the existing aeration tank is divided into two compartments and the extra aeration volume is added to create a long-MCRT process, providing an aerobic MCRT of 3.4 days. For ER and *in-situ* approach, the extra volumes are used for the enricher-reactor and reaeration tank, respectively. The ER is designed as an SBR, receiving sludge centrate, and the reaeration tank is a CFSTR, receiving recycled sludge and high-strength return water. The fraction of recycled sludge that flows through the reaeration tank is adjustable, and when there is no flow of the recycled sludge added to the reaeration tank, the *in-situ* approach becomes an ER approach.

Table 4.5 Designed bioaugmentation scenarios under overloaded conditions

Scenarios	Main reactor		Side reactor	
	Volume (m ³)	MCRT ⁺ (day)	Volume (m ³)	MCRT (day)
1. No bioaugmentation	16450	2.9	0	-
2. Parallel plants	6725	2.4	9725	3.4
3. Enricher reactor	13450	2.4	3000	3.1
4. <i>In-situ</i> approach	13450	2.4	3000	1.0

+ MCRT calculated neglecting selector volume

Figure 4.4 shows the simulation results of various bioaugmentation scenarios under stressed conditions. When the plant flow is doubled (200%) and at lower temperature (15°C), average effluent ammonia nitrogen of the control case (increased aeration volume and no bioaugmentation) normally ranges from 4 to 12 mg-N/L but increases to

approximately 30 mg-N/L at the peak load on day 8). The effluent ammonia of the parallel plant approach is the combined effluent of the two lines: the side with longer MCRT (augmentation source) always performs better. The parallel process provides only limited improvement for N-removal, reducing approximately 1 to 2 mg-N/L lower of the effluent ammonia than no bioaugmentation. Both ER and *in-situ* provide improved N-removal. Full nitrification can be achieved at the low loading period of each day, the ammonia break through at the daily peak is approximately 30% of the control case. At the peak load on day 8, only marginal benefit is provided. The ER and *in-situ* approach provide nearly equal ammonia removal, but at all times are better than the control and parallel plant cases.

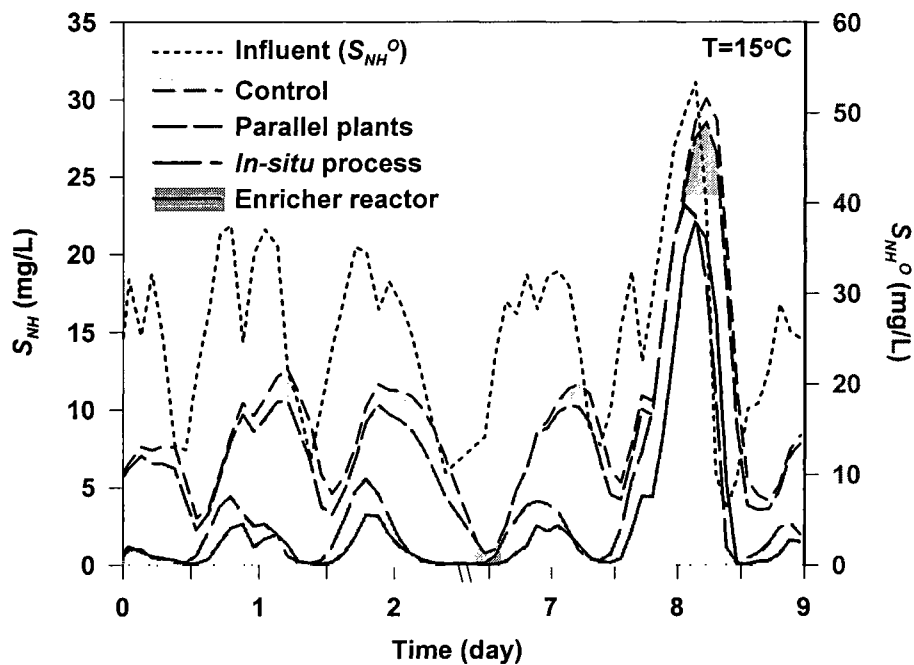


Figure 4.4 Simulation results of nitrogen removal under stressed conditions (doubled plant loadings, lower temperature) and with various bioaugmentation scenarios

4.3.3 Effects of Temperature and Aeration Volumes

Sensitivity analyses were performed to investigate the effects of changing temperature and aeration volume on the performances of various bioaugmentation scenarios. Figure 4.5 (a) and (b) show the average percent removal of ammonia, and the biomass fraction of nitrifying cultures over the total active MLVSS under different operation temperatures, respectively.

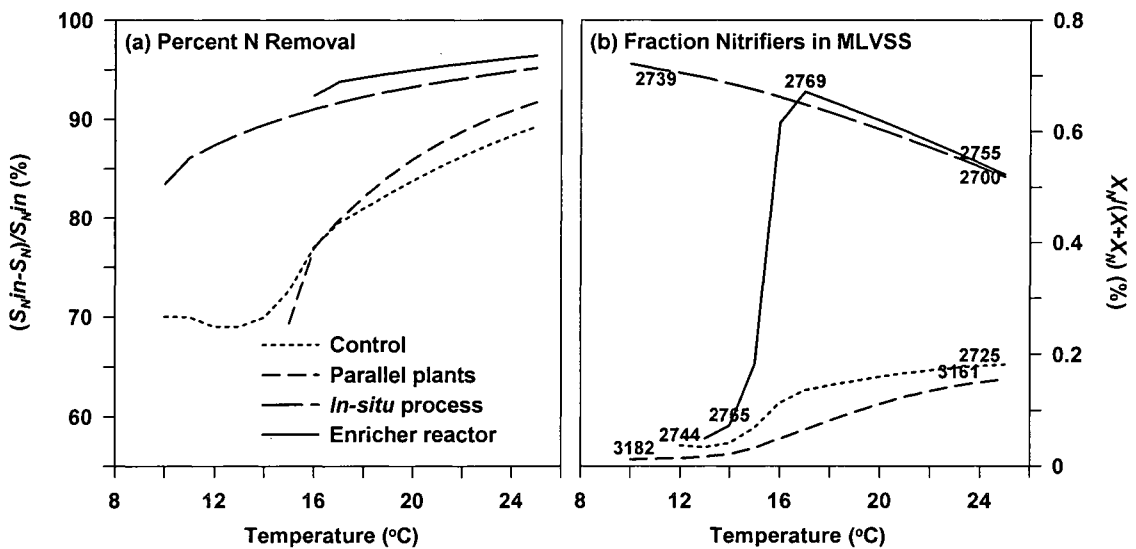


Figure 4.5 Simulations of various bioaugmentation scenarios under changing temperature of the main reactors. Two parameters are plotted against operation temperatures: (a) percent removal of ammonia, and (b) fraction of autotrophic species over MLVSS (number labels). Bioaugmentation scenarios are compared at the same level of seed loadings and aeration volumes (including control with no bioaugmentation).

Ammonia removal in all approaches increases with operation temperature, as expected.

For the control study, ammonia removal increases from 70 % at 14°C to approximately 87% at 25°C. The parallel plant approach provided lower ammonia removal than the control when the operating temperature is lower than 16°C, which is possibly due to

incomplete nitrification in the long-MCRT side. The parallel plant approach provided slightly higher N-removal than the control when the temperature was more than 16°C, and provided approximately 90% removal at 25°C. Both the *in-situ* approach and ER approach improve ammonia removal. For the *in-situ* approach at least 85% of ammonia can be removed when operation temperature is more than 10°C, and at 25°C the removal increases to 95%. The performance of the ER approach is similar to the *in-situ* approach, but a key difference is the effect of temperature below 16°C; below 16°C, the ER approach begins to lose nitrification and cannot bioaugment the main reactor. As shown in Figure 4.5(b), the nitrifying biomass declines as the temperature decreases below 17°C. The parallel plant approach has the highest MLVSS (numbers along lines indicate MLVSS concentrations in mg/L).

Figure 4.6 shows the simulated effects of changing the additional reactor volume (the original value of 3000 m³ corresponds to 22% of the total volume) on the performance of different bioaugmentation scenarios at 20°C. The extra volume increased average removal from 80 to 88% for the control case. The parallel plant approach provides slightly higher ammonia removal than the control but is only distinguishable from the control below 50% increase. The ER approach and *in-situ* approach provide significantly higher ammonia removal than the other alternatives: approximately 95% removal can be achieved, but both approaches require a minimum additional aeration volume to be effective (10% for *in-situ* and 20% for ER). The percent nitrifying cultures of total MLVSS are shown in Figure 4.6(b) and support the other results. The parallel plant

approach has the highest MLVSS and lowest fraction of nitrifying culture, as discussed earlier. The critical additional aeration volumes for *in-situ* and ER approaches are negatively related to operation temperatures. When temperature decreased from 20°C to 12°C, the requirements of additional aeration volume increased from 10 to 20% for *in-situ* process and to 50% for the ER approach.

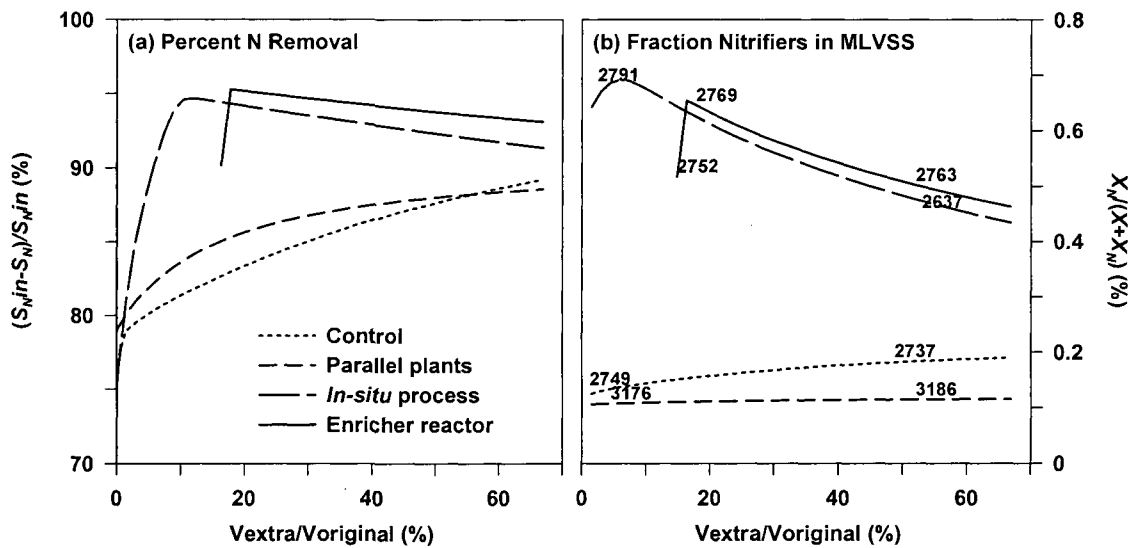


Figure 4.6 Simulations of various bioaugmentation scenarios under changing extra aeration volumes. Two parameters are plotted against percent additional volumes: (a) percent removal of ammonia, and (b) fraction of autotrophic species over MLVSS (number labels). Bioaugmentation scenarios are compared at the same level of seed loadings and operation temperature.

4.3.4 Comparison between *In-situ* and ER Approaches

Among the three main bioaugmentation approaches, the parallel plant approach may be the simplest to operate but operates at the greatest MLVSS concentration. This occurs because the overall MCRT of the parallel process is higher than the control case. This

means that the burden on the clarifiers can be higher. The benefit of the parallel process is that it can treat additional carbonaceous load. In many cases, the need for a parallel plant is not only to nitrify but to treat the additional load from subscriber growth. Therefore a parallel plant may be completely justified for this reason and its ability to bioaugment, albeit limited, is “free.” The *in-situ* and ER approaches will provide improved nitrification efficiency but will not increase the carbonaceous treatment capacity.

Simulation results showed that both *in-situ* approach and ER approach provided beneficial effects to N-removal, but which approach is more applicable will likely be plant-specific. The *in-situ* approach shows higher efficiency at low temperature and requires less aeration volume to grow the nitrifying biomass by reaeration, but the ER approach performs slightly better at higher temperature and above a minimum volume increase of approximately 22%.

Growing nitrifying species separately from the recycled sludge isolates the nitrifiers from toxic or nitrifier-inhibitory compounds in the process influent. Smith et al. (2008) showed that biodiversity of nitrifying species was better preserved in the isolated ERs than in the reaeration reactors, when both received the high ammonia sludge supernatant as enrichment substrate. Using molecular biology, they showed that the *in-situ* approach produces a monoculture of the nitrifying species in the augmented reactor, whereas multi-cultures were always found in reactors augmented by off-line SBRs (ER). It may be

easier to manage the alkalinity loss in the *in-situ* approach since the entire recycle stream is available to buffer the pH decline. Alternatively, the Enricher, if operated as an SBR, may be able to nitrify and denitrify.

4.4 Conclusion

1. Bioaugmentation is a proposed technique to improve nitrogen removal and this chapter compares three major approaches: 1) the parallel plant approach; 2) ER approach; and 3) the *in-situ* approach. All three approaches increase the MCRT of nitrifying biomass and provide improvements for nitrogen removal, but the *in-situ* and enricher reactor approaches are significantly better than the parallel plant approach.
2. Simulation results of a full-scale treatment plant defined the critical reaction temperature and the minimum volume for bioaugmentation scenarios to be effective. For the specific plant sizes considered, the *in-situ* approach requires at least 10°C and the ER approach 16°C to provide the beneficial effects of bioaugmentation. The minimum volume of reaeration tank for the *in-situ* approach is approximately 10% of the main reactor whereas 20% additional volume is required for the ER approach.
3. The *in-situ* approach and ER approach are both beneficial to improve ammonia removal and are comparable in performance, but which is more suitable to upgrade a full-scale “carbon-only” process requires plant-specific investigation. The *in-situ* approach will likely be more useful at lower temperature while the ER approach will likely be more advantageous in the presence of inhibitory compound(s).

5. MONITORING AERATION EFFICIENCY

5.1 Introduction

Municipal wastewater treatment plants have been converted to fine pore diffusers which have resulted in significant energy savings. Fine pore diffusers work well but suffer from fouling and scaling problems, which rapidly decrease performance and significantly increase energy costs (Rosso and Stenstrom, 2006a). Fouled diffusers not only suffer a significant drop in oxygen transfer efficiency (OTE, %) but also have increased back pressure, typically defined as dynamic wet pressure (DWP, includes pressure drop as well as pressure to overcome surface tension). The combination of decreased efficiency and higher pressure drop increase power consumption and often degrade process performance. Due to different wastewater composition and treatment operations, the cleaning frequency of diffusers is site-specific, and may not be easily observable without off-gas measurements.

The off-gas technique developed by Redmon et al. (1983) is the process water OTE measurement with the highest accuracy and precision (ASCE, 1997), and it is the only technique that can determine OTE in real-time. This technique measures the oxygen content in the air leaving the surface of the aeration tank, and the OTE is calculated by the mass balance of oxygen between ambient air (20.95% mole fraction) and off-gas. Libra et al. (2002) applied the off-gas method to compare the performance of several different aeration devices. Rosso et al. (2005) showed that transfer efficiency is a function

of diffuser air flux and mean cell retention time (MCRT), based upon more than 100 tests at more than 30 plants. The impacts of fouling on plant economics and the need for diffuser cleaning have also been described (Rosso and Stenstrom, 2005).

Although OTE measurement using the off-gas technique does not require air flow rate measurement, it can be easily measured and used to calculate the oxygen transfer rate (OTR, kg O₂ transferred per hour), or the oxygen uptake rate (OUR, mg O₂/L/hour). Oxygen uptake rate is useful since it indicates the oxygen requirement, or the metabolism of microorganisms. With a time-series measurements of OUR, transient conditions in the bioreactor can be evaluated for activated sludge modeling and/or process control, such as optimization of the sludge recycle rate, contacting pattern and plant configuration (Stenstrom and Andrews, 1979); to verify the storage function of substrates (Goel et al., 1998; Third et al., 2004), the simultaneous uptake and growth of the heterotrophic and autotrophic biomasses (Beccari et al., 2002; Marsili-Libelli and Tabani, 2002), nitrification (Guisasola et al., 2003), denitrification (Puig et al., 2005; Third et al., 2004), and endogenous respiration (Koch et al., 2000).

Respirometers are the most common way of measuring OUR and have as their goal monitoring OUR in real-time over a wide-range of DO concentrations. These instruments may be limited to well-controlled environments since they usually measure at only a single point in an aeration tank. Examples of respirometry for process control include off-line procedure and steady-state calculations (Beccari et al., 2002; Guisasola et al.,

2003) and *in-situ* instrumentation for real-time control (Spanjers et al., 1998; Marsili-Libelli and Tabani, 2002; Sin et al., 2003), and are also being applied to sequencing batch reactors (SBR) (Baeza et al., 2002; Third et al., 2004; Puig et al., 2005). The difficulty of using these methods relates to the cost and maintenance requirements of a respirometer. The theory and benefits are sound but the methodology has not been applied routinely to a large number of treatment plants.

Off-gas analysis has been shown as an appropriate method to access the oxygen uptake rate under varying process conditions, and does not require a specific DO concentration for measurement. Therefore a lightly loaded process at higher DO concentration or an overloaded process at near zero DO concentration can be evaluated. Yuan, et al. (1993) and Tzeng et al (2003) applied off-gas measurements of the covered high purity oxygen (HPO) activated sludge process reactors to calibrate the oxygen transfer functions in a structured model and to evaluate process control systems. Jenkins et al. (2004) used real-time off-gas analysis to calculate the change in air flow needed to affect a change in DO concentration, which was then used in a feed forward DO control strategy.

Schuchardt et al. (2005) used real-time off-gas analysis for OTE and off-gas carbon dioxide concentration to separately estimate the heterotrophic and nitrifying loads.

Off-gas monitoring has rarely been coupled with mathematical modeling to reduce aeration costs. Off-gas monitoring can provide real-time measurement for several of the models' state variables, which creates a validated model to calculate aeration power cost. Aeration power is a function of aeration efficiency, DWP, power rates, and plant loads.

Power rates often vary during the day, with late afternoons during warm months typically being the most costly. Plant flows vary with human activities, and large diurnal fluctuation in flow rate and wastewater composition are typical. If the increases in power consumption are in phase with higher power rates, then the cost of aeration can be quite large. Alternatively, if the peak in aeration power can be made to occur when power costs are minimal, savings are possible. The availability of real-time monitoring data of OTE, load and power cost can be combined in a model that can be optimized to minimize power cost, within the constraints of feasible plant operation.

In our experience, of the more than 30 plants evaluated with off-gas testing, only one plant managed any aspect of their operations to take advantage of off-peak power costs. Part of the reason for this may be the unavailability of OTE measurements as well as inflexibility in process operations. The availability of simple, inexpensive off-gas analyzers (Stenstrom et al., 2007), increasing emphasis on conservation, and more frequent use of variable power pricing policies by power companies, should encourage treatment plant operation to maximize power consumption during low-price periods, typically late at night. The ability to take advantage of low cost power will depend on both the availability of data as well as flexibility in plant operation. Off-line equalization of wastewater flows, which has most often been used previously to improve pollutant removal efficiency or facilitate plant operations, is one tool for reducing peak loadings.

The objective of this chapter is to demonstrate how real-time OTE monitoring can be used to reduce power costs. A simplified design of an off-gas analyzer with simplified digital electronics to provide real-time data is presented. A case study of a 10 MGD plant that has offline equalization is used to illustrate the potential savings. The plant was evaluated in multiple off-gas tests which were used to construct a demonstration of how to reduce power costs. A time-series analysis of the field experiments is presented and includes measurements of OTE, OTR, α factors in 24-hour cycles. Two examples are presented: the first shows the advantages of diffuser cleaning and the second shows the benefits of off-line equalization.

5.2 Material and Methods

5.2.1 Field Experiments

Field tests were performed in a full-scale treatment plant with the capacity of approximately 38,000 m³/day (10 MGD or 125,000 population equivalent). The plant uses an activated sludge process that nitrifies and denitrifies using the modified Ludzack-Ettinger (MLE) concept, and the MCRT is controlled to approximately 7 days. Figure 5.1 shows a schematic diagram of the tested plant and the hood positions for 24-hour tests, and Table 5.1 shows the operating conditions of the plant. The total volume of aeration tanks is approximately 14,800m³. The anoxic zones comprise 33% of the total aeration tank volume. Two polishing tanks follow the four parallel MLE tanks and comprise 27% of the total volume. All aeration zones are equipped with fine-pore, membrane strip diffusers. The primary effluent contains 300 mg/L of total COD and 40

mg-N/L of ammonia on average, and is equalized by diverting peak flows to an off-line storage tank (not shown in Figure 1), which are then pumped back during the low flow period. In this way peak loads on the process are reduced from 2800 m³/hour to a maximum 1800 m³/hour. For the 24 hour tests, primary effluent samples were collected hourly and analyzed for dissolved organic carbon (DOC), chemical oxygen demand (total COD), and ammonia nitrogen (NH₃-N). Organic nitrogen was measured using the plant's composite sampler and was assumed constant during the day for the purposes of the simulations.

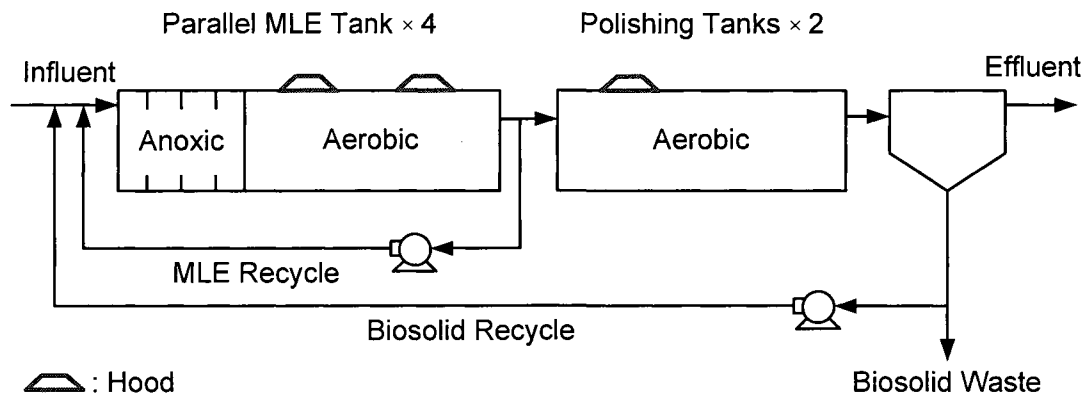


Figure 5.1 Schematic Diagram of the tested treatment plant (headworks, primary clarifier, equalization basin and disinfection facilities not shown)

An initial off-gas test and two sets of 24-hour tests were performed. The initial test was performed eight months after the diffusers were installed and was used to confirm the aeration system's performance. Hoods (2.2 m² area) were used in eight positions in the initial test which lasted only eight hours. Only three hood positions (see Figure 5.1) were used in the 24 hour tests, and the initial test was used to select hood positions that were representative of the tanks. The 24-hour tests involved only one process tank (Tank

4) and one polishing tank. The first 24-hour tests evaluated the diffusers under normal operation conditions, 13 months after the diffusers were installed, and the second 24-hour test was performed immediately after *in-situ* liquid acid cleaning, after 21 months of operation. The flow-weighted average values among the three hood positions are shown. The oxygen efficiency (OTE), air flux, DO, and the α factor were measured or calculated by the three hood positions.

Table 5.1 Operation background of tested treatment plant

Properties	Values	
Volume of anoxic zone (m ³)	4,800	
Volume of aerobic zone (m ³)	10,000	
MCRT (day)	7	
pH	7.2	
MLVSS (mg/L)	2,300	
Flow conditions	Range	mean
Influent flow rate (m ³ /hour)	0550 – 2800	1550
Equalized flow rate (m ³ /hour)	0615 – 1800	1550
Total COD (mg/L)	155 – 350	300
DOC	34.5 – 83.5	57
COD/DOC	4.66 – 7.28	5.73
Ammonia (mg-N/L)	27 – 57	40
Organic Nitrogen (mg-N/L)	4 – 18	10
Wastewater temperature (°C)	22 – 27	24
Ambient air temperature (°C)	4 – 36	21

To apply the 24 hour tests to the entire plant, the OTEs and OURs for each hood position were air-flow weighted to create an average for Tank 4 and polishing basin 1. The averages were applied to the other tanks and basin. This is reasonable since the diffusers were installed at the same time, no cleaning had been performed, and the influent flow split among the tanks was equal (confirmed in the initial off-gas test).

5.2.2 Design of a Real-Time Off-gas Analyzer

Figure 5.2 shows a schematic of the automated monitoring system. It is similar to the original analyzer (Redmon et al.) but has several important differences to facilitate automation. The majority of the off-gas (~ 99%) travels through the flow tube and bypasses the rest of the instrumentation. The gas flow rate is measured by a hot wire anemometer or mass flow meter that produces no pressure drop in the flow tube upon insertion. This avoids the use of a vacuum cleaner to overcome the pressure drop associated with rotameters, and simplifies measurement since pressure balancing is not required. A small fraction (~16 mL/sec) of the off-gas passes through a drying column and a fuel cell that produces a signal that is proportional to oxygen partial pressure. A relay alternates flow between off-gas and air, which serves as a reference gas. The pressure balancing valve is used to provide the same pressure drop as the drying column and small flow meter. An op-amp is used to condition the signal which is then recorded. The output alternates between off-gas and reference gas, and the reference gas provides calibration for each measurement.

The measuring process can be switched on and off to provide the desired number of measurements, and one measurement every 15 minutes appears to be adequate to capture all the process changes. For routine process monitoring, such as proposed in this study, a fixed hood in a single position can be used. Multiple hoods or hood positions must be used if it is desired to obtain the spatial variability of OTE and OUR across an aeration tank. Development of this analyzer is funded by the California Energy Commission (CEC) and Southern California Edison Inc. The CEC insists that the products of the research project be in the public domain, and they are pursuing a contract for construction of inexpensive analyzers. More than one version of the real-time analyzer has been used in this project and they were compared to the conventional analyzer for quality assurance. A real-time analyzer is needed for 24-hour measurement, since it is impractical to keep operators working continuously. Stenstrom et al (2007) provides more detail on the analyzer construction, including more specific information on the components.

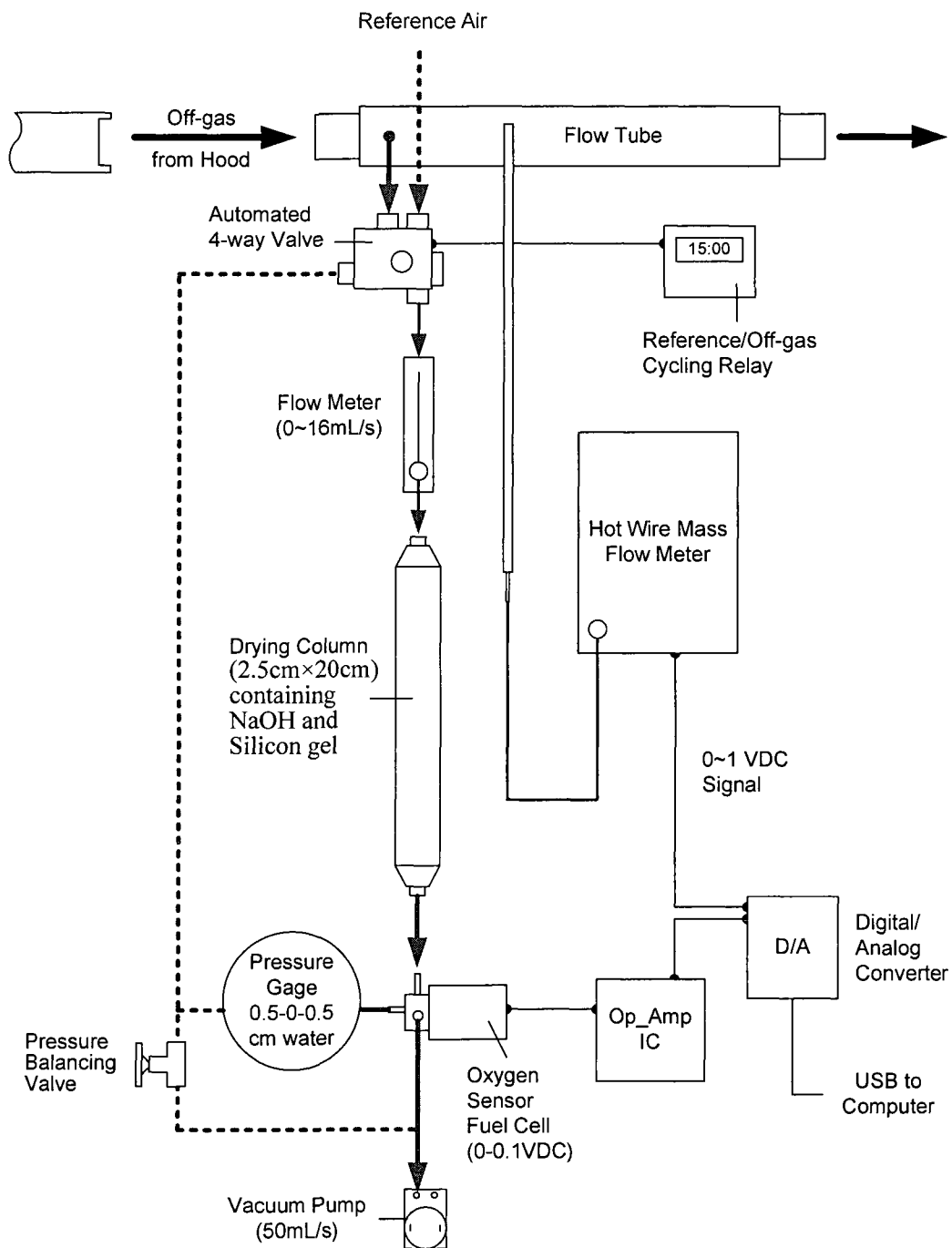


Figure 5.2 Schematic of a real-time off-gas monitoring system.

5.2.3 Oxygen Uptake Rate Model

A dynamic model was developed to simulate the oxygen balance and energy conservation opportunities for a 24-hour cycle. The modeling approach was based on Lawrence and McCarty (1970) using Monod kinetics. It was desired to create the simplest possible model that adequately simulates the OUR. This allows a number of simplifications, such as considering total COD as opposed to soluble and particulate COD separately. The model simulates the transient conditions of five components: carbonaceous substrate (total COD), ammonia, nitrate, heterotrophic biomass, and nitrifier biomass. The volumetric flow rate of equalized primary effluent and pollutant concentrations measured from hourly grab samples were used to calculate the total oxygen demand, or the oxygen uptake rate (OUR). In this study, OUR and OTR are different by definition: OTR represents the gas transfer capacity of aeration system, and OUR is the mass oxygen per unit volume consumed to degrade certain pollutants. The difference between the two parameters in a continuous-flow stirred tank reactor (CFSTR) is a function of non-steady state conditions as well as the sources of oxygen demand, and can be expressed as follows:

$$\frac{dDO}{dt} = \frac{1}{\theta_H} (DO^0 - DO) + OTR - OUR_N - OUR_C - OUR_D \quad 5.1$$

where θ_H = hydraulic retention time (hour)

DO^0 = influent dissolved oxygen concentration (mg/L)

OUR_C = OUR of substrate consumption (mg/L-hour)

OUR_N = OUR of nitrification (mg/L-hour)

OUR_D = OUR of biomass decay (mg/L-hour)

Wastewater aeration is commonly controlled at near constant DO, and the time constant associated with oxygen transfer ($\sim 1/K_{La}$, with K_{La} typically ranging from 2 to 10 hr^{-1}) is rapid compared to the time constants for substrate and biomass change. Therefore, the derivative term of DO in Eq.5.1 can be assumed to be negligible, transforming the equation to a steady state or algebraic calculation.

In this study, OTR in Eq.5.1 was calculated from off-gas tests. Data collected from the three hood positions were compared to clean water data using relationships described in the ASCE/EWRI standards (2006, 1997), as follows:

$$OTR = \alpha \cdot \left[\frac{\beta C_{\infty}^* - DO}{C_{\infty 20}^*} \right] \cdot \theta^{T-20} \cdot SOTR \quad 5.2$$

where β = correction factor for dissolved solids (1/day)

θ = temperature correlation coefficient

C_{∞}^* = saturated dissolved oxygen concentration (mg/L)

super- or subscript of 20 = standard conditions at 20°C

The relationships between substrate consumption and biomass growth are based on Monod kinetics. For example, the mass balances of ammonia (S_{NH}) and autotrophic biomass (X_N) can be expressed as:

$$\frac{dS_{NH}}{dt} = \frac{1}{\theta_H} \cdot (S_{NH}^O - S_{NH}) - \frac{k_N S_{NH}}{K_N + S_{NH}} \cdot X_N \quad 5.3$$

$$\frac{dX_N}{dt} = \frac{1}{\theta_H} \cdot (X_N^O - X_N) - \frac{X_N}{\theta_X} + Y_{XN}^{NH_3-N} \cdot \frac{\mu_N S_N}{K_N + S_N} \cdot X_N - K_d \cdot X_N \quad 5.4$$

where k_N = maximum uptake rate of NH_3-N (g NH_3-N /gCOD-day)

K_N = half velocity coefficients of NH_3-N (mg-N/L)

K_d = decay coefficient (gVSS/gVSS-day)

θ_X = mean cell retention time (day)

$Y_{XN}^{NH_3-N}$ = mass yield of X_N on NH_3-N (gCOD/g NH_3-N)

Balances for heterotrophic substrate consumption and nitrite oxidation can be written in a similar fashion. Since nitrite was never observed, the nitrogen balance can be further simplified by considering it as a single step process with ammonia oxidation limiting.

The OUR needed to consume each substrate is equal to the growth rate with appropriate stoichiometric yields, and the consumption for ammonia can be written as follows:

$$\text{OUR}_N = Y_{\text{DO}}^{\text{NH}_3\text{-N}} \cdot \frac{k_N S_{\text{NH}}}{K_N + S_{\text{NH}}} \cdot X_N \quad 5.5$$

where $Y_{\text{DO}}^{\text{NH}_3\text{-N}}$ = mass oxygen demand of nitrification (gO₂/gNH₃-N)

Heterotrophic OUR is calculated in a similar fashion but the yield term is slightly different, since the carbonaceous substrate (S) is defined in units of total COD (mg/L) or oxygen equivalents (Stenstrom and Andrews, 1979), as follows:

$$\text{OUR}_C = Y_{\text{DO}}^S \cdot \frac{k_S S}{K_S + S} \cdot X \quad 5.6$$

where Y_{DO}^S = mass oxygen demand of heterotrophic growth (gO₂/gCOD)

k_S = maximum substrate uptake rate (gCOD/gCOD-day)

K_S = half velocity coefficients of heterotrophic growth (mg/L)

Similarly, the oxygen consumption of biomass decay can be calculated by the decay coefficient as:

$$\text{OUR}_D = Y_{\text{DO}}^X \cdot K_d \cdot X \quad 5.7$$

where Y_{DO}^X = oxygen demand of decay (gO₂/gCOD).

The oxygen consumption from the decay of nitrifier biomass is assumed negligible.

Therefore, OTR can be obtained by substituting the oxygen consumption of COD

degradation (Eq.5.5), nitrification (Eq.5.6), and cell decay (Eq.5.7) into equation 5.1, and can be calculated as:

$$\text{OTR} = \frac{1}{\theta_H} \cdot \text{DO} + Y_{\text{DO}}^S \cdot \frac{k_S S}{K_S + S} \cdot X + Y_{\text{DO}}^{\text{NH}_3\text{-N}} \cdot \frac{k_N S_{\text{NH}}}{K_N + S_{\text{NH}}} \cdot X_N + Y_{\text{DO}}^X \cdot K_d \cdot X \quad 5.8$$

Equation 5.8 uses total COD and the rate must be the average of the rates for soluble and particulate substrate. Deviation from this rate will occur a significant portion of the COD is stored and later oxidized, since the simple model cannot mechanistically simulate storage products. Deviation was observed between the modelled and measured OUR, and we attribute it to the delayed oxidation of storage products. The precise definition of the storage products can be debated. The ASM 1 and ASM 3 and the Clifft and Andrews models have differing treatments of storage products. For the purposes of this study it is sufficient to notice that there is a delayed OUR associated with storage products. The delay in the exertion of OUR will be important because it delays or modifies the peak OUR.

The model was specifically developed to study the oxygen balance between oxygen demand and oxygen transfer, and to serve as a base to calculate aeration energy. We deliberately chose a model with few state variables in order to validate a simple linkage from measured data (off-gas analysis and a series of influent grab samples) to energy cost, by assuming constant DO and single reaction rate for influent COD.

5.3 Results and discussion

5.3.1 The 24-Hour Experiments

Figure 5.3 shows the volumetric plant flow before and after equalization, α SOTE, α factor, COD and air flow rate (AFR) measured or calculated for the first 24-hour transient test. The AFR increases dramatically during the periods of high loading period to maintain the required DO. The increase is larger than simple stoichiometry requires because of the reduced efficiency of the diffusers at higher AFR. This plant has a phase shift between COD and flow, and it is partly attributed to the off-line equalization, which fills when the primary influent COD is high and empties when the primary influent COD is low. The α factor is also changing and is lowest when the COD is the highest. This occurs because the surfactants (detergents, soaps, fats and oils) that are present in the influent and contribute to COD, take longer to degrade at higher concentration and have greater influence on aeration (Rosso and Stenstrom, 2006b). The reduction of efficiency with increased COD concentration is unfortunate, since the period of greatest aeration rate occurs at the lowest aeration efficiency. The top panel shows the wastewater flow rate and the impact of off-line equalization; the peak flow is maintained less than 1800 m³/hour (or 11.4 MGD) by storing the primary effluent during high flow periods. Results of the 24-hour test 2 showed similar pattern as test 1.

The large change in α factor should have special significance for designers. The alpha factor ranged from about 0.25 to 0.55. Aeration systems should be designed with the needed “turn up” and “turn down” capacity to accommodate such changes.

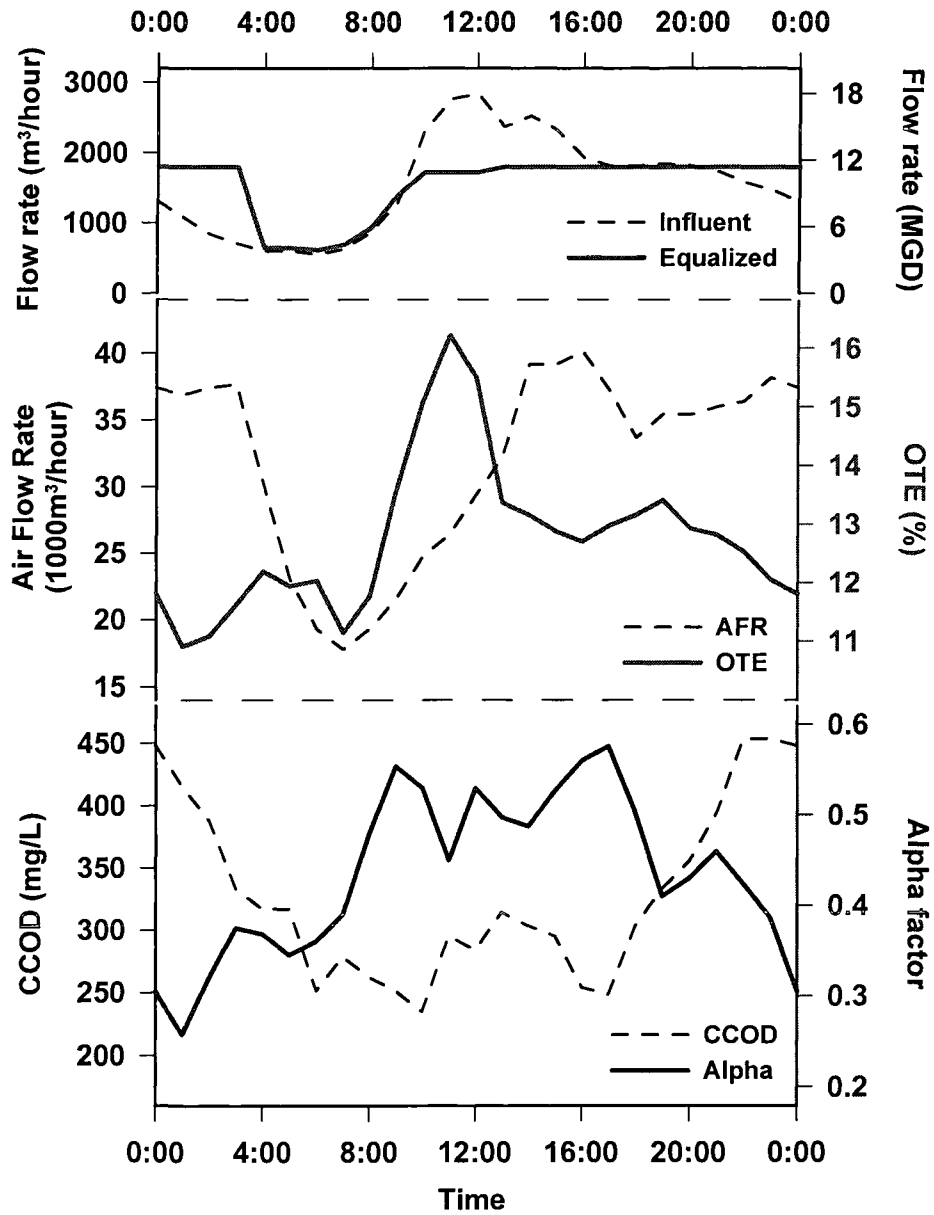


Figure 5.3 Influent, partially equalized flow rate, oxygen transfer efficiency (OTE), air flow rate (AFR), load, and alpha factor during a 24-hr cycle.

Figure 5.4 shows the data from the two 24-hour tests, before and after cleaning, plotted as a function of the α SOTE and air flux (air flow rate per unit of diffuser area, $\text{m}^3 \cdot \text{hour}^{-1} \cdot \text{m}^{-2}$ or SCFM/ft²). The α SOTE is calculated from the OTE data shown in the middle panel of Figure 5.3 by adjusting the temperature, DO concentration, etc. to standard conditions.

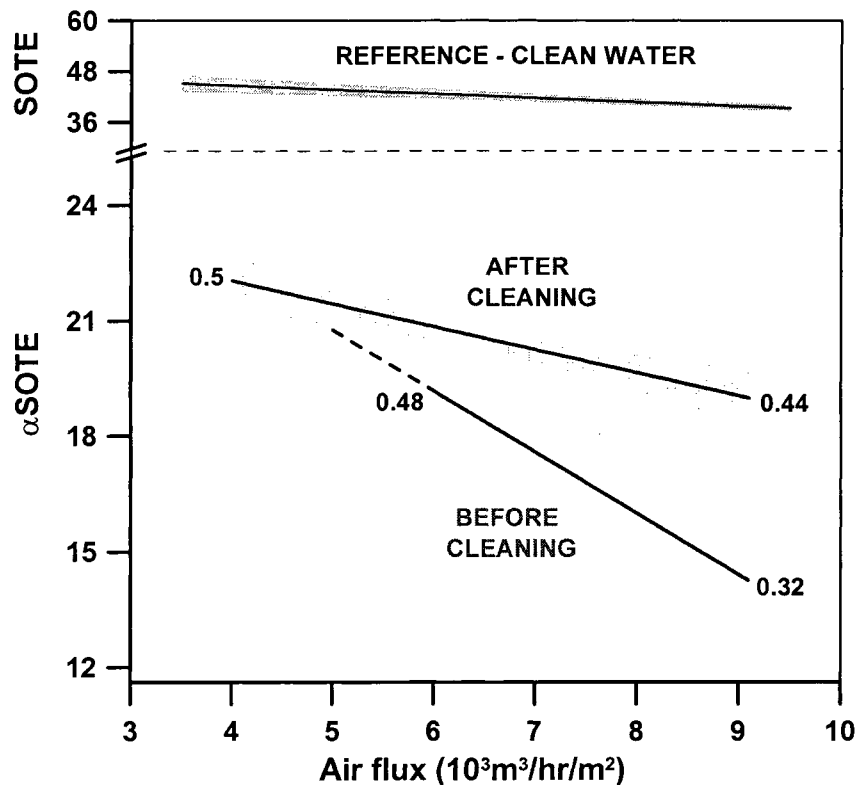


Figure 5.4 Correlation between α SOTE, alpha factors, and diffuser air flux for both 24 hour tests. (curved zones represents 85% confidence interval and alpha factors are shown as number labels).

The clean water test results are shown at the top of Figure 5.4, and were measured in a warranty shop test. The α factors were calculated by dividing the α SOTE by the SOTE for the same diffuser air flux. The differences between clean and fouled α factors (fouled

α factors are often written as α_F factors) is dramatic with α for fouled diffusers declining at a greater rate with increasing air flux. This occurs because there are fewer open pores or slits with fouled diffusers, and the air flow per pore becomes greater, increasing bubble size. This and other impacts on alpha have been described in our other work (Rosso et al., 2005, Rosso and Stenstrom, 2006b).

5.3.2 Oxygen Demand Simulation

The previously described model was used to calculate the total OUR for microbial reactions. Table 5.2 shows a matrix formulation of the kinetics and yield coefficients of pollutants and treatment by-products for all the reactions, including heterotrophic growth, nitrification, and biomass decay.

Table 5.2 Matrix of mass yield from stoichiometry.

Reactions	Reacting compounds or products					Reaction kinetics, (mg/L/hour)
	S	S _{NH}	DO	X	X _N	
	gCOD	g-N	gO ₂	gCOD	gCOD	
Heterotrophic growth	-1	-0.04	-0.51	0.49		$\frac{k_S S}{K_S + S} \cdot X$
Nitrification		-1	-4.33		0.17	$\frac{k_N S_N}{K_N + S_N} \cdot X_N$
Biomass decay		0.08	-1	-1		$K_d \cdot X$

Table 5.3 shows the validated Monod kinetics used in our simulations. The parameters are within the range of commonly observed parameters (Metcalf and Eddy Inc., 2003, Poduska and Andrews, 1975) and were manually adjusted to provide the best fit with off-gas measurements.

Table 5.3 Monod kinetics of activated sludge model at 20°C.

Parameters	Value
1. Heterotrophic species	
Maximum uptake rate, k_s , gCOD/gCOD-day	6
Half-velocity of substrate, K_s , mg/L	30
Yield coefficient, Y , g COD/g COD	0.5
Decay coefficient, K_d , gVSS/gVSS-day	0.06
2. Autotrophic	
Maximum uptake rate, k_N , gNH ₃ -N/gVSS-day	1.08
Half-velocity of substrate, K_N , mg-N/L	1.05
Yield coefficient, Y_N , gCOD/gNH ₃ -N	0.17
Decay coefficient, K_{dN} , gVSS/gVSS-day	0.12

Figure 5.5 shows the oxygen demand and oxygen transferred over a 24-hour cycle. The graph shows the three calculated OURs: heterotrophic growth, nitrification, and biomass decay. The OTR, measured by off-gas analysis, should equal the total OUR, but in the low loading part of the day, 3 AM to 10 AM, more oxygen transfer occurs that is predicted by the model. The explanation is the delayed OUR associated with metabolizing storage products or particulate COD, which have a slower reaction rate, and is not included in the model. This creates a delay or shift in transfer and is frequently

observed in full-scale plants. The top of Figure 5.5 shows the transient MCRT, which is a dynamic calculation of MCRT. The biomass waste rate is held constant, but other process aspects are not constant.

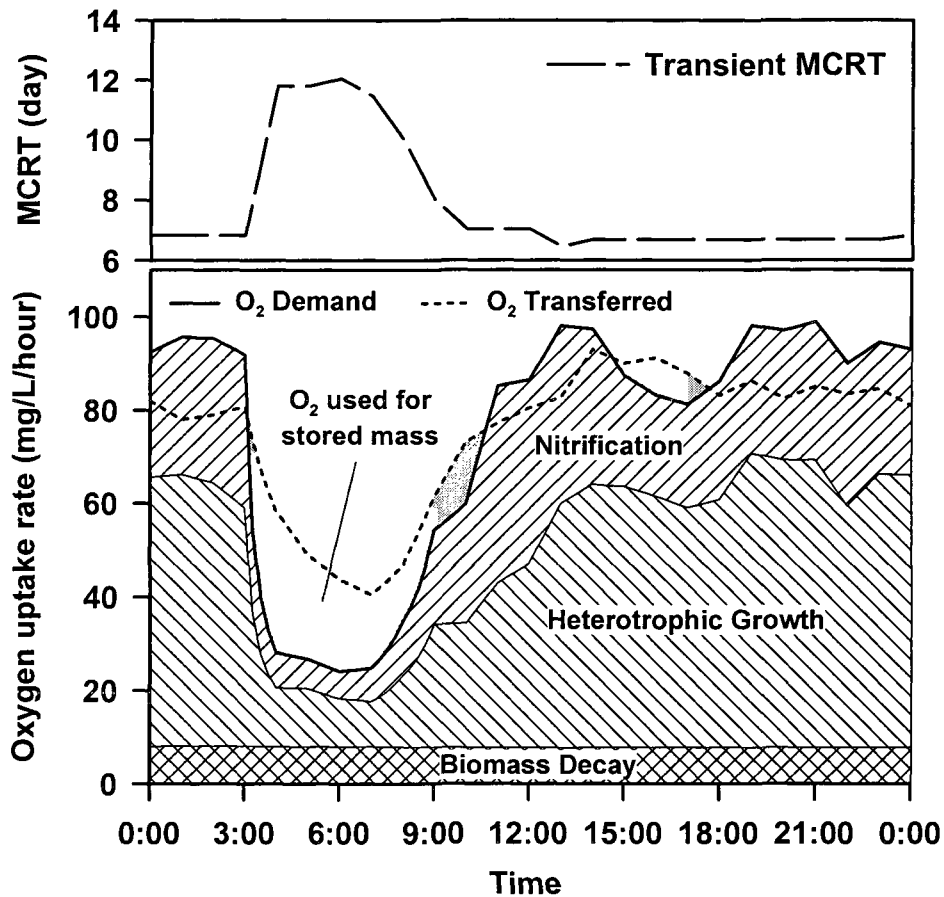


Figure 5.5 Simulated oxygen uptake rate versus the rate of oxygen transferred (measured by off-gas tests) during the 24-hour cycle.

Equation 5.8 provided a good fit between observed OTR and OUR with the exception of peak and low flow periods. This occurs because the simple Monod model does not include the production and consumption of storage products (Andrews and Stenstrom,

1979). This is not necessarily a fault, since it allows for the observation of changes in storage product concentration, which becomes important when trying to equalize aeration energy consumption.

The degradation of stored mass during the low-loading period is caused by the changing F/M (food and mass) ratio. Substrate consumption in activated sludge is performed by a two-stage function: 85% of the organic substrate can be rapidly incorporated into the biomass but is not immediately degraded (Heukelekian et al., 1947), and are preserved as stored mass for later cell metabolism. Many structured models have adopted this two-stage reaction to perform better fitness with real conditions (Busby and Andrews, 1975; Stenstrom and Andrews, 1979, Cliff and Andrews, 1983; Gujer et al., 1999). The commonly used Lawrence and McCarty (1970) approach was selected for simplicity and the ability to show the importance of storage products. Although it does not simulate the rapid uptake of substrate as performed in structured models (Henze et al., 1987, Melcer et al., 2003, Tzeng et al., 2003), it provides sufficient information to calculate the oxygen demand of nitrification and heterotrophic growth.

The impact of storage product formation is to help equalize the OUR. After equalization, approximately 10% of the heterotrophic uptake occurs during the low flow period, which reduces the maximum OUR and increases the minimum OUR. This is helpful for controlling the plant, since the “turn up” and “turn down” ratios are reduced.

5.3.3 Remarks on Air Supply System

Current control techniques for aeration systems are typically based on feedback signals provided by dissolved oxygen (DO) probes immersed in the aeration tanks. Dissolved oxygen concentration is an effect of oxygen transfer, and is an important indicator of proper process conditions. When the DO is too low, bacterial metabolism is inhibited and the sludge composition may change, reducing the treatment efficiency or even causing process failures (i.e., low DO sludge bulking). Conversely, high DO may pose problems for denitrification zones (which require anoxic conditions), and represents excessive energy consumption (Ferrer, 1998; Serralta et. al., 2002). Many studies have focused on improvement of the DO control systems (Ferrer, 1998, Ma et. al., 2004). To optimize the energy consumption of aeration systems, the best blower control strategy is to supply the minimum amount of process air to the wastewater treatment, yet meeting substrate removal requirements. The adoption of a low-cost, on-line off-gas instrument should be considered. Off-gas testing measures the exact mass transfer, not only an effect of it, therefore offering a new tool for accurate energy calculations.

5.3.4 Application I. – Energy Savings by Optimal Cleaning of Fine-Pore Diffusers

A time-series of off-gas measurements offers a tool for monitoring the decline in α SOTE with diffuser fouling. This application shows a strategy to estimate the energy costs for diffuser system before and after cleaning processes using the results of our off-gas experiments. Diffuser maintenance is site-specific and can be between once every six months to more than 2 years, and the net present value of the energy wastage can be

calculated. The most economically favourable cleaning schedule can be determined, and the methodology has been demonstrated by Rosso and Stenstrom, 2006a. Table 5.4 shows the average oxygen transfer data gathered from the three off-gas tests: Test 0 is the reference test, which was performed 8 months after diffuser installation; Test 1 was performed five months after Test 0 and Test 2 was performed immediately after cleaning. Our results suggest that after five months' operation oxygen transfer efficiency decreased from 18.3% to 16.3%, providing an increase of air flow from 240,000 m³/day to 290,000 m³/day. The cleaning procedure recovers the α SOTE from 16.1% to 18.6%, reducing energy requirements from 235 kW to 193 kW, or approximately 18% of the total power consumption. Furthermore, since Test 1 was performed eight months before diffuser cleaning and the conditions of diffuser fouling could be more serious during this period, the actual total saving must be greater than the calculated savings.

Table 5.4 Results of off-gas tests (averages from various time and hood positions).

Properties	Test 0	Test 1	Test 2
Diffuser conditions	Reference	Before cleaning	After cleaning
a. Plant conditions			
DO (mg/L)	1.6	1.9±0.6	2.5±1.0
Temperature (°C)	27	22±0.3	27±0.3
b. Measured by off-gas tests			
α SOTE (%)	18.3	16.3	18.5
Air flux (10 ³ m ³ /s/m ²)	1.75	2.03	1.78
c. Calculated parameters			
Operational air flow rate (m ³ /day)	240,000	290,000	240,000
Aeration energy (kW)	192	235	193

The net present worth of the energy wastage can be compared to the cleaning costs, after Rosso and Stenstrom (2005, 2006a). The power wasted (bar plot), normalized per kg of oxygen transferred, in the tested aeration tank is shown in Figure 5.6. The power wastage is defined as the power consumption exceeding the initial power requirement for new diffusers. The total power requirements (solid line), increases after start-up due to diffuser fouling. The diffuser cleaning frequency can be easily defined by comparing the cumulative wasted power costs and the site-specific cleaning costs. If the cumulative wasted power costs approach the cleaning cost, cleaning should be performed.

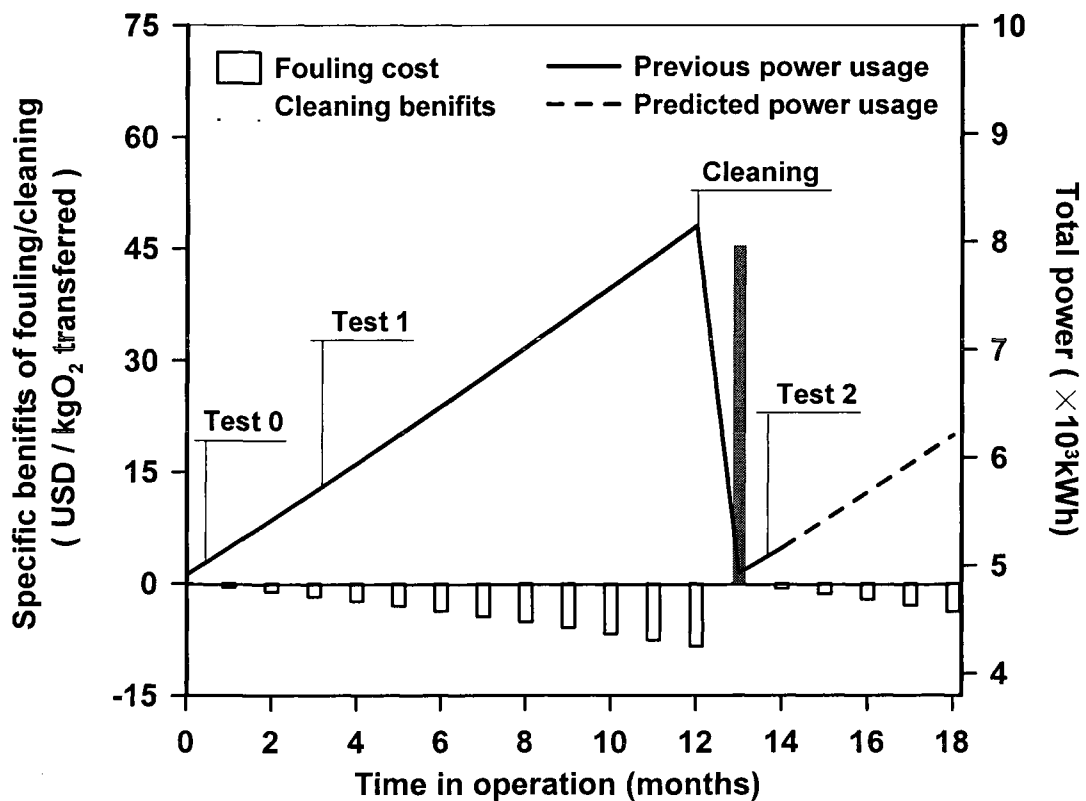


Figure 5.6 Energy expenditure of aeration cost. Total power consumption is calculated by the off-gas test results, which total power = initial power + power wasted.

5.3.5 Application II. – Optimization of the Peak Power Loadings

In addition to quantifying energy wastage due to diffuser fouling, the real-time off-gas test provides useful information to assist plant operation. As discussed, aeration energy is a function of oxygen requirements, which vary with plant loads and during the diurnal load cycle. Equalization tanks are commonly used in wastewater treatment to compensate peak flows and to improve system stability for process control. Typically, equalization attempts to provide a uniform influent volumetric flow into the treatment process. In geographic locations where power cost varies with time of day or season, cost-savings and power savings are not necessarily the same, as the following example illustrates. In this case, different strategies for off-line equalization should be considered.

Figure 5.7 shows the hourly blower power drawn in the 24-hour cycle, obtained by the off-gas analysis (solid line), and the hourly industrial power rate (bars) in hot periods (peak rate) and average periods (average rate) (Southern California Edison, 2007). It is clear that the power consumption is not optimally managed: the high loading period of power consumption is in phase with the high-power-cost period during the afternoon (1pm-8pm), and the cheapest power costs always occur at low loading period (4am-10am). Significant savings can be realized if the plant flow is shifted to diurnal periods associated with lower power rates.

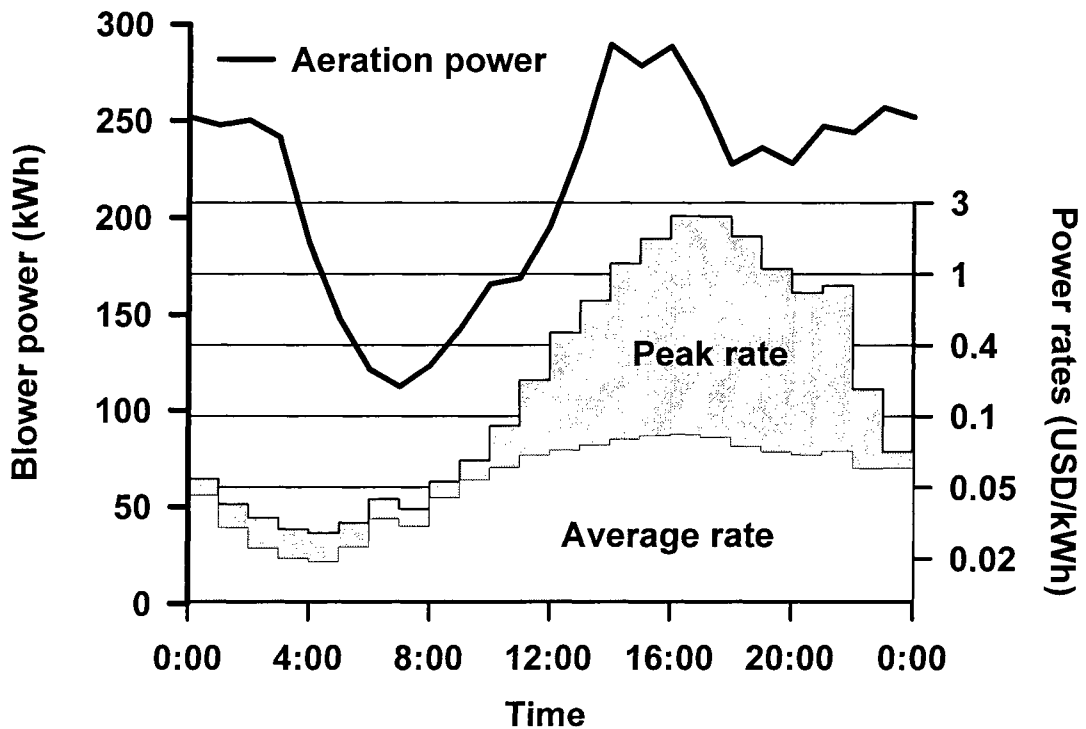


Figure 5.7 Energy consumption of blowers versus the hourly power rate (California, U.S.).

Using the previously described model, three off-line storage scenarios were simulated: 1) current operation to limit peak plant flow to 1800 m³/hr; 2) increased storage to create a constant plant flow, and 3) further increased storage to shift the peak power consumption to periods with lowest power rate. Current operation requires approximately 5000 m³ of storage while options 2 and 3 require the storage volume to increase to 7,500 and 10,000 m³, respectively. The power costs were calculated based on the power consumption times the power rates, for both peak and average conditions. In the simulations, the influent flow rates were slightly adjusted to simulate the extra OTR during the low loading period. Alpha factor is assumed to be constant, and SRT is the same as the current operation (7days). Figure 5.8 shows the flow rates and power cost, but only for the peak power rate

condition, while Table 5.5 shows power cost for both peak and average conditions, The case with no equalization was also simulated and shown in Table 5.5. The patterns of power costs for the low cost periods appear similar in the graphs because the rate is so low that the differences are not obvious; however, for high rate periods the optimized flow provides significant reduction in cost, which is obvious in Figure 5.8. It can be noted that longer hydraulic retention time in the aeration basins themselves can help create an equalized OUR, as shown in the middle panel of Figure 5.8.

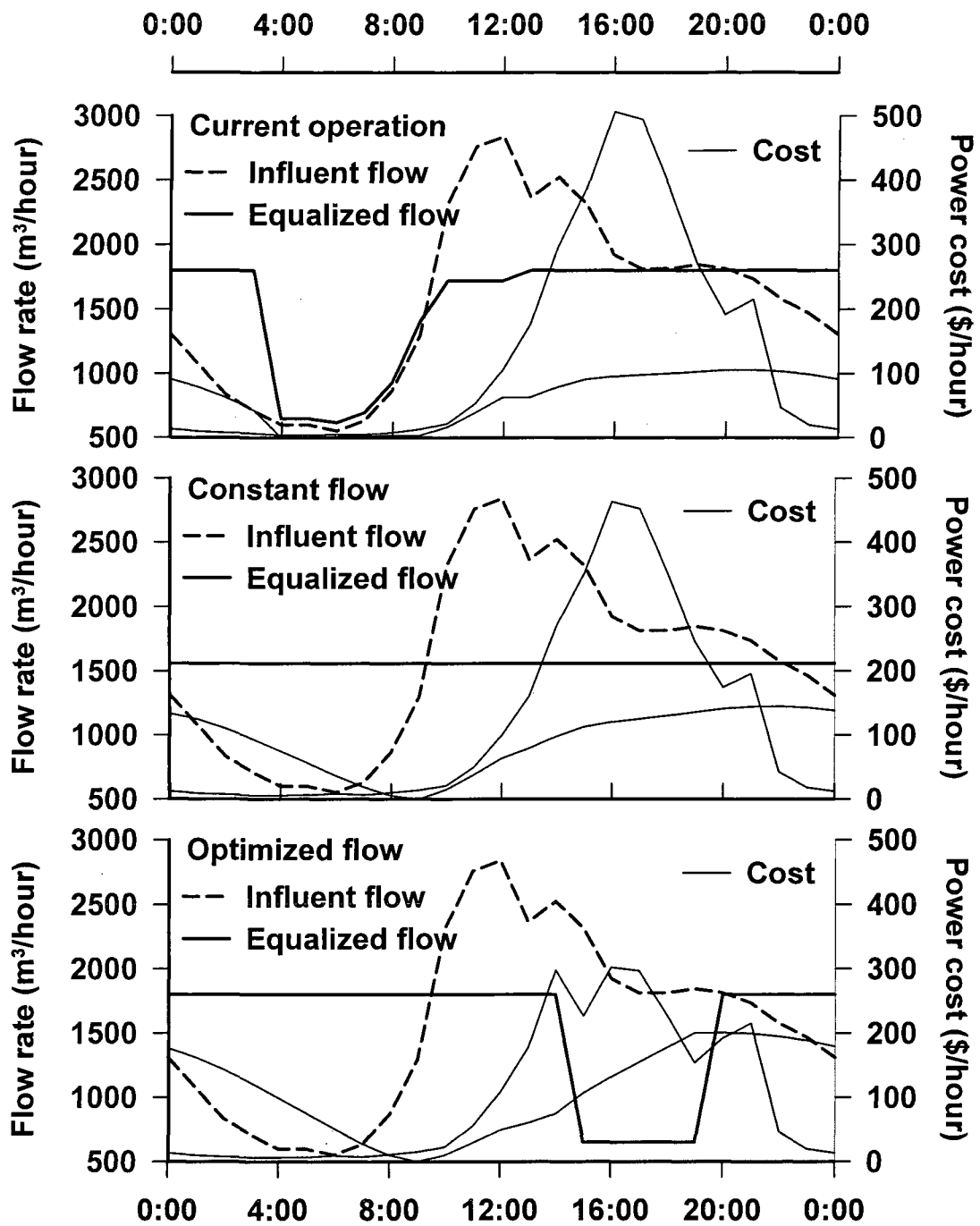


Figure 5.8 Energy saving practices by flow control. Shaded area represents the volume wastewater stored in the equalization basin.

Table 5.5 summarizes the power cost and the potential savings created by flow equalization. The results show significant savings of the three storage scenarios using flow equalization compared to the reference scenario with no flow storage. The various potential savings are shown for peak and average conditions, as well as a yearly estimate, based on two months at peak rate and five months each of summer and winter rates. The current operating strategy of limiting peak flows can save up to 8% during the peak season, 5 to 6% during average winters and summers, and 6% on a yearly basis. If the flow can be adjusted to shift the low loading period, which ordinarily occurs at night, to the power rate peak hours in the afternoon, up to 31% of savings can occur in the peak season, or 16% on a yearly basis. In the studied treatment plant with an average ambient temperature of 21°C, treating 38,000 m³/day (10MGD), or approximately 125,000 P.E., moving the peak to the early morning will create \$80,000 of power savings every year. Perhaps the most important conclusion is that complete equalization to constant plant flow, which greatly simplifies plant operation and improves effluent quality, produces significant power savings as well.

The power savings has an additional advantage for reducing green house gas emissions. Power companies typically maximize usage of their most efficient plants and minimize the use of their least efficient plants. Typically, night time operation uses as much hydro and nuclear sources as possible, and the oldest, least efficient plants (i.e., stand-by plants) are operated only during peak periods in the hottest weather. The heat rate for the most efficient natural gas burning plants is approximately 10,550 kJ/kWh (10,000 BTU/kWh).

Table 5.5 Aeration costs of different plant operation strategy.

Operation Scenarios	High flow (m ³ /hour)	Low flow period	Wastewater stored (m ³)	Power cost (USD/1000m ³)			Potential savings			Yearly Savings	CO ₂ Credit (g/kWh)
				Peak	Avg Summer	Avg Winter	Peak	Avg Summer	Avg Winter		
0. No equalization	2550	12am-7am	0	95.1	10.0	10.5	-	-	-	-	-
1. Current operation	1800	3am-7am	5,000	87.7	9.4	10.0	8%	6%	5%	6%	19
2. Constant flow	1550	-	7,500	80.5	8.9	9.7	15%	11%	8%	10%	36
3. Optimized flow	1800	2pm-6pm	10,000	65.9	8.5	9.5	31%	15%	10%	16%	59

Note: Unit of power cost = U.S dollars per unit volume thousand cubic meter wastewater treated

Peak = summer season (June-Sept.) with temperature higher than 35°C

Summer = summer season with average temperature = 24°C

Winter = winter season (Oct.-May) with average temperature of 15°C

CO₂ production for unit heat generation = 0.049 gCO₂/KJ

The least efficient gas burning plants in routine daily operation have a heat rate of approximately 13,700 kJ/kWh (13,000 BTU/kWh). During high demand times such as in the summer when system load is very high, the stand-by plants are used, which have a heat rate of approximately 19,000 kJ/kWh (18,000 BTU/kWh). The ability to shift peak power consumption to the early morning saves power and also reduces green house gas emissions by increasing the utilization of the most efficient power plants. If the flow is shifted to the low loading period, approximately 1200 kJ/kWh (1120 BTU/kWh) can be saved. The CO₂ savings or credit for equalization ranges from 19 to 59 g of CO₂ per kWh.

5.4 Conclusions

4. This chapter illustrates the ability of a real-time off-gas analyzer to provide useful information to characterize plant operation and in particular to estimate aeration power consumption.
5. The results of 24-hour experiments showed that OTE vs. OTR, and COD vs. α factor are negatively correlated, which is the first observations of α factors as a function of diurnal plant loading. The results provide supporting evidence for previous observations that load (i.e., surface active agents) depresses oxygen transfer and α factors.
6. The impact of loading and diffuser air flow rates in response to increased loadings result in large changes in α factor. Designers need to be aware of the changes and the need to provide process flexibility to allow operators to respond to varying α actors.

7. The energy savings from diffuser cleaning were demonstrated using off-gas tests at different times (before and after cleaning). After cleaning, aeration power was reduced at least 18% due to increased oxygen transfer efficiency.
8. Flow equalization reduces aeration cost by 5 to 31% depending on the season and the available volume for storage. Completely equalizing flow to a constant rate saves nearly as much as shifting the peak loading to the low power rate periods (early morning hours). Yearly savings for the anticipated number of peak, summer and winter periods is 6% for peak limiting, 10% complete equalization and 16% for peak shifting.
9. The required off-line storage, as a percent of average flow was 13 % for peak limiting, 19% for complete equalization and 27% for peak shifting. The actual requirement will be site specific but should be similar.

6. QUANTIFYING NITROGEN REMOVAL BY MONITORING OFF-GAS O₂/CO₂

6.1. Introduction

Nitrification/denitrification (NDN) with activated sludge process (ASP) is the most popular technique to remove nitrogenous pollutants in municipal wastewater. The activated sludge process consists of many different types of active bacteria, often called “active mass” in structured ASP models, and which can have a wide range of biodegradation mechanisms for different types of pollutants. Consumption of carbonaceous compounds and denitrification are generally performed by heterotrophic bacteria, and nitrification is performed by autotrophic bacteria. The performance of an ASP highly depends on bacteria activities. In aeration basins, many criteria must be carefully maintained to provide a suitable habitat for microorganisms, especially for nitrifiers, such as proper pH (Painter, 1970, 1983), temperature, sufficient oxygen concentration (Stenstrom and Poduska, 1980) and adequate mean cell retention time (Poduska and Andrews, 1975).

Among these growth factors, an important aspect of process operation is the oxygen transfer efficiency (OTE). Nitrification failure can easily occur if sufficient oxygen can not be supplied for nitrifying bacteria. The off-gas procedure developed by Redmon et al. (1983) is the most accurate method to estimate OTE and has been widely applied for testing aeration basins under process conditions (ASCE, 1997). The test can measure the various off-gas mole fractions and it is common to only measure oxygen mole fraction.

The CO₂ mole fraction can be easily measured if an additional analyzer, such as a CO₂ absorption tube or infrared sensor is used.

The by-products of the treatment of carbonaceous and nitrogenous compounds in activated sludge processes are different, and can be measured by off-gas analysis, the relative amounts of CO₂ produced and oxygen consumed can become the basis for a new method of analyzing nitrification efficiency. The goal of this paper is to understand the relationships and develop a method for estimating nitrification efficiency of a full-scale ASP bioreactor. The proposed method is based upon the differences in CO₂ production. The molar fraction of carbon dioxide in the off-gas should be greater if nitrification is limited, or the ratio of nitrogenous compounds in total BOD is smaller.

The main problem of the proposed method is the “super-saturate” of dissolved carbon dioxide due to change of pH. At normal pH, carbon dioxide concentration in gas phase is a function of dissolved CO₂ concentration, influent alkalinity, and pH. When pH changes, dissolved carbon dioxide acts as a buffer and shifts the fraction between carbonic acid (CO_{2q}) and bicarbonate (HCO₃⁻) to adsorb or release hydrogen ions. Since CO₂ transfer relates to the concentration of carbonic acid, increasing fraction of bicarbonate creates a supersaturate condition and most of the dissolved CO₂ stay in the processing water.

Hellinga et al., (1996) calculated the ratio of carbon dioxide production rate (CPR) and oxygen uptake rate (OUR) for different wastewater compositions. The authors demonstrated that the off-gas measurement is useful to evaluate the reactivity of

carbonaceous substrate (i.e. COD/TOC ratio), but they also suggested that the changes of CPR was very small due to bicarbonate equilibrium when estimate nitrification. Similar discussions were also presented in other studies (Nogita et al., 1982; Minkevich and Neubert, 1985; Spérandio and Paul, 1997).

Experimental and modeling works have been developed in many studies to evaluate or simulate the supersaturated conditions of dissolved CO₂ in bioreactors. Pratt et al. (2003, 2004) used titrimetric technique with off-gas analysis, called on-line titrimetric and off-gas analysis (TOGA), to calculate the effect of changing pH in batch systems.

Hydrogen ion production rate (HPR) was measured by monitoring the shift of pH due to *in-situ* titration, and CPR was monitored in the off-gas using a mass spectrometer. By knowing HPR and CPR, the transfer rate of oxygen, nitrogen and carbon dioxide was calculated using stoichiometry. Weissenbacher et al. (2006) proposed a simplified model to take account the effect of pH shift or change in alkalinity to off-gas CO₂. Instead of simulate alkalinity and pH shift, the authors used on-line pH measurements as input signals to practically estimate CPR. This modelling approach is similar to what will be used in this paper.

The goal of this paper is to demonstrate how online off-gas O₂/CO₂ measurements can be used to evaluate nitrification performance. Online off-gas tests were performed in full-scale wastewater treatment plant, and the relationships between oxygen uptake, carbon dioxide production, change of pH, and nitrification performance were investigated.

The mathematical model was built to simulate the temporal concentrations of the major components in wastewater and its exhausted gas, and off-gas measurements were applied to validate the model. The model was used to create a profile between off-gas O₂/CO₂ and reaction status of carbonaceous substrate/ammonia, and also to predict ammonia discharge.

6.2 Materials and methods

6.2.1 Off-Gas Tests

Off-gas test is the process measurement method commonly used to estimate of fine-pore diffuser efficiency (ASCE, 1997). The method uses a floating hood on the surface of aeration basin to collect off-gas and the mole fractions of O₂ and CO₂ are measured. In the standard guideline of ASCE, oxygen transfer efficiency (OTE, %) is calculated by comparing the oxygen content in the supplied air and the off-gas; and the alpha factor (α) is evaluated by taking the ratio of standardized OTE of process water conditions to clean water condition. Off-gas tests can also measure the air flow rate passing through the hood. The total air flow of the aeration system can be estimated by weighting the area of hood to tank surface.

Oxygen transfer rate (OTR, mg/L/hour) can be calculated by comparing to clean water data of standard conditions (20°C, 0 mg/L of dissolved oxygen, 1 atm, 0 salinity), using relationships described in the ASCE/EWRI standards (2006, 1997), or by multiplying OTE to air flow rate if available, as followed:

$$OTR = \frac{O_2^{IN} - O_2^{OUT}}{O_2^{IN}} \cdot \frac{Q_g^{HOOD}}{V^{TANK}} \cdot \frac{Area^{TANK}}{Area^{HOOD}} \quad 6.1$$

and CO₂ transfer rate (CTR, mg/L/hour) can be calculated by a similar fashion:

$$CTR = \frac{CO_2^{OUT} - CO_2^{IN}}{CO_2^{IN}} \cdot \frac{Q_g^{HOOD}}{V^{TANK}} \cdot \frac{Area^{TANK}}{Area^{HOOD}} \quad 6.2$$

6.2.2 Background of tested Treatment Plant

Field experiments were performed in the wastewater treatment plant of Waßmannsdorf, Germany. Table 6.1 shows the wastewater composition and operation properties of the tested plant. The plant is a middle size NDN plant with capacity of approximately 32,000 m³/day (8.2 MGD). The volume of aerobic zone is 13450m³, counts approximately 53% of the total volume of the aeration tank. The average influent total COD is approximately 600 mg/L, and ammonia concentration is approximately 50 mg-N/L.

Table 6.1 Wastewater composition of the tested treatment plant

Property	Range	Mean
Plant flow, m ³ /hour	550-1,900	1,350
Total COD, mg/L	467-808	600
Soluble COD, mg/L	195-386	280
Ammonia, mg-N/L	41.0-58.4	50
Organic-Nitrogen, mg-N/L	11.6-20.4	15
MLVSS, mg/L	3000-4200	3600

Figure 6.1 shows the schematic diagram of the wastewater treatment process and the sampling locations. The real-time off-gas tests were performed by an online monitoring device which measured the partial O_2 by a fuel cell and CO_2 content by an infrared sensor. The analyzer recorded hood air flux and O_2/CO_2 contents once per every two hours. Measured data from four time periods were selected in this study; each period lasted at least 10 days and was in different season. Time-series influent and effluent data were monitored during the testing period for model validation, including plant flow, COD, ammonia, nitrate, DO, MLVSS, and pH.

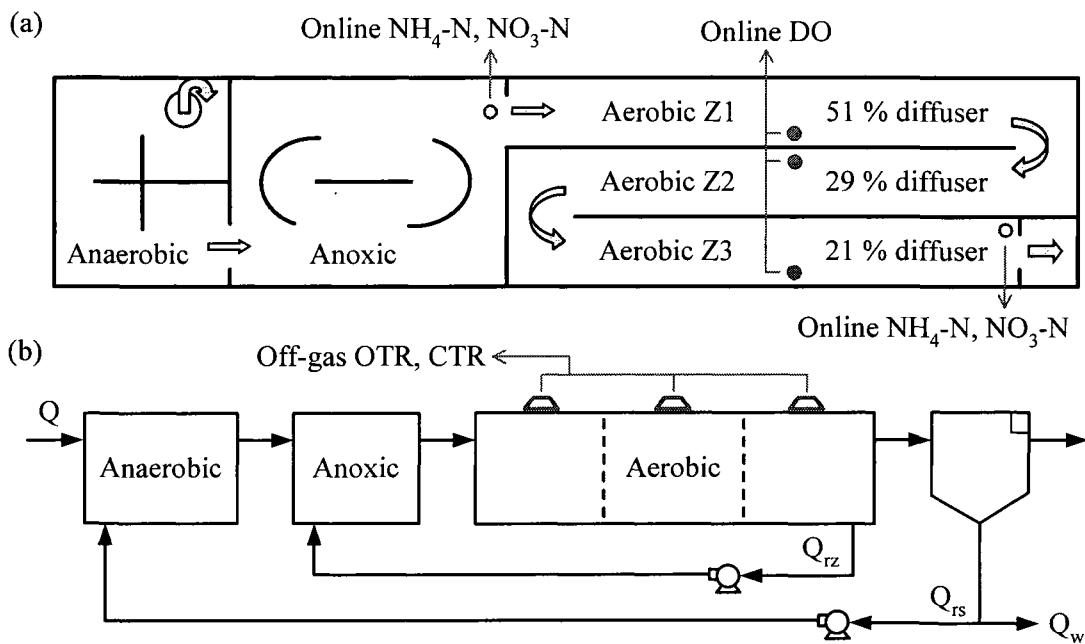


Figure 6.1 (a) Tank geometry and (b) schematic diagram of tested wastewater treatment plant (Waßmannsdorf, Berlin, Germany). Symbols show the monitored parameters and sampling locations.

6.2.3 Activated Sludge Model

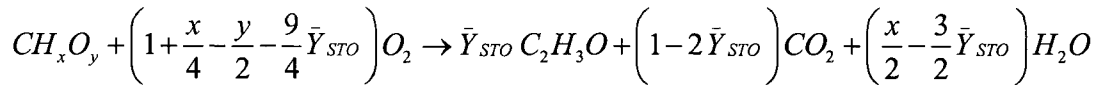
The activated sludge model is developed based on the general Activated Sludge Models No.3 of Gujer et al. (1999) with modifications as Cliff and Andrews (1981), and Sin et al. (2005). The modification was made to simulate the simultaneous direct growth and storage for substrate uptake, which better describes the growth of heterotrophic bacteria (Krishna and van Loosdrecht, 1999) and has a well-defined yield calculation: Sin et al. (2005) used the parameter δ to define the yield coefficients of direct heterotrophic growth ($Y_{H,S}$), substrate storage (Y_{STO}), and heterotrophic growth ($Y_{H,STO}$) on stored mass as:

$$Y_{H,S} = \frac{4\delta - 2}{4.2\delta + 4.32} \cdot \frac{4.2}{4}; \quad Y_{STO} = \frac{4\delta - 2}{4.5\delta} \cdot \frac{4.5}{4}; \quad \text{and} \quad Y_{H,STO} = \frac{4.5\delta - 0.5}{4.2\delta + 4.32} \cdot \frac{4.2}{4.5} \quad 6.3$$

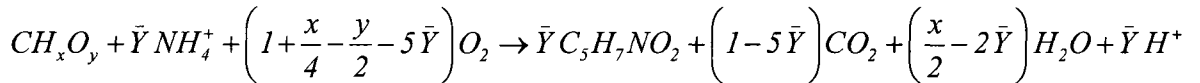
The model simulates the temporal concentrations of carbonaceous substrate (S), stored mass (X_{STO}), heterotrophic (X_H), autotrophic (X_A), and inert biomass (X_I) in the biological phase; dissolved oxygen (S_{DO}), carbon dioxide (S_{DCD}), ammonia (S_{NH}), and nitrate (S_{NO}) in the liquid phase; and oxygen (O_2), carbon dioxide (CO_2) contents in the gas phase. To accurately calculate the mass production/consumption of each simulated compound, stoichiometry was derived for all reactions. In this model, all forms of carbonaceous substrates (rapidly degradable CODs, slowly degradable CODs, or stored CODs) are expressed as CH_xO_y with constant x, y , stored mass is C_2H_3O , and $C_5H_7NO_2$ is used for all bacteria species (heterotrophic or nitrifying bacteria). The value of x and y were originally assumed unknown and then validated with whole plant mass balancing. The five reactions which occur simultaneously in the reactor are: 1) the store of carbonaceous

substrate; 2) the direct growth of heterotrophic biomass; 3) growth of heterotrophic biomass on stored mass; 4) nitrification; and 5) biomass decay; and the stoichiometry of each reaction can be expressed as followed:

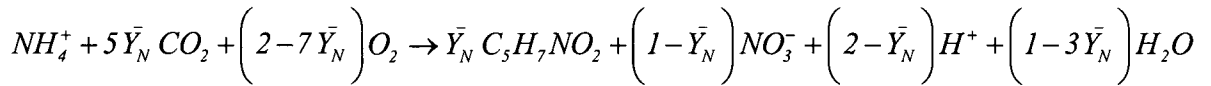
Storage of carbonaceous substrate: 6.4



Growth of heterotrophic bacteria (growth on stored mass use $x = 1.5, y = 0.5$): 6.5



Nitrification: 6.6



Endogenous respiration or biomass decay:



Table 6.2 shows the kinetics and the simulated components in a matrix form similar to the IWAQ ASP model, which the mass balance equations can be developed by adding the multiplication of the coefficients listed in the column and the process rate of each reaction in the right end column. The coefficients in each column are calculated from stoichiometry, and Monod functions are assumed to simulate various cell growth criteria. Simulations of dissolved O_2 and CO_2 shown in the next section provide examples of using the proposed model structure.

Table 6.2 Model matrix of yield coefficient and model kinetics

Reactions	S						Reaction kinetics (mg/L/day)	
	S gCOD	S_{NH} gN	X_{STO} gCOD	X_H gCOD	X_N gCOD	S_O gO ₂	S_{CO2q} gCO ₂	S_{HCO3-} gCO ₂
1 Storage of carbonaceous substrate	$-\frac{1}{Y_{STO}}$		1			$-Y_{O}^{STO}$	Y_{CO2}^{STO}	$k_{STO} \cdot M_O \cdot M_S \cdot X_H$
2 Direct synthesis of heterotrophic bacteria	$-\frac{1}{Y_{H,S}}$	$-Y_{NH}^{H,S}$		1		$-Y_{O}^{H,S}$	$Y_{CO2}^{H,S}$	$\mu_{MAX,S} \cdot M_S \cdot M_O \cdot M_{NH} \cdot X_H$
3 Heterotrophic growth on stored mass		$-Y_{NH}^{H,STO}$	$-\frac{1}{Y_{H,STO}}$			$-Y_{O}^{H,STO}$	$Y_{CO2}^{H,STO}$	$\mu_{MAX,STO} \cdot M_S \cdot M_O \cdot M_{NH} \cdot \frac{f_{STO}^2}{K_{STO2} + f_{STO} \cdot K_{STO1}} \cdot X_H$
4 Nitrification		$-\frac{1}{Y_N}$		1		Y_{O}^{NH}	$-Y_{CO2}^{NH}$	$\mu_A \cdot M_{NH,N} \cdot M_{O,N} \cdot X_N$
5 Endogenous respiration		Y_{NH}^X		-1		$-(1-f_{XI})$	Y_{CO2}^X	$b_H \cdot X_H$
6 Oxygen transfer					1			$\alpha K_L a \cdot (S_O^* - S_O)$
7 Carbon dioxide transfer							1	$\alpha K_L a_{CO2} \cdot (S_{CO2}^* - S_{CO2q})$
8 Bicarbonate equilibrium							-1	$1 \left(k_1 + k_2 \cdot 10^{pH-14} \right) \cdot S_{CO2q} - \left(k_{-2} + k_{-1} \cdot 10^{pH} \right) \cdot S_{HCO3-}$

Note: $f_{STO} = X_{STO}/X_H$; $f_{H_2CO_3} = S_{H_2CO_3} / (S_{H_2CO_3} + S_{HCO_3^-} + S_{CO_3^{2-}})$; $M_S = S_S / (K_S + S_S)$; $M_O = S_O / (K_O + S_O)$; $M_{NH} = S_{NH} / (K_N + S_{NH})$

6.2.4 Simulation of Gas Transfer

Mass balance of DO is estimated by the oxygen uptake rate (OUR) and oxygen transfer rate (OTR). In this study, OTR represents the gas transfer capacity of aeration system, and OUR is the mass oxygen per unit volume consumed to degrade certain pollutants.

The mass balance of DO can be expressed as:

$$\frac{dS_o}{dt} = \frac{Q_l}{V}(S_o^{IN} - S_o) + OTR - OUR_N - OUR_C - OUR_D \quad 6.8$$

In the model, simulation of oxygen transfer across the gas/liquid interfaces is based on the well-known two film theory (Lewis and Whitman, 1924), which can be expressed as:

$$OTR = \alpha K_L a \cdot (S_o^* - S_o) \quad 6.9$$

OUR_C , OUR_N , and OUR_D represent the oxygen uptake of substrate consumption, nitrification, and biomass decay, respectively. The oxygen uptake rate needed to consume each substrate is equal to the growth rate with appropriate stoichiometric yields. Since all the required parameters are given in Table 6.2, only an example is presented here: OUR_N for the consumption of ammonia can be written as follows:

$$OUR_N = Y_O^{NH} \cdot k_N \cdot \frac{S_{NH}}{K_n + S_{NH}} \cdot \frac{S_o}{K_o + S_o} \cdot X_N \quad 6.10$$

In Eqn. (9), Y_O^{NH} is the oxygen demand of ammonia oxidation by nitrifiers and is derived from Eqn. (6). The relationship between Y_O^{NH} (g O₂/g NH₃-N) and molar yield Y_N can be expressed as:

$$Y_O^{NH} = \frac{2 - 7Y_N}{Y_N} \cdot \frac{32}{113} \cdot \frac{1}{1.42} \quad 6.11$$

Oxygen demands of heterotrophic and endogenous respiration are calculated in a similar fashion. By combining all reactions to Eqn. 8, transient DO and OTR can be simulated and to match the off-gas measurements for model validation.

Simulation of carbon dioxide transfer is more complex than oxygen because of the CO_{2q}/bicarbonate equilibrium, as formally discussed. In addition to the reaction kinetics described by the bacteria activities, such as CO₂ uptake for autotrophic growth (CUR), production due to heterotrophic growth and biomass decay (CPRs), and the CO₂ transfer rate (CTR) to off-gas, an additional term was used for pH equilibrium. The mass balance of dissolved CO₂ (S_{CO2q}) a separate function for bicarbonate balance (S_{HCO3-}), and the off-gas CO₂ (CO_2) can be expressed as:

$$\frac{dS_{CO2q}}{dt} = \frac{Q_l}{V} (S_{CO2q}^{IN} - S_{CO2q}) - CTR - CUR_N + CPR_C + CPR_D - r_{HCO3-} \quad 6.12$$

$$\frac{dS_{HCO3-}}{dt} = \frac{Q_l}{V} (S_{HCO3-}^{IN} - S_{HCO3-}) + r_{HCO3-} \quad 6.13$$

$$\frac{dCO_2}{dt} = \frac{Q_g}{V} (CO_2^{IN} - CO_2) + CTR \quad 6.14$$

Spérandio and Paul (1997) estimated the transformation rate of bicarbonate (r_{HCO3-}) using the CO₂ transformation kinetics (k_1, k_2) and the CO₂ dissociation constants (K_1, K_2), which can be expressed as:

$$r_{HCO_3^-} = (k_1 + k_2 \cdot 10^{pH-14}) \cdot S_{CO_2q} - (k_{-2} + k_{-1} \cdot 10^{pH}) \cdot S_{HCO_3^-} \quad 6.15$$

where $k_{-1}=k_1/K_1$; $k_{-2}=k_2/K_2$

The concentration of bicarbonate and CO_{2q} changes with pH: when pH decreases, bicarbonate gains proton and transformed to CO_{2q} , whereas increase CO_2 stripping, and vice versa. If pH shift is too significant, off-gas CO_2 measurements may be upset. Fortunately, biological treatment processes requires and is normally controlled at constant pH, the changes of CO_2 transfer due to pH shifting should be small. Based on this assumption, modeling efforts can be applied to correct the off-gas measurements of CO_2 . In this study, pH changes associated with periodical plant alkalinity measurement was used as input signal to adjust the CO_2 simulation.

CTR is simulated with a similar fashion as OTR and the mass transfer coefficient ($\alpha K_L a_{CO_2}$) was calculated based on the $\alpha K_L a$ of O_2 measured by off-gas tests. The saturated concentration $S_{CO_2}^*$ can be calculated by Henry's Law; whereas all the relationships can be expressed as:

$$CTR = \alpha K_L a_{CO_2} \cdot (S_{CO_2}^* - S_{CO_2q}) \quad 6.16$$

$$\alpha K_L a_{CO_2} = 0.91 \cdot \alpha K_L a \quad 6.17$$

$$S_{CO_2}^* = H_{CO_2} \cdot S_{CO_2q} \quad 6.18$$

Model parameters were validated by matching the online measured ammonia concentration, off-gas OTR, and CTR with the simulation results. And then the model

will be used to study the effects of pH shifting and to estimate removal performance of carbonaceous/nitrogenous pollutants.

6.3 Results and Discussion

6.3.1 Primary Analysis of Off-Gas Data

Table 6.3 shows the operation conditions and the average measurement data during the four testing periods. The average DO and off-gas data are relatively constant during the year, but the mean cell retention time (MCRT) and effluent NH_3 changes largely with water temperature. MCRT increased from approximately 8 days at summer to 15.5 days during winter to perform better nitrification.

Table 6.3 Average plant monitoring results and off-gas tests

Property	Testing period			
	T1-May	T2-July	T3-Nov	T4-Jan
Temperature, °C	19.8	21.5	17.1	14.0
MCRT, day	7.9	8.0	11.0	15.5
DO, mg/L	1.4	1.5	1.6	1.7
Effluent NH_3 , mg-N/L	0.25	0.27	0.47	1.15
Gas transfer coefficient $\alpha K_L a$, 1/hour	4.5	4.4	4.3	4.0
Off-gas OTR, mg/L/hour	43.4	36.3	36.4	34.5
Off-gas CTR, mg/L/hour	43.4	41.1	40.5	37.1

Figure 6.2 shows the results of online off-gas monitoring and nitrification conditions. Examples of two testing periods were performed: a) summer time with average liquid temperature of 20°C; and b) winter time with temperature of 14°C. The upper panel of each Figure shows the transient nitrification status of the process, and results of OTR

versus CTR were shown in the lower panels. To visualize the general idea and potential of the proposed strategy, the scale and limits of each Y-axis were modified to perform the relationship among different parameters.

The plant performed full nitrification during most of the days at summer except one or two days with extremely high loadings; but during winter ammonia was not completely removed at most of the days except low loading hours (midnight to early morning). The results of OTR follow the plant loads well, as expected, and with a constantly 2 to 3 hours' lagging. One important observation between OTR measurement and nitrogen loadings is the nitrification limit. When shock loading occurred and plant operations can not match with the increase (upper panel, shaded area with high influent nitrogen load, date 7/17, 1/20, and 1/21), ammonia was discharged. This observation served a good example of the real-time OTR monitoring since DO was still at constant (~1.9 mg/L) during this period and did not provide information about this fail of nitrification..

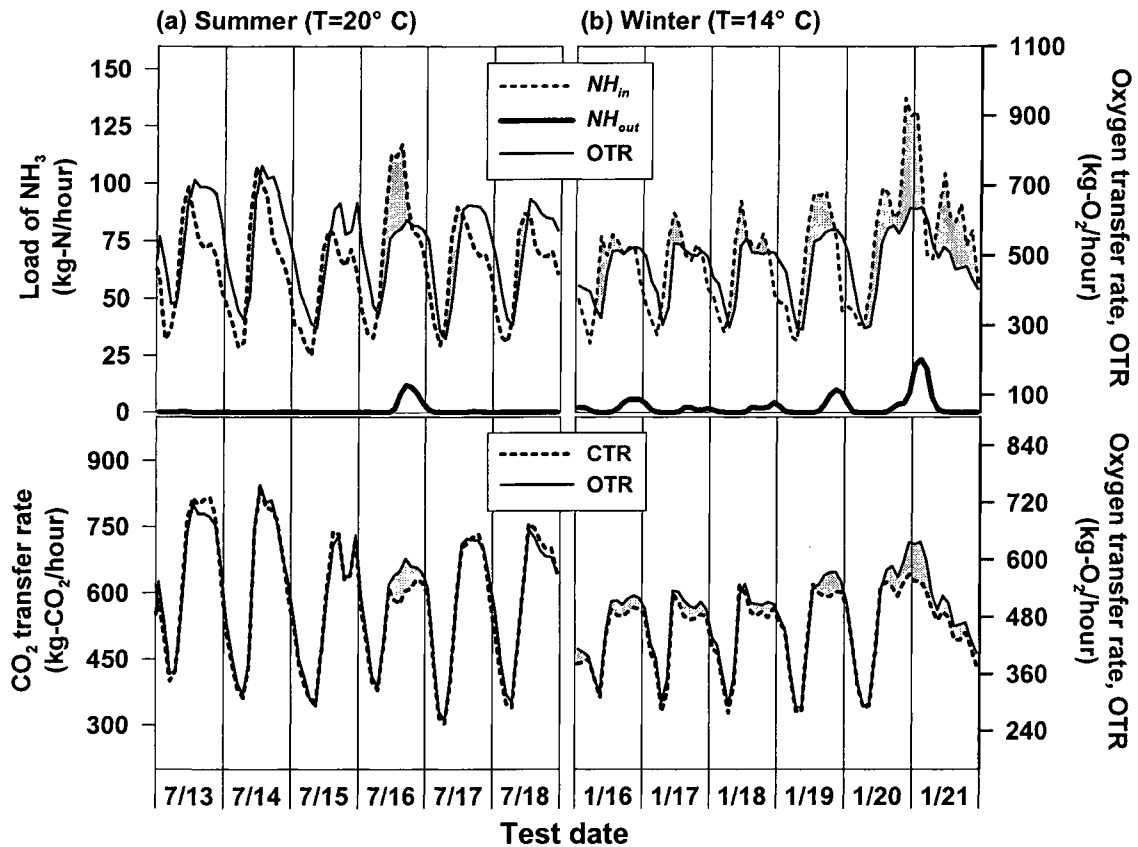


Figure 6.2 Experiment results of real-time off-gas tests and nitrification status in a full-scale ASP. Two columns shows the data collected from two seasons: (a) summer with average temperature of 20°C; and (b) winter of 14°C. Nitrification status versus oxygen transfer rate (OTR) measured by off-gas tests is plotted on the top rows; and carbon dioxide transfer rate (CTR) compared to OTR is plotted on the bottom. Difference between CTR and OTR can be observed at NH₃ break period.

Similar strategy and observation was also found to CTR and OTR. When the plant loads are under control and ammonia is fully nitrified, CTR match well with OTR; but at ammonia overloading period, CTR is lower than OTR (lower panel, shaded area). Figure 6.3 shows the correlations between CTR and OTR at the fully nitrified period versus the ammonia overloading period. This figure contains all the measurements of four testing periods and confirmed the lower CTR/OTR ratio during the ammonia overloading period.

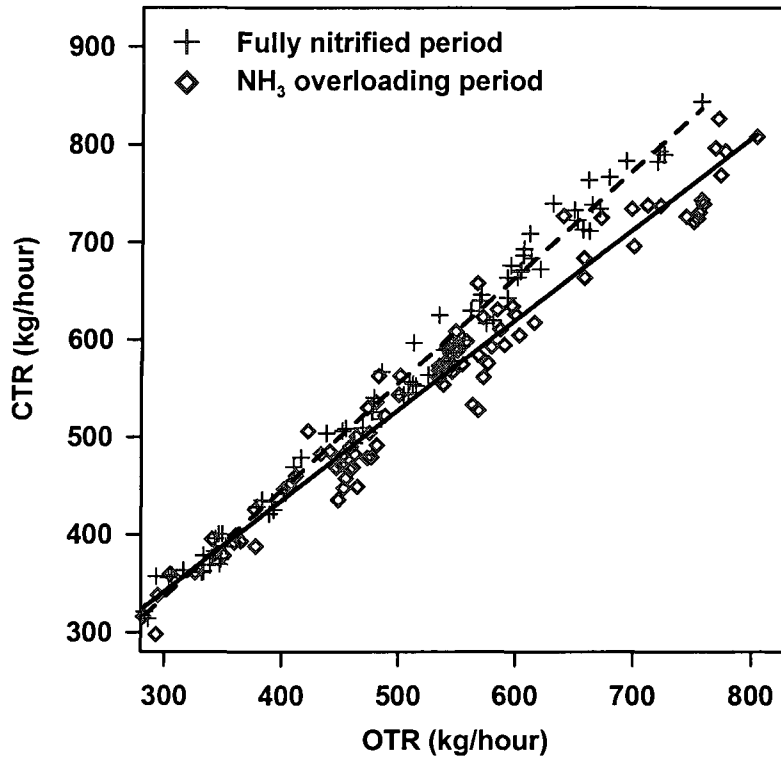


Figure 6.3 Correlations of off-gas measured CTR and OTR at ammonia overloading period and fully nitrified period. Distinguishable higher OTR can be observed during the ammonia breakthrough period.

An explanation of this lower CTR during overloaded periods is higher oxygen demand of nitrifiers. Nitrification failure may be caused by various reasons, as formally discussed, such as insufficient MCRT, DO, or toxic inhibition. No matter what the reason is, during this period, nitrifiers consume all the available oxygen but still not available to oxidize all the influent ammonia. While at the same time the heterotrophic species still consume most of the carbonaceous substrate and oxygen, producing the same amount of carbon dioxide and lowering the ratio of CTR/OTR.

Simulation works were performed to understand the relationship between bacteria activities and gas transfer. Table 6.4 shows the fates of carbon (kg-C/hour) and oxygen (kg-O₂/hour) in the full-scale treatment process. The long-term average of measurement data, including plant loads, off-gas data, online DO, and sludge wasting rate was used to calculate the total CO₂ in the liquid phase and to understand the effect of super-saturation. The calculated total liquid phase CO₂ (CO_{2q} + HCO₃⁻) was 253.4 mg/L, and the saturated dissolved CO_{2q} ($S_{CO_2}^*$) was 54.7 mg/L (from off-gas CO₂).

Table 6.4 Mass balance of special elements

Transfer rate of special element	In	Out
Carbon (kg-C/hour)		
Total substrate (CH _x O _y)	+455.5	
Biosolids wastage (C ₅ H ₇ NO ₂)		-218.1
Gas transfer out as CO ₂		-144.8
Discharged liquid phase CO ₂		92.6
Oxygen (kg-O₂/hour)		
Total substrate (CH _x O _y)	+289.8	
Gas transfer in as O ₂	+492.8	
Gas transfer out as CO ₂		-386.2
Biosolids wastage (C ₅ H ₇ NO ₂)		-116.3
Discharged DO		-2.2
Discharged NO ₃		-33.1
Discharged liquid phase CO ₂		246.9

Based upon the two calculated concentrations, fraction of HCO_3^- was estimated and confirmed with measured alkalinity and pH. The results showed that CO_2 equilibrium was in a manageable range and can be calculated. The oxygen content in the carbonaceous substrate (CH_xO_y) was also defined, whereas C:H:O = 1:1.5:0.48. This empirical formula was then used in stoichiometry (Eqn. 6.4 and 6.5) to calculate the yield coefficients (Table 6.2) for dynamic simulations.

6.3.2 Model Calibration and Sensitivity Analysis

The model was calibrated by seeking the least square errors between simulated OTR, CTR, effluent ammonia and the measured data. Table 5 shows the parameters which are less sensitive in this study, or have well-defined empirical values, i.e. heterotrophic growth rate, μ_{max} , half-velocity coefficient, K_n , K_s , and K_d .

Table 6.5 Selected Monod kinetics used in simulations

Parameter	Heterotrophic	Autotrophic
Maximum uptake rate, $\mu_{max20^\circ\text{C}}$ (1/day)	3	calibrated
Half-velocity coefficient, substrate, K_s	20	-
Half-velocity coefficient, ammonia, K_n	0.1	1.05
Half-velocity coefficient, DO, K_o	0.5	1.0
Decay coefficient, K_d	0.06	0.06
Temperature factor, θ	0.0693	0.0844

Figure 6.4 shows the calibrated parameter values versus temperatures. The parameters are more sensitive for nitrification and CO₂ simulation, including the maximum ammonia uptake rate (k_N), storage coefficient (δ), and COD/TOC ratio. For all the parameters the influences of temperatures are very significant: ammonia uptake rate (k_N) and carbon-oxidation ratio (COD/TOC ratio) increased dramatically with temperature, and the decrease of δ suggested that higher fraction of substrate uptake was used in direct synthesis then storage during summer.

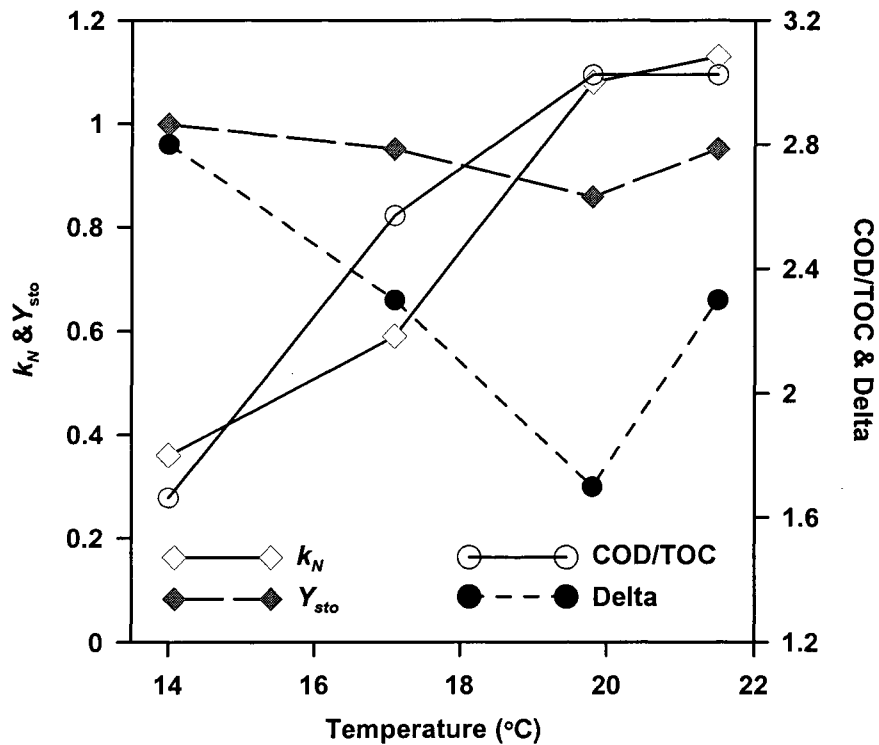


Figure 6.4 Calibrated parameter values at different testing temperatures.

Sensitivity analysis was performed to estimate the potential simulation errors of CTR caused by changes of pH. The study tested the percent differences of simulated CTR with changing pH (ΔpH vary from -1.0 to +1.0) and at three different pH levels (influent pH=6~8, see Figure 5). As previously discussed, the model assumed no transformation between dissolved CO_2 and bicarbonate when change of pH = 0 ($r_{\text{HCO}_3^-} = 0$, Eqn. 13-15), therefore at this point the best prediction of CTR can be provided. Changes in CTR varied with pH conditions; for example, when pH decreased from 7.0 to 6.0, the model over estimated CTR by approximately 60%, but if pH increased from 7.0 to 8.0 the error became 20% under estimate.

Based upon the proposed strategy, CTR can be calculated under the assumption that the change of pH (ΔpH in the Figure) does not change dramatically in a short period.

Treatment plants normally equipped with pH control system to fix the pH at constant: online measurements from the tested plant showed a very stable change in pH at all time (pH change from 6.95 to 6.80, $\Delta\text{pH} = -0.15$). The percent shift of simulated CTR due to this change of pH become a constant (~10%) and can be calibrated. The consistently good fits between simulated CTR and measurements confirmed this hypothesis, as shown in Figure 6.6.

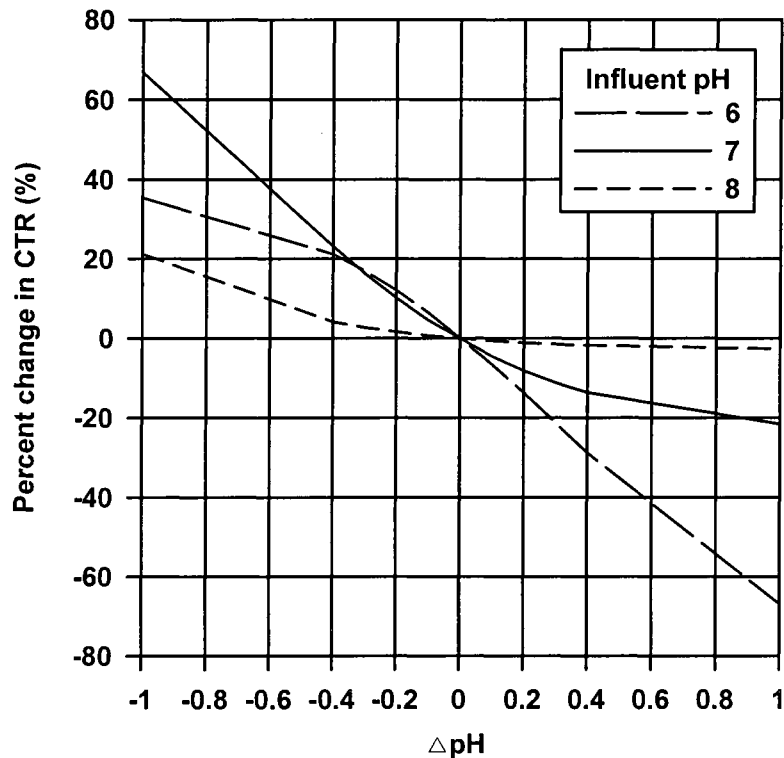


Figure 6.5 Effects of unexpected pH change to CPR simulations.

6.3.3 Dynamic Simulation

Figure 6.6 shows an example of the simulated effluent ammonia, OTR, and CTR versus measured data during a monitoring period. Simulated OTR and CTR fit well with measured data after model calibration, and the model successfully predicted the discharged of ammonia. The simulation result demonstrated that ammonia discharge is caused by nitrifying limitation due to plant operation (e.g., temperature, aeration volume, MCRT), and decreased oxygen transfer is the response of this limitation. The model predicted slightly higher OTR and lower DO than measured data at nitrogen overloading periods, possibly due to the use of transient $\alpha K_L a$ for gas transfer. In the model, simulated DO was used to limit the rate of bacteria growth, but this parameter changes very fast

with $\alpha K_L a$. In the real condition, DO is constant and oxygen uptake is the result of bacteria activities but not the limiting factor. Difference of the two creates small uncertainties for each simulation of OTR and DO, but does not affect the summation. The more important prediction of reaction rates of pollutant consumption and mass balance of ammonia is not affected. Disregard the reason to cause the incomplete nitrification, off-gas data provide useful information to estimate the oxygen shortage in real-time.

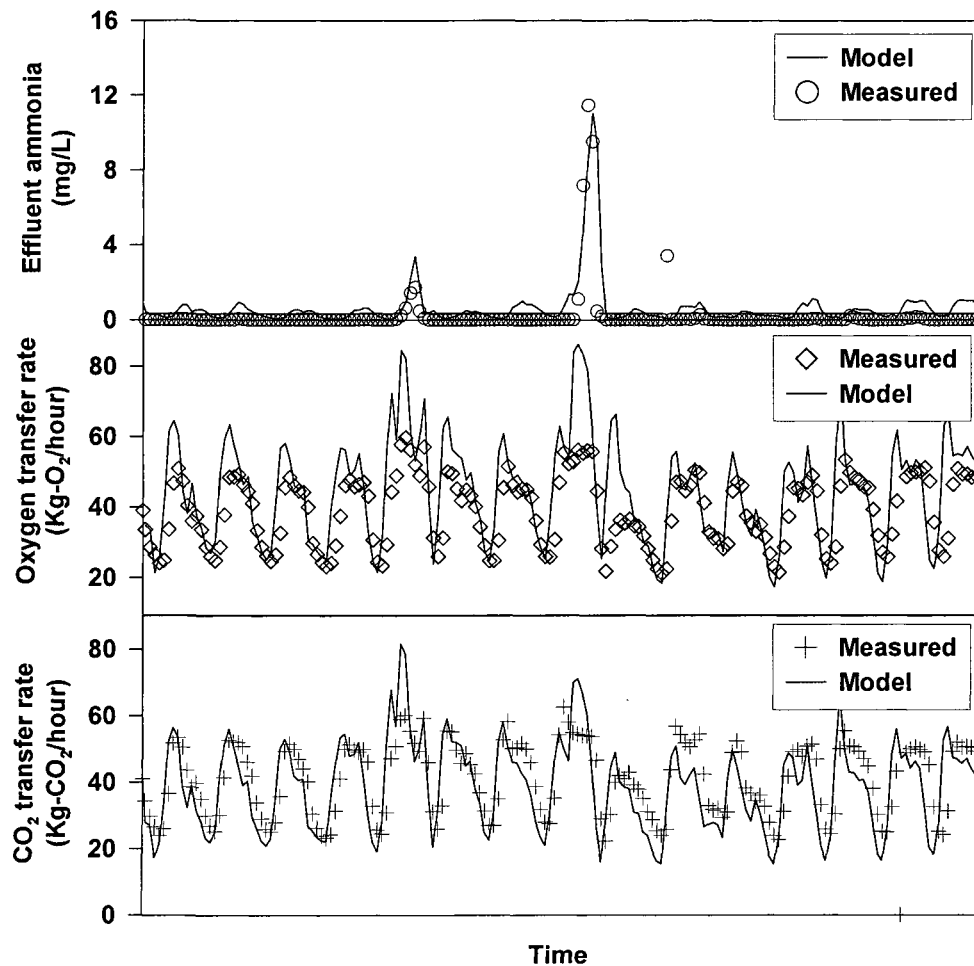


Figure 6.6 Simulation results of the three parameters. Effluent ammonia can be predicted by comparing simulation results of oxygen and CO₂ transfer to the measured data.

Based upon the simulation results, a control strategy to predict nitrification was proposed using off-gas monitoring data and activated sludge model (see Figure 7). The activated sludge model for different monitoring sections can be validated by periodical plant measurements and off-gas data. At each section the calibrated model can be used to evaluate the dynamic ammonia consumption and predict the discharge with only information of off-gas monitoring. Immediate response for the nitrogen discharge, such as effluent flow equalization or temperate increase of MCRT, can be made based on the real-time monitoring results.

6.4 Conclusions

- 1 This study presented a strategy of using online off-gas O₂ and CO₂ monitoring to predict nitrification performance. The ratio of carbon dioxide transfer rate (CTR) to oxygen transfer rate (OTR) decreased during ammonia overloading periods.
- 2 Simulation results showed that rapid change of pH may significantly affect the accuracy of CTR estimation; but in a well controlled environment (i.e. aeration tank with pH control), the uncertainty may be reduced and become manageable by regular measurements of pH and alkalinity.
- 3 Off-gas monitoring provides useful information to evaluate the nitrification status and off-gas CO₂ data can be valuable for model calibrations. The model successfully simulated CTR and was used to predict the ammonia discharge based upon off-gas monitoring and pH adjustment.

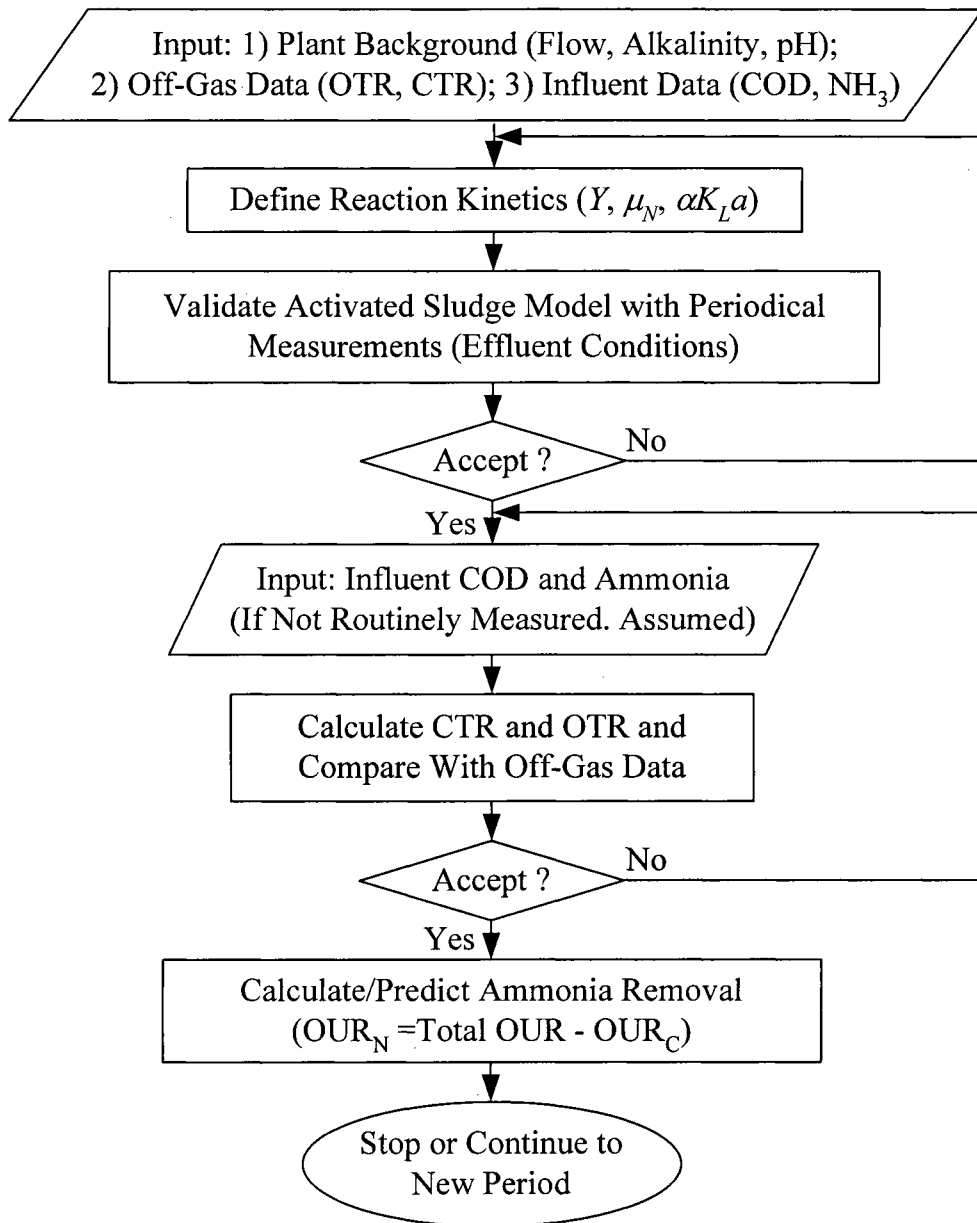


Figure 6.7 Block diagram of using off-gas monitoring and activated sludge model to estimate nitrification performance.

Nomenclature

CO_2	Carbon dioxide mole fraction in off-gas (mole/L)
CH_xO_y	Empirical formula of carbonaceous substrate
S_o^*	Saturated dissolved oxygen concentration (mg/L)
S	Carbonaceous substrate (mg/L)
K_d	Decay coefficient (1/day)
K_s	Half velocity coefficient (mg/L)
K_n	Half velocity coefficient of nitrification (mg/L)
K_o	Half velocity coefficient of DO (mg/L)
O_2	Oxygen mole fraction in off-gas (mole/L)
Q_g	Air flow rate (m ³ /day)
Q_l	Volumetric flow rate (m ³ /day)
OTR	Oxygen transfer rate (mg/L/day)
OUR	Oxygen uptake rate (mg/L/day)
V	Volume (m ³)
X	Cell concentration (mg COD/L)
Y	Yield coefficient (g COD biomass/g COD substrate)
\bar{Y}	Molar yield (mole biomass/mole substrate)
$\alpha K_L a$	Gas transfer coefficient under processing conditions (1/day)
k_N	Maximum uptake rate of ammonia (g NH ₃ -N/g COD-day)
$r_{HCO_3^-}$	Transfer rate to bicarbonate
θ	Temperature correlation coefficient
δ	Storage coefficient
μ_{max}	Maximum substrate uptake rate (g/g-day)

Subscripts or Superscripts

<i>C</i>	Consumption of carbonaceous substrate
<i>D</i>	Cell decay
<i>CO_{2q}</i>	dissolved carbon dioxide
<i>HCO₃₋</i>	bicarbonate
<i>H,S</i>	direct synthesis of heterotrophic biomass
<i>H,STO</i>	heterotrophic growth on stored mass
<i>N</i>	autotrophic species, nitrifiers
<i>O</i>	dissolved oxygen
<i>NH</i>	ammonia
<i>STO</i>	stored mass
<i>IN</i>	influent

7. CONCLUSIONS

This dissertation discussed the major strategies to improve the activated sludge processes, including bioaugmentation to enhance treatment performance of the “target pollutant(s)” and developing online monitoring strategy/instrument to guarantee nitrogen removal and/or reduce aeration costs. The benefits were demonstrated in four thrusts, described in separate chapters.

Mathematic models were developed and validated with experiment data. After calibration, all the models successfully reproduced the measurement results and were used to investigate the observed phenomenon of special interests. Specific conclusions of each thrust are as follows:

1. The benefits of bioaugmentation using the ER-process were demonstrated, showing enhanced target compound removal, improved resistance to shock loads and more rapid reacclimation to the introduction of a toxic compound. The benefits occur with low amounts of bioaugmentation (1 to 2% by reactor biomass). At higher bioaugmentation levels a large fraction of the added mass decays, reducing the benefits of bioaugmentation. The simulation model was useful to quantify the biomass decay rate, which obviously must occur, but is not easy to measure. The increased decay rate explains the reduced relative benefits of bioaugmentation at higher bioaugmentation levels. Simulation results show that the *in-situ* process is superior at longer MCRTs, but the ER-process has the advantage of not exposing the entire biomass to high concentrations of potentially toxic enrichment substrates, as well as being able to accommodate more than one target compound.
2. Three major bioaugmentation approaches were evaluated to improve nitrogen removal: 1) the parallel plant approach; 2) ER approach; and 3) the *in-situ* approach. All three approaches increased the MCRT of nitrifying biomass and provided

improvements for nitrogen removal, but the *in-situ* and enricher reactor approaches were significantly better than the parallel plant approach. The *in-situ* approach and ER approach are both beneficial for improving nitrification, but the choice of process for upgrading a “carbon-only” process will require a plant-specific investigation. The *in-situ* approach will likely be more useful at lower temperature while the ER approach will likely be more advantageous in the presence of inhibitory compound(s).

3. The ability of a real-time off-gas analyzer to estimate aeration power consumption was illustrated. The results of 24-hour experiments showed that OTE vs. OTR, and COD vs. α factor are negatively correlated, which provides supporting evidence for previous observations that load (i.e., surface active agents) depresses oxygen transfer and α factors. The energy savings from diffuser cleaning were demonstrated using off-gas tests before and after cleaning. After cleaning, aeration power was reduced at least 18% due to increased oxygen transfer efficiency. Flow equalization reduces aeration cost by 5 to 31% depending on the season and the available volume for storage. Completely equalizing flow to a constant rate saves nearly as much as shifting the peak loading to the low power rate periods. Yearly savings for the anticipated number of peak, summer and winter periods is 6% for peak limiting, 10% complete equalization and 16% for peak shifting.
4. A strategy of using online off-gas O₂/CO₂ monitoring to monitor and control nitrification performance was presented. The ratio of carbon dioxide transfer rate (CTR) to oxygen transfer rate (OTR) decreased during ammonia overloaded periods. Simulation results showed that frequently change of pH may significantly affect the accuracy of CTR estimation; but the uncertainty may be manageable in a well controlled environment (i.e. aeration tank with pH control). Off-gas monitoring provides useful information to evaluate the nitrification status and off-gas CO₂ data can be valuable for model calibrations. The model successfully simulated CTR and can be used to predict the ammonia discharge.

REFERENCES

- American Society of Civil Engineering (2006) *ASCE Standard Measurement of Oxygen Transfer in Clean Water*, ASCE 2-91, New York, NY.
- American Society of Civil Engineering (1997) *ASCE Standard Guidelines for In-Process Oxygen Transfer Testing*, ASCE 18-96, 345 E. 47th St, New York, NY.
- Andrews, J. F. (1972) Dynamic models and control strategies for wastewater treatment processes. *8th Annual Workshop in Nassau, Bahamas.*, 301-349. Association of Environmental Engineering Professors.
- Babcock, R. W. Jr., Ro, K. S., Hsieh, C. C., and Stenstrom, M. K. (1992) Development of an off-line enricher-reactor process for activated sludge degradation of hazardous wastes. *Res. J. Wat. Environ. Fed.* **64**(6), 782-791.
- Babcock, R. W. Jr., and Stenstrom, M. K. (1993) Use of inducer compounds in the enricher-reactor process for degradation of 1-naphthylamine wastes. *Res. J. Wat. Environ. Fed.* **65**(1), 26-33.
- Babcock, R. W. Jr., Chen, W., Ro, K. S., Mah, R. A., and Stenstrom, M. K. (1993) Enrichment and kinetics of biodegradation of 1-Naphthylamine in activated sludge. *Appl. Environ. Micro.* **39**(2), 264-269.
- Baeza, J. A., Gabriel, D., and Lafuente, J., (2002) In-line fast OUR (oxygen uptake rate) measurements for monitoring and control of WWTP, *Water Sci. Technol.*, **45**(4-5), 19-28.
- Beccari, M., Dionisi, D., Giuliani, A., Majone, M., and Ramadori, R., (2002) Effect of different carbon sources on aerobic storage by activated sludge, *Water Sci. Technol.*, **45**(6), 157-168.
- Bogusch, E. D. (1987) Nitrification with sludge reaeration and ammonia enrichment.

United States Patent. #4,705,633.

- Boon, N., Top, E., M., Verstraete, W., and Siciliano, S. (2003) Bioaugmentation as a tool to protect the structure and function of an activated-sludge microbial community against a 3-Chloroaniline shock load. *Appl. Environ. Micro.* **69**(3), 264-269.
- Bouchez, T., Patureau, D., Dabert, P., Juretschko, S., Dore, J., Delgenes, P., Moletta, R., and Wagner, M. (2000) Ecological study of a bio-augmentation failure, *Environ. Microbiol* **2**(2), 179-190.
- Box, M. J. (1965) A new method for finding multiple extrema of a function of n variables, *Computer J.*, **8**, 45-52.
- Busby, J. B. and Andrews, J. F., (1975) Dynamic modelling and control strategies for the activated sludge process, *J. Water Pollut. Control Fed.*, **47**(5), 1055-1080.
- Cardinal, L. C. (1989) Degradation and biotransformation of isophorone, xylenols, cresols and polyaromatic hydrocarbons in acclimated activated sludge: Use of enrichment reactors to enhance this process, Ph.D. thesis, Univ. of Calif., Los Angeles.
- Cardinal, L. C., and Stenstrom, M. K. (1991) Enhanced biodegradation of polyaromatic hydrocarbons in the activated sludge process. *Res. J. Wat. Environ. Fed.*, **63**(7), 950-957.
- Carrio, L., Sexton, J., Lopez, A., Gopalakrishnan, K., Sapienza, V. (2003) Ammonia-nitrogen removal from centrate: 10 years of testing and operating experience in New York City. *Proceedings of the Water Environment Federation 73th Annual Conference & Exposition, Los Angeles, CA.*
- Capela, S., Gillot, S., Héduit, A., (2004) Comparison of oxygen-transfer measurement methods under process conditions. *Wat. Environ. Res.*, **76**(3), 183-188.
- Cliff, R. C., and Andrews, J. F. (1986) Gas-Liquid Interactions in Oxygen Activated

- Sludge. *Journal of Environmental Engineering*. **112**(1), 61-77.
- Cliff, R. C., and Andrews, J. F. (1981) Predicting the Dynamics of Oxygen Utilization in the Activated Sludge Process, *J. Water Pollut. Control Fed.*, **53**(7), 1219.
- Colour Index (2007) Intermediates of Production, p. 6405. Chorley and Pickersgill Ltd., Leeds, Great Britain.
- Constantine, T. A. (2006) North American experience with centrate treatment technologies for ammonia and nitrogen removal. *Proceedings of the Water Environment Federation 76th Annual Conference & Exposition, Los Angeles, CA.*
- Cliff, R. C., and Andrews, J. F. (1981) Predicting the Dynamics of Oxygen Utilization in the Activated Sludge Process, *J. Water Pollut. Control Fed.*, **53**(7) 1219.
- Cliff, R. C., and Andrews, J. F. (1986) Gas-Liquid Interactions in Oxygen Activated Sludge. *Journal of Environmental Engineering*, **112**(1): 1986, 61-77.
- Daigger, G. T. and Grady, C. P. L. (1982) The Dynamic of Microbial Growth on Soluble Substrates: A Unifying Theory. *Wat. Res.*, **16**: 365-382.
- Daigger, G. T., Norton, L.E., Watson, R.S., Crawford, D., and Sieger, R.B. (1993) Process and Kinetic Analysis of Nitrification in Coupled Trickling Filter/Activated Sludge Processes. *Water Environ. Res.*, **65** (6), 750-758.
- Dold, P. L., and Marais, G.v.R (1986) Evaluation of the general activated sludge model proposed by the IAWPAC task group. *Wat. Sci.Tech*, **18**: 63-89.
- Drury, D. D., Dezham, P., Torres, B., Ooten, K., and Gabb, D. (1995) A novel process for nitrogen removal from belt press filtrate. *Wat. Environ. Tech.*, **7**(9): 1-29.
- Ferrer, J., (1998) Energy saving in the aeration process by fuzzy logic control. *Water Sci. Technol.*, **38**(3), 255-263.
- Federal Register (1974) OSHA Rules and Regulations, Sec. 1910.93d alpha-Naphthylamine. **39**, 23548.

- Gapes, D., Pratt, S., Yuan, Z., and Keller, J. (2003) Online titrimetric and off-gas analysis for estimating nitrification processes in wastewater treatment. *Water Res.* **37**: 2678-2690.
- Gernaey, K., Petersen, B., Nopens, I., Vanrolleghem, P. (2002) Modeling Aerobic Carbon Source Degradation Processes using Titrimetric Data and Combined Respirometric-titrimetric Data: Experimental Data and Model Structure. *Biotechnol Bioeng.* **79**(7):741– 753.
- Goel, R., Mino, T., Satoh, H., and Matsuo, T., (1998) Intracellular storage compounds, oxygen uptake rates and biomass yield with readily and slowly degradable substrates. *Water Sci. Technol.*, **38**(8-9), 85-93.
- Grutsch, J. F., Mallatt, R. C., Streely, B. F. (1978) Process for the purification of waste water. *United States Patent.* #4,073,722.
- Gujer, W., Henze, M., Mino, T. and van Loosdrecht, M.C.M. (1999) Activated Sludge Model No.3. *Wat. Sci. Tech.*, **39**(1), 183-193.
- Guisasola, A., Baeza, J. A., Carrera, J., Casas, C., and Lafuente, J., (2003) An off-line respirometric procedure to determine inhibition and toxicity of biodegradable compounds in biomass from an industrial WWTP. *Water Sci. Technol.*, **48**(11), 267-275.
- Gujer, W., Henze, M., Mino, T. and van Loosdrecht, M.C.M. (1999) Activated Sludge Model No.3. *Wat. Sci. Technol.*, **39**(1), 183–193.
- Head, M. A., and Oleszkiewicz, J. A. (2004) Bioaugmentation for nitrification at cold temperatures. *Wat. Res.*, **38**(3), 523-530.
- Head, M. A., and Oleszkiewicz, J. A. (2005) Bioaugmentation with nitrifying bacteria acclimated to different temperatures. *J. Environ. Eng.*, **131**(7), 1046-1051.
- Hellinga C.; Vanrolleghem P.; van Loosdrecht M.C.M.; Heijnen J.J. (1996) The potential

- of off-gas analyses for monitoring wastewater treatment plants. *Wat. Sci. Tech.* **33**(1), 13–23.
- Henze, M., Grady Jr., C. P. L., Gujer, W., Marais, G.v.R., and Matsuo, T. (1987) Activated sludge model No.1., *IAWPRC Sci. and Technol. Report 1*, IAWPRC, London.
- Henze, M., Gujer, W., Mino, T., Matsuo, T., Wentzel, M. C. and Marais, GvR (1995) Activated Sludge Model No.2. *Wat. Sci. Tech.*, **31**(2): 13-23.
- Henze, M., Gujer, W., Takahashi, M., Matsuo, T., Wentzelt, M. C., Marais, GvR, and Van Loosdrecht, C.M. (1999) Activated Sludge Model No.2D, ASM2D. *Wat. Sci. Tech.* **39**(1): 165-182.
- Hockenbury, M.R., and Grady, C.P. Jr. (1977) Inhibition of Nitrification-Effects of Selected Organic Compounds. *J. Wat. Pollut. Control Fed.*, **49**(5), 768-777.
- Hsieh, C.-C., Ro, K. S., and Stenstrom M. K. (1993) Estimating emissions of 20 VOCs. I: surface aeration. *Journal of Environmental Engineering, ASCE*, **119**(6): 1077-1098.
- Hsieh, C.-C., Babcock, R. W., and Stenstrom M. K. (1993) Estimating emissions of 20 VOCs. II: diffused aeration. *Journal of Environmental Engineering, ASCE*, **119**(6): 1099-1118.
- Hwang, H. J., and Stentrom, M. K. (1985) Evaluation of fine-bubble alpha factors in near full-scale equipment, *J. WPCF* **57**: 1141-1151.
- Iranpour, R., Stenstrom, M.K. (2001) Relationship between Oxygen Transfer Rate and Airflow for Fine-Pore Aeration under Process Conditions, *Wat. Environ. Res.* **73**(3), 266-275.
- Jenkins, T. E., Redmon D. T., Hilgart, T. D., Monsoriu, J. D. D. T., Fox, I. T., (2004) Controlling wastewater treatment processes. *United States Patent*. #0,112,829.
- Katehis, D., Murthy, S., Wett, B., Locke, E., and Bailey, W. (2006) Nutrient removal from

- anaerobic digester side-stream at the blue plains AWTP. *Proceedings of the Water Environment Federation 76th Annual Conference & Exposition*, Dallas, TX.
- Koch, G., Kuhni, M., Gujer, W., and Siegrist, H. (2000) Calibration and validation of activated sludge model No.3 for Swiss municipal wastewater, *Wat. Res.* **34**(14), 3580-2590.
- Kos, P. (1998) Short SRT (solids retention time) nitrification process/flowsheet. *Wat. Sci. Tech.*, **38**(1), 23-29.
- Krause, S., Cornel, P., and Wagner, M. (2003) Comparison of different oxygen transfer testing procedure in full-scale membrane bioreactors, *Wat. Sci. Tech.* **47**(12): 169-176 .
- Krhutková, O., Novak, L., Pachmanova, L., Wanner, J., Kos, M. (2006) *In-situ* bioaugmentation of nitrification in regeneration zone – practical application and experience in large plants. *Wat. Sci. and Tech.*, **53**(12), 39-46.
- Krishna C, van Loosdrecht, MCM. (1999) Substrate flux into storage and growth in relation to activated sludge modelling. *Water Res.* **33**(14), 3149-3161.
- Lawrence, A. W., and McCarty, P. L. (1970) Unified basis for biological treatment design and operation. *J. Sanitary Eng. Div. ASCE*, **96**, 757-778.
- Lee, C.-Y. (1996) Discussion of “How input active biomass affects sludge age and process stability” by B. E. Rittmann. *J. Environ. Eng.*, **123**(1), 101-103.
- Lee, C.-Y. (1997) Model of Bacteria-Supplement Kinetics. *Journal of Environmental Engineering.*, **123**(8), 809-812.
- Libra, J.A., Schuschardt, A., Sahlmann, C., Handschag, J., Wiesmann, U., Gnirss, R., (2002) Comparison of the efficiency of large-scale ceramic and membrane aeration systems with the dynamic off-gas method, *Wat. Sci. Technol.*, **46**(4-5),

317-324.

- Ma, Y., Peng, Y., Wang, S., (2004) Feedforward-feedback control of dissolved oxygen concentration in a predenitrification system, *Bioprocess Biosyst Eng.*, **27**(4), 223-228.
- Marsili-Libelli, S., and Tabani, F., (2002) Accuracy analysis of a respirometer for activated sludge dynamic modelling, *Wat. Res.*, **36**(5), 1181-1192.
- McCann, J., Choi, E., Yamasaki, E., and Ames, B.N. (1975) Detection of Carcinogens as Mutagens in the Salmonella/microsome test: Assay of 300 Chemicals. *Proc. Nat. Acad. Sci. USA, Med. Sci.*, **72**(12), 5135-5139.
- Melcer, H., Dold, P. L., Jones, R. M., Bye, C. M., Fakacs, I., Stensel, H. D., Wilson, A. W., Sun, P., and Bury, S. (2003) *Methods for Wastewater Characterisation in Activated Sludge Modeling*, Water Environment Research Foundation (WERF), Alexandria, VA, USA.
- Metcalf and Eddy Inc., (2003) *Wastewater Engineering: Treatment, Disposal, Reuse*, 4th Ed., McGraw-Hill, New York, N.Y.
- Metcalf and Eddy Inc. (2003) *Wastewater engineering: treatment, disposal, reuse*, 4th Ed., McGraw-Hill, New York, N.Y.
- Mossakowska, A., Reinius, L.-G., Hultman, B. (1997) Nitrification reactions in treatment of supernatant from dewatering of digested sludge. *Wat. Environ. Res.* **69**(6), 1128-1133.
- Muller, A., Wentzel, M.C., Loewenthal, R.E., and Ekama, G.A. (2003) Heterotrophic Anoxic Yield in Anoxic Aerobic Activated Sludge Systems Treating Municipal Wastewater, *Water Res.*, **37**: 2435-2441.
- Neethling, J. B., Spani, C., Danzer, J., and Willey, B. (1998) Achieving nitrification in pure oxygen activated sludge by seeding, *Wat. Sci. and Tech.*, **37**(4-5), 573-577.

- Newbry, B. W., (1998) Oxygen-transfer efficiency of fine-pore diffused aeration system: energy intensity as a unifying evaluation parameter. *Water Environ. Res.*, **70**(3), 323-333.
- Nogita, S., Watanabe, S., Baba, K. (1982) Basic studies on carbon dioxide/ air control system for activated sludge processes. *Water Res.* **16**(6) 1017-1024.
- Novák, L. and Havlíková, D. (2004) Performance intensification of Prague wastewater treatment plant. *Wat. Sci. and Tech.*, **50**(7), 139-146.
- Painter, H. A., (1970) A Review of Literature on Inorganic Nitrogen Metabolism in Microorganisms, *Water Res.*, **4**:393-450.
- Painter, H. A., Loveless, J. E. (1983) Effect of Temperature and pH Value on the Growth-Rate Constants of Nitrifying Bacteria in the Activated Sludge Process, *Water Res.*, **17**: 238-248.
- Parker, D. and Wanner, J. (2007) Review of approaches for improving nitrification through bioaugmentation, *Proceedings of the Water Environment Federation 77th Annual Conference & Exposition*, San Diego, CA.
- Pitter, P. (1976) Determination of Biological Degradability of Organic Substances. *Wat. Research.*, **10**(3), 231-235.
- Plaza, E., Trela, J., and Hultman, B. (2001) Impact of seeding with nitrifying bacteria on nitrification process efficiency. *Wat. Sci. and Tech.*, **43**(1), 155-164
- Poduska, R. A. and Andrews, J. F., (1975) Dynamics of nitrification in the activated sludge process. *J. Water Pollut. Control Fed.*, **47**(11), 2599-2619.
- Puig, S., Corominas, LI., Vives, M. T., Balaguer, M. D., and Colprim, J., (2005) Development and implementation of a real-time control system for nitrogen removal using OUR and ORP as end point, *Ind. Eng. Chem. Res.*, **44**(9), 3367-3373.

- Pratt, S., Yuan, Z., Gapse, D., Dorigo, M., Zeng, R., and Keller, J. (2003) Development of a Novel Titration and Off-gas Analysis (TOGA) Sensor for Study of Biological Processes in Wastewater Treatment Systems. *Biotechnol Bioeng.*, **81**(4): 482-495.
- Pratt, S., Yuan, Z., Keller, J. (2004) Modeling Aerobic Carbon Oxidation and Storage by Integrating Respirometric, Titrimetric, and Off-gas CO₂ Measurements. *Biotechnol Bioeng.*, **88**(2): 135-147.
- Redmon, D.T., Boyle, W.C. and Ewing, L. (1983) Oxygen transfer efficiency measurements in mixed liquor using off-gas techniques. *J. Water Pollut. Control Fed.*, **55**(11), 1338-1347.
- Rittmann, B. E. (1996) How input active biomass affects sludge age and process stability. *J Environ. Eng.*, **122**(1), 4-8.
- Rittmann, B. E. (1996) Closure of "How input active biomass affects sludge age and process stability." *J. Environ. Eng.*, **123**(1), 103.
- Ro, K. S., Babcock, R.W., and Stenstrom, M. K. (1997) Development of a biological process to treat water contaminated with trace-level toxic compounds, *Wat. Research*, **31**(7), 1687-1693.
- Rosso, D., and Stenstrom, M. K. (2005) Comparative economic analysis of the impacts of mean cell retention time and denitrification on aeration systems, *Water Res.*, **39**(16), 3773-3780.
- Rosso, D, Iranpour, R. and Stenstrom, M. K. (2005) Fifteen years of off-gas transfer efficiency measurements on fine pore aerators: key role of sludge age and normalized air flux, *Wat. Env. Res.*, **77**(3), 266-273.
- Rosso, D., and Stenstrom, M.K. (2006a) Economic implications of fine pore diffuser aging, *Wat. Environ. Res.*, **78**(8), 810-815.

- Rosso, D., and Stenstrom, M.K. (2006b) Surfactant effects on α -factors in aeration systems, *Wat. Res.*, **40**(7), 1397-1404.
- Salem, S., Berends, D., Heijnen, J. J., and van Loosdrecht, M. C. M. (2003) Bio-augmentation by nitrification with return sludge. *Wat. Res.*, **37**(8), 1794-1804.
- Salem, S., Berends, D., Heijnen, J. J., and van Loosdrecht, M. C. M. (2002) Model-based evaluation of a new upgrading concepty for N-removal. *Wat. Sci. and Tech.*, **45**(6), 169-176.
- Salem, S., Moussa, M. S., van Loosdrecht, M. C. M. (2006) Determination of the decay rate of nitrifying bacteria, *Biotechnol Bioeng.* **94**(2), 252-262.
- Schuchardt, A., Libra, J. A., Sahlmann, C., Handschag, J., Wiesmann, U., and Gnirss, R., (2005) Potential of OUR and OTR measurements for identification of activated sludge removal processes in aerated basins. *Wat. Sci. Technol.*, **52**(12), 141-149.
- Scott, T.S. (1962) Carcinogenic and Chronic Toxic Hazards of Aromatic Amines. Elsevier Publishing Co., New York, N.Y., 16.
- Serralta, J., Ferrer, J., Borrás, L., and Seco, A. (2004) An Extension of ASM2d including pH Calculation. *Water Res.*, **37**: 2678-2690.
- Serralta, J., Ribess, J., Seco, A., Ferrer, J. (2002) A supervisory control system for optimizing nitrogen removal and aeration energy consumption in wastewater treatment plants. *Wat. Sci. Technol.*, **45**(4-5), 309-316.
- Sin, G., Malisse, K., and Vanrolleghem, P. A. (2003) An integrated sensor for the monitoring of aerobic and anoxic activated sludge activities in biological nitrogen removal plants. *Wat. Sci. Technol.*, **47**(2), 141-148.
- Sin, G., Guisasola, A., De Pauw, D. J. W., Baeza, J. A. Carrera, J., Vanrolleghem, P. A. (2005) A New Approach for Modelling Simultaneous Storage and Growth

- Processes for Activated Sludge Systems Under Aerobic Conditions. *Biotechnol Bioeng.* **92**(5), 600-613.
- Smith, R. C., Saikaly, P. E., Zhang, K., Thomatos, S., and Oerther, D. B. (2008) Ecological engineering of bioaugmentation from side-stream nitrification, *Wat. Sci. and Tech.*, **57**(12), 1927-1933.
- Southern California Edison (2007) *Schedule of Real Time Pricing*. <http://www.sce.com/>
- Spanjers, H., Vanrolleghem, P. A., Olsson, G., and Dold, P. L. (1998) *Respirometry in the Control of Activated Sludge Process: Principles*. IAWQ, London.
- Spérandio, M., and Paul, E. (1997) Determination of Carbon Dioxide Evolution Rate Using On-Line Gas Analysis During Dynamic Biodegradation Experiments. *Biotechnol Bioeng.* **53**(3), 243-252.
- Speckhart, F. H., and Green, W. L. (1976) *A Guide to using CSMP- the Continuous System Modeling Program*, Prentice-Hall, Inc. Englewood Cliffs, N.J.
- Staff (1974) Final Rules Set for Exposure to Carcinogens. *Chem. and Eng. News.* **52**, (6) 12.
- Standard Methods for the Examination of Water and Wastewater (2005) 21th Ed., Am. Public Health Assoc., Washington, D.C., 2.75.
- Stenstrom, M. K. (1979) Models for oxygen transfer: Their theoretical basis and implication for industrial wastewater treatment, *Processing 33rd Purdue Industrial Waste Conference*, **33**: 679-686, Ann Arbor.
- Stenstrom, M. K., and Andrews, J. F. (1979) Real-time control of activated sludge processes, *J. Env. Engr. Div.*, **105**(2), 245-260.
- Stenstrom, M. K., and Gilbert, R. G. (1981) Effects of alpha, beta and theta factors in design, specification and operations of aeration systems, *Wat. Res.*, **15**(6), 643-654.

- Stenstrom, M. K., Kido, W., Shanks, R. F., and Mulkerin, M. (1989) Estimating Oxygen Transfer Capacity of a Full-scale Pure Oxygen Activated Sludge Plant. *J. WPCF* **61(2)**: 208-220.
- Stenstrom, M. K., Kido, W. H., Shanks, R. F., and Mulkerin, M. (1989) Estimating Oxygen Transfer Capacity of a Full Scale Pure Oxygen Activated Sludge Plant, *Journal of the Water Pollution Control Federation*, **61**: 208-220.
- Stenstrom, M. K. and Poduska, R. A. (1980) The Effect of Dissolved Oxygen Concentration on Nitrification. *Water Res.* **14**: 643-649.
- Stenstrom, M. K., Rosso, D., Leu, S.-Y., and Larson, L. (2007) Energy-conservation in fine-pore diffuser installation in activated sludge processes, *Final Report 2005-2007* for Southern California Edison, contract number: 500-03-001. www.seas.ucla.edu/stenstro/reports.
- Stenstrom, M. K., Cardinal, L., and Libra, J. (1989) Treatment of hazardous substances in conventional biological treatment plants. *Environ. Prog.* **8(2)**, 107-112.
- Stephenson, D., and Stephenson, T. (1992) Bioaugmentation for enhancing biological wastewater treatment. *Biotech. Adv.* **10(4)**, 549-559.
- Van Aalst– van Leeuwen, M., Pot, M., van Loosdrecht, M., (1997) Kinetic Modeling of Poly (h-hydroxybutyrate) Production and Consumption by *Paracoccus Pantotrophus* under dynamic substrate supply. *Biotechnol Bioeng* **55(5)**:773–782.
- Van Limbergen, H., Top, E. M., and Verstraete, W. (1998) Bioaugmentation in activated sludge: current features and future perspectives, *Appl. Microbiol. Biotechnol.* **50(1)**, 16-23.
- Tzeng, C. J., Iranpour, R., and Stenstrom, M. K. (2003) Modeling and control of oxygen transfer in the HPO activated sludge process, *J. Env. Engr., ASCE.*, **129(5)**,

402-411.

- Wagner, M., and Pöpel, H. J. (1996) Surface active agents and their influence on oxygen transfer. *Wat. Sci. Technol.*, **34**(3-4), 249-256.
- Wanner, J., Kos, M., Grau, P. (1990) An innovative technology for upgrading nutrient removal activated sludge plants. *Wat. Sci. Tech.*, **22**(7-8), 9-20.
- Weissenbacher, N., Lenz, K., Mahnik, S., Wett, B., and Fuerhacker, M., 2006, Determination of activated sludge biological activity using model corrected CO₂ off-gas data. *Wat. Res.* **41**(7), 1587-1595.
- Wichern, M., Lubken, M., Rlomer, R., and Rosenwinkel, K.-H. (2003) Efficiency of the Activated Sludge Model no.3 for German wastewater on six different WWTPs, *Wat. Sci. Tech.*, **47**(11): 211-218.
- Yuan, W., Okrent, D., and Stenstrom, M. K. (1993) Model calibration for the high-purity oxygen activated sludge process – algorithm development and evaluation, *Wat. Sci. Tech.* **28**(11-12), 163-171.
- Zilverentant, A. (1999). Process for the treatment of wastewater containing specific components e.g. ammonia. Patent PCT/NL99/00462, WO0005177.
- Zimmerman, R. A., Bradshaw, A. T., Richard, D. (2004) *Acclimation of nitrifiers for activated sludge treatment: a bench-scale evaluation*, Moorhead, Minnesota.